Pricing of Embedded Options

Implementing stochastic interest rates and stochastic spread

Jan Müller

Master's thesis
2022:E19

Lund University

Faculty of Science
Centre for Mathematical Sciences
Mathematical Statistics

Centrum Scientiarum Mathematicarum

Abstract

Given the current market climate, in an era of negative interest-rates, the Hull-White model has regained popularity in the eyes of investors. This thesis aims to extend this model to incorporate credit risk, to allow the modelling of credit derivatives such as diff swaps, defaultable corporate bonds and credit default swaps. This process can be achieved in a number of ways, by utilising either two one-factor models or one two-factor model. Additionally, notable generalisation procedures are outlined to extend the modelling framework to incorporate popular one-factor short rate alternatives such as Black-Karasinski. Finally, calibration methods of the input variables are discussed as well as determining sensitivity metrics directly from the lattice trees themselves, used in hedging these derivatives which is of particular interest in practical applications.

Keywords— Option pricing, Callable bonds, Affine term structure models, Hull-White one-factor, Hull White two-factor, Trinomial trees, Short rate, Default intensity, Swaption volatilities, Black-76, Credit derivatives, Calibration, Optimisation.

Credit Derivatives - Seeking the fair value

All people, at some point in their life will likely seek a loan or mortgage from a bank, friend or private institution. Interest rates govern the cost of these luxuries, and are influenced by a range of factors including political influence, inflation and government intervention. This process is difficult enough to model itself, but it is not the only factor. A financial institution will also assess the inherent cost of risk (among other things), the ability of the borrower to repay their loan.

Corporations face the same dilemma. In an effort to raise capital, corporations often issue stocks or bonds rather than borrowing from banks or other financial institutions. Bonds are of particular interest, as they are cheaper and do not afford the owner of the bond any control of the company. Additionally, the interest paid from the issuer to the owner of the bond is usually less than that offered by the bank. This allows the corporation in invest in their growth and other projects.

That being said there is at least one distinguishing feature between a company and a government, a risk of default. Most governments are assumed to be risk-free and this is reflected in the cost and yield of their bonds. Corporate bonds are an attractive investing opportunity to a lender, where a greater risk is likelier to return a greater reward. Similar to stocks, bonds also have option features, where it is possible for the issuer to call their bond at a pre-determined price at pre-specified dates. There is one exception, the price of this exercisibility is embedded in the option price. It is not a stand alone product as in the case of the stock market.

Calculating the fair price of the bond, and in turn the cost of this embedded option is far from trivial. Apart from financial statements, there are additional factors such as market risk, operational and systematic risk as well as increased regulations which could influence the fair price of the bond. Thus, modelling this inherent default risk into a suitable yield curve is an art form.

Once all the relevant data has been obtained, one must still contend with a modelling framework to capture all the underlying information. A family of models, denoted affine term-structure models, are popular in practice. These models are particularly useful at relating the prices of bonds to market data, more specifically the yield curve. One of it's most popular children, the Hull-White model is making a revival in recent years due to the nature of the market, with many government curves yielding close to zero or in fact, negative interest rates.

This thesis will attempt to model the aforementioned underlying risks in the popular one-factor Hull-White interest rate model. Notably, this model will be extended to incorporate the default risk of corporations and other financial institutions. In doing so, the fair price of a corporate defaultable bond will be modelable. Additionally, the framework will provide a template to model a range of other credit derivatives such as credit default swaps. Finally, a routine will be established to allow this framework to be further extended under the class of affine term-structure models. This will outline the flexibility of the modelling framework from an investors' perspective, allowing the capture of the inherent risks under different modelling assumptions.

Acknowledgements

I would like to thank Capital Four, most specifically Nicolai and Rasmus for their willingness to provide their expertise and guidance throughout the thesis duration and Torben for making this thesis possible. Additionally to my danish compatriots, Camilla and Nellie for the thorough discussions and sharing in the struggle and battles in navigating through and ensuring the models worked as intended.

I would also like to thank my friend, Jim Öhman who provided the necessary support and advice required through challenging times in the wake of the pandemic.

Finally, I would like to thank my supervisor Magnus Wiktorsson who was always available to discuss and provide the time necessary to understand underlying concepts and discuss common interests outside the world of academia.

Jan Müller

List of Figures

List of Tables

List of Acronyms

ATM At-the-money.

BS Black-Scholes.

COBYLA Constrained Optimization by Linear Approximation.

HW Hull-White.

IQR Inter-quartile Range.

JF Jenks-Fischer.

LIBOR London Interbank Offered Rate.

MD Multiple Defaults.

MSE Mean-squared Error.

NS Nelson-Siegel.

NSS Nelson-Siegel-Svensson.

OAS Option-adjusted Spread.

OTC Over-the-counter.

OTM Out-of-the-money.

RMV Recovery of Market Value.

RP Recovery of Par.

RT Recovery of Treasury.

SMM Standard Market Model.

VIF Variance-Inflation Factor.

YTC Yield to Call.

YTM Yield to Maturity.

YTW Yield to Worst.

ZCB Zero Coupon Bond.

ZR Zero-Recovery.

Table of Contents

1 Introduction

Bonds are financial instruments which represent loans made by investors to borrowers. These borrowers, typically governments and corporations use bonds to raise capital and in turn pay back the principal over an agreed upon term structure and interest rate. These products are quite attractive to borrowers, as in contrast to stocks, do not offer the investor any control of the company.

Derivatives on the other hand are financial products, whose value is derived from an underlying asset. One form of these derivatives are options, whose contract offers the buyer an opportunity to buy or sell these assets at pre-determined times and prices. The embedded option combines the two; bond and option into one stand alone product. These derivatives became more sophisticated and available to a wider audience after the Renaissance. As time went by, these securities attracted the attention of scientists such as Bachelier and Bronzin, who were able to model and develop the foundations of the products which are sold in the market today.

Modeling the prices of these bonds is complex as they are influenced by a host of external factors which are intricate to model. The most popular variable to consider are interest rates. Interest rates are affected by a host of factors such as inflation, supply and demand, political decisions and government intervention. These interest rate models often assume a default-free interest rate, such as those obtained from government treasury term structures. Corporate bonds add an extra dimension, where default is a viable additional variable to consider. As a result, bond credit rating businesses such as S&P and Moody's have categorized bonds based on their risk, assigning a rating to each bond based on a range of factors including industry, bond seniority and time to maturity. High rated bonds are considered investment grade, representing a reduced risk of default and deemed reliable. In contrast, high-yield bonds have lower credit grades than their investment grade counterparts, as a result paying higher yields to entice investors.

This thesis will initially outline one way to value and price these corporate defaultable callable bonds. This will be achieved by replicating the work by Schönbucher [1], who outlined one possible way of modelling the short rate while also incorporating the probability of default using two one-factor Hull-White models, for the short rate and default intensity, respectively. The resulting tree structure can be generalised to price a range of credit default derivatives such as digital default swaps, default swaps and credit spread options. Moreover, once both stochastic processes are established, methods will be proposed to calibrate each respective one-factor model, as well as the combined two-factor trinomial tree.

The initially proposed Hull-White model will initially be assumed to have constant calibration parameters and equidistant time steps. In practice, it may be desirable to vary the time steps during the modeling process, such that payment dates, coupons and strike dates exactly match the contract specifications. Section 7.2 will outline methods to impose these constraints in a one-factor case. Due to the properties and methodology of the two-factor modeling process, it is easy to apply the one-factor modeling extension to the proposed two-factor model.

Additionally, one can make use of useful properties of the family of affine term structure models to provide a generalisation of the Hull-White model. Most notably, the Hull-White model allows the possibility for the short rate or default intensity to become negative, a property which is particularly undesirable in the latter case. As such, the Black-Karasinksi model, which follows a lognormal $f(r) = \ln(r)$ process, will be proposed as an alternative in Section 7 to modeling either the short-rate or default intensity.

Finally, as interest rates and corporations can be heavily affected by their shareholders, regulations and government intervention, it may be desired to add additional constraints or flexibility to the drift and volatility structures in the diffusion processes. Furthermore, historical models such as Ho-lee and Hull-White suffer from the possibility for interest rates to become negative whereas Black-Karasinksi does not perform well in low interest rate environments. In recent years, Hainaut and MacGilchrist [2] as well as Beliaeva and Nawalkha [3] have provided notable alternative short rate models. The consensus is that a short rate model should be chosen such that the chosen model both fits market prices and is similarly consistent with empirical research on the behavior of interest rates [4]. In addition, one must ensure not only that the calibration parameters match the prices of standard interest rate options as closely as possible but the calibrating instrument is not too similar to the interest rate derivative. The choice of model is thus more important as the derivative being priced becomes more exotic. Section 7.3 and Section 7.4 provide procedures for dealing with these more complex structures. In doing so, this thesis provides both choices for modeling and generalising the underlying stochastic processes as well as a generalised framework for the pricing of credit derivatives under a binomial or trinomial tree structure.

2 Definitions

2.1 Bond

Bonds represent a loan made by an investor to a borrower. Bonds come in a variety of forms and characteristics, including mortgage-backed securities, municipal bonds, corporate, savings and treasury bonds. This thesis will focus on treasury and corporate bonds. In addition, when referring to a bond it is assumed that the bond is a fixed rate bond, paying out the same level of interest at each payment date.

2.2 Cash Flow

The cash flow is the net amount of cash or equivalent transferring in and out of a company. In the derivative space, this corresponds to coupon payments which are traditionally paid out quarterly, semi-annually or annually, based on the contract specifications. Additionally, cash flows also entail the loan amount disbursed from the lender to the borrower at the start of the loan and can also occur at non-deterministic times, such as when an option is exercised.

2.3 Zero-Coupon-Bond

A zero-coupon bond (ZCB) is a bond that does not offer coupon payments, yet trade at a discount, offering a profit at maturity where the owner redeems the face value of the bond. Let $P(0,T)$ be defined as the price of a ZCB, with a face value of \$1 maturing at time T. The price of such a bond can thus be expressed as:

$$P(0,T) = e^{-rT}, \tag{2.1}$$

where $r = r(T)$ is the yield at time T.

2.4 Callable Bond

A callable bond is redeemable, where the issuer has the right to exercise the option on the bond and pay off their outstanding debt prior to the bonds maturity date. In doing so, the investors principal is returned and the remaining interest payments are stopped. This is an attractive

feature for the issuer and thus, investors are compensated with a more attractive interest rate. The price of a callable bond can thus be de-constructed into the price of a non-callable bond and the price of the underling option. Thus:

$$P(0,T)^C = P(0,T) + \Pi_c, \tag{2.2}$$

where $P(0,T)^C$, $P(0,T)$ and Π_c correspond to the price of the callable bond, the price of the non-callable bond and the price of the option, respectively.

2.5 Bond Yield

The bond yield is the return an investor receives on a bond, expressed as a percentage of notional. In turn, the price of the bond is the interest rate which would ensure that the discounted value of all future cash flows would be equal to its current price. This is denoted as the yield-to-maturity (YTM).

$$P(t,T) = \sum_{t=1}^{T} \frac{C_t}{(1+y)^t}, \tag{2.3}$$

where y corresponds to the yield and C_t to the cash flow at time t. Eq.2.3 can be solved by popular root solving algorithms such as Newton-Raphson. In the case of callable bonds, yield-to-call (YTC) and yield-to-worst (YTW) represent the yield of a bond expiring at a call date at a given strike rate. In the case of multiple strike dates, YTW is simply the lowest bond yield obtained from all possible strike dates.

2.6 Forward Rates

The forward rates are the quoted interest rates obtainable in a future point of time. These rates are implied from the current zero rates. The instantaneous forward rate is thus the forward rate obtainable at an infinitesimally small time in the future.

$$F(t,T) = -\frac{\partial}{\partial T} \ln P(t,T), \quad T > t, \tag{2.4}$$

The instantaneous instantaneous forward rate can similarly be defined as:

$$F_T(t,T) = -\frac{\partial}{\partial T} F(t,T), \quad T > t, \tag{2.5}$$

2.7 Term-Structure

More commonly known as the yield curve, the term-structure represents the relationship between interest rates or bond yields over different terms to maturity.

2.8 Spread

A spread depicts the difference in yield between a risk-free bond and another debt security with the same maturity. There are a number of spread options to choose from, such as yield spread, option-adjusted spread (OAS) or zero-volatility spread (Z-spread). A more thorough description is provided in [5]. In the case of corporate bonds, the spread compensates the investor for credit risk as well as reduced liquidity. For the purposes of this thesis, the spread will be defined as the difference between a government issued security of a given maturity and a corporate bond yield of the same maturity.

2.9 Market Conventions

When pricing a bond, there are a number of pricing conventions one needs to take account of and are stipulated in bond contracts. These include lockout periods, settlement days, day count conventions and notice periods etc. Though these features impact the price of the bond, unless otherwise stipulated, they are ignored. The day count convention is assumed to be Actual 365, which assumes a daily interest rate in a 365-day calendar year.

3 The Dataset

The data used in the analysis of this thesis consists of corporate bond contract static data (issue and maturity dates, coupons, calendar codes, industry, coupon frequency etc) and daily market prices from January 2016 until April 2021. Additionally, risk-free bond prices are obtained for a number of European countries including Germany, France and the United Kingdom as well as the United States and Canada. Due to the sensitivity of the data, implementation guidelines will be proposed, yet results may be withheld and instead replaced with publicly available reference data. For the purposes of this thesis, government issued treasury bonds will be assumed to be risk-free. Swaption volatilities, calibrated from interest rate swap options are obtained from Bloomberg for the same aforementioned dates and treasury curves, which are required for the calibration of the short rate models. Finally, recovery rates for selected industries and bond seniority are provided by Moodys [6]. Additionally unless otherwise stated, all figures and illustrated examples are created using data from the reference literature by John C.Hull [7] or Philipp Schönbucher [1] and provided in Appendix A, Appendix B and Appendix C.

4 The Model

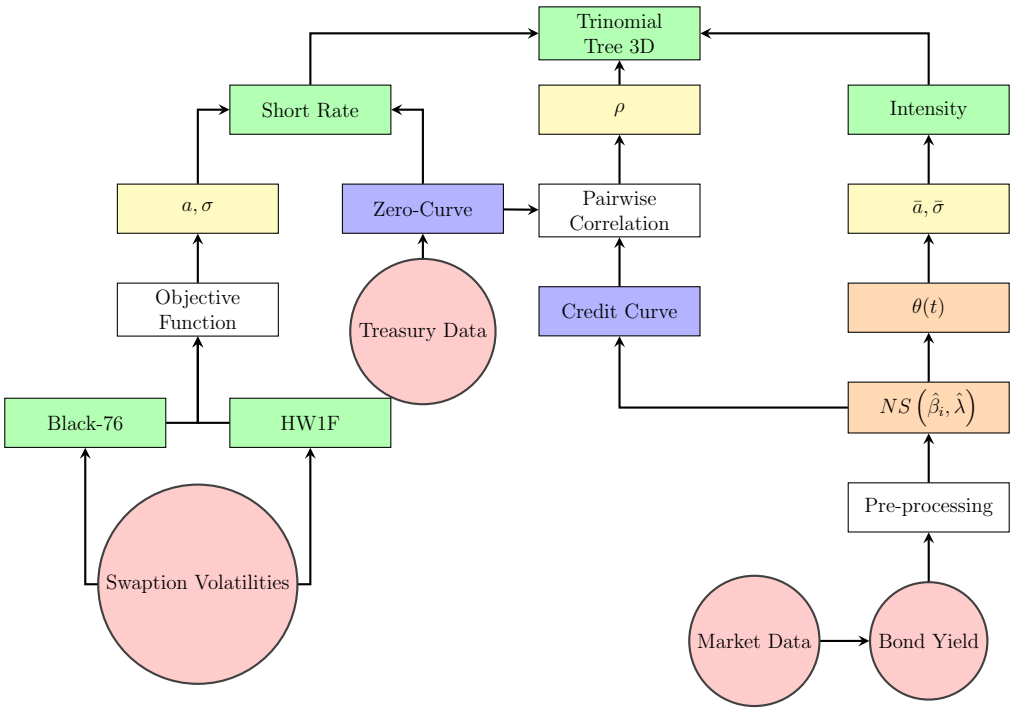

Figure 4.1: Overview of the construction of a two-factor stochastic interest rate and default intensity model.

The thesis can be divided into three main sections; the 2d-model, the 3d-model and the calibration of the model parameters. These model parameters are further sub-categorized into short rate, intensity and correlation respectively. In the case of the short-rate, one begins by obtaining swaption volatilities from a relevant source. These derivatives are over-the-counter (OTC) and thus sourced from Bloomberg. These volatilities are used to determine the underlying Swaption market prices using the Black-76 model and the Hull-White implied model values for a chosen a and σ. The optimal parameters are calibrated using a suitable objective function.

Similarly, one must obtain the corresponding calibration parameters from an intensity model, which carries the underlying default risk of the credit derivative. This is achieved by calculating the bond yields of a time series of daily market prices, processed to obtain smooth curves for yield, spread, or default intensity and finally fitted to a suitable model to allow interpolation. By fitting the Hull-White functional form to this interpolated function, the implied intensity parameters $\bar{a}$ and $\bar{\sigma}$ are obtainable by a suitable calibration procedure.

The final parameter ρ, which is the correlation between the two stochastic processes is obtainable using a historical pairwise correlation comparison of the two benchmark curves.

The calibration parameters a and σ, (or analogously $\bar{a}, \bar{\sigma}$) form the basis in constructing a two-dimensional trinomial lattice tree, under the Hull-White model. This leads to a number of modelling options. One can choose to model each of the stochastic processes independently (each with their own term structure) and then incorporate correlation or to model a two-factor stochastic process with a single term-structure and embedded correlation. This thesis' main focus is the pricing of corporate defaultable bonds, whereby the former will be required and utilised.

One begins by modeling the short-rate process independently under the Hull-White model. This tree can be calibrated to the observed zero-rate curve and is capable of being used to price credit derivatives and determining sensitivity metrics. One could analogously build an intensity based two-dimensional tree.

In order to construct the three-dimensional tree, one combines the calibrated short-rate and non-calibrated intensity based tree. Correlation and default are introduced and the tree is calibrated to the intensity curve. This tree is now capable of pricing credit derivatives and calculating sensitivity metrics such as the Greeks. A summary of the modeling process is exhibited in Fig 4.1.

5 Short-Rate Model

Interest rates are affected by a host of factors such as inflation, supply and demand, political decisions and government intervention which makes the modeling of interest rates quite complex. Short-rate models attempt to simplify this complexity. The short rate represents the continuously compounded and annualized interest rate which can be borrowed for an infinitesimally short period of time on a corresponding term structure. Thus, by modeling the evolution of these short rates over time, one can estimate the evolution of interest rates and price interest rate derivatives.

5.1 Affine Term-Structure Models

One popular framework for the modelling of interest rates is using affine term-structure models. A model is classified as an affine term-structure model if the continuously compounded spot

rate $R(t,T)$ can be written in the form

$$R(t,T) = \alpha(t,T) + \beta(t,T)r(t), \tag{5.1}$$

where α and β are deterministic functions of time and $r(t)$ is a vector short rates [8]. This criteria is satisfied if the price of a zero-coupon bond can be written as

$$P(t,T) = A(t,T)e^{-B(t,T)r(t)}, \tag{5.2}$$

and thus setting $\alpha(\cdot), \beta(\cdot)$ to

$$\begin{aligned} \alpha(t,T) &= -\frac{\ln(A(t,T))}{T-t}, \\ \beta(t,T) &= \frac{B(t,T)}{T-t}. \end{aligned} \tag{5.3}$$

This Vasicek model (1977) was of notable historical importance when applying this class of models to interest-rate modelling. Unfortunately due to an endogenous modelling of the term-structure of interest rates, the initial term structure did not match that of the market, irrespective of the choice of model parameters [8]. Ho-Lee (1986) first proposed a rectification of this conundrum, by modelling the term-structure exogenously. This model operated under a binomial tree structure and failed to capture mean reverting dynamics. Hull and White (1990) successfully managed to provide a solution, by introducing a time-varying parameter to the Vasicek Model. Additionally, a key underling assumption is that the short rate process $f(r)$ follows an Ornstein-Uhlenbeck process with a reversion level that is a function of time. This model provided an exact match to the term-structure of interest rates. The short rate process $f(r) = r$ became known as the Hull-White Extended Vasicek Model or simply, the Hull-White model. The model assumed a Gaussian distribution for the short-rate at each time t and provided analytically tractable zero-coupon bond prices. Furthermore, they introduced an additional time-varying parameter which could to used to match a term-structure of volatilities. The model had one drawback, that interest rates could be negative under certain conditions. This led to the development of the Black-Karasinski model (1991) which addressed these issues. That being said, the Hull-White model has once again become popular due to it's applicability in modern day dynamics where interest rates are both negative and/or close to zero [8]. Some popular arbitrage-free short-rate models are illustrated in Tab 5.1. For the purposes of this thesis, the Hull-White one-factor model will be utilised and extended to incorporate default intensity and in-turn provide a framework for pricing credit derivatives, most notably corporate defaultable bonds.

Table 5.1: Popular one-factor arbitrage free short-rate models.

Model	**Expression**
Ho-Lee	$dr_t = \theta_t dt + \sigma dW_t$
Hull-White	$dr_t = (\theta_t - ar_t)dt + \sigma dW_t$
Black-Derman-Toy	$d\ln(r) = (\theta_t + \frac{\sigma_t'}{\sigma_t}\ln(r))dt + \sigma_t dW_t$
Black-Karasinski	$d\ln(r) = (\theta_t - \Phi_t \ln(r))dt + \sigma_t dW_t$

6 Hull-White Model

The Hull-White model is a no-arbitrage mean reverting model which is capable of fitting term structures of interest rates and a member of these class of affine term-structure models. The instantaneous short rate r, using the Hull-White model can be illustrated as:

$$dr = (\theta(t) - a(t)r(t))\,dt + \sigma(t)dW(t), \tag{6.1}$$

where $\theta(t)$ is a deterministic function, $a(t)$ and $\sigma(t)$ are time-dependent factors and $W(t)$ is a standard Brownian motion [7]. It is assumed the time steps in the tree remain constant, though Section 7.2 illustrates a procedure where this procedure can be extended to include non-constant time steps. For the basis of a lattice based one-factor short rate model, it is assumed that the mean-reversion factor and volatility are constant, i.e. $a(t) = a$ and $\sigma(t) = \sigma$. Additionally, it is assumed that the Δt period rate, $R(t)$, follows the same process as $r(t)$. It can be shown that the difference between the instantaneous short rate process $r(t)$ and the Δt-period rate R(t) is a deterministic time-dependent function such that (Appendix D):

$$r(t) - R(t) = r(0)e^{-at} + \int_0^t e^{-a(t-s)}\theta(s)ds. \tag{6.2}$$

Thus, by modelling the distribution of $R(t)$ it is possible to model the distribution of $r(t)$, where this deterministic offset is determined during calibration, with the matching of the interest-rate term structure. The Δt period-rate $R(t)$ is defined as:

$$dR = (\theta(t) - aR)\,dt + \sigma dW(t). \tag{6.3}$$

The model then comprises of two steps, denoted forward and backward branching/propagation, respectively. The forward branching stage aims to model the instantaneous short rate process while the backward branching models the pricing of the derivative. In the case of callable bonds (and non-callable bonds), this entails initiating the price at the end nodes to the face value of the bond at expiry, discounting accordingly through each of the nodes, adding coupons and early exercise where applicable to obtain the price of the bond at the root node.

6.1 Forward Branching

The forward branching consists of two steps, modelling the process of R^*, which is assumed to follow the same process as $r = R$, and then calibrating this tree to the term-structure of interest rates.

6.1.1 Constructing the Un-calibrated Lattice

The lattice based tree can be viewed as a discretization of the underlying continuous stochastic process. The first stage in building a trinomial tree is to construct a tree for a variable R^*, where $\theta(t) = 0$ and follows the process:

$$dR^* = -aR^*dt + \sigma dW_t, \tag{6.4}$$

and the process is symmetrical about zero. Furthermore, it is assumed that this process follows a normal distribution, whose mean and variance can be expressed as:

$$\begin{aligned} Z = R^*(t + \Delta t) - R^*(t) &\in N(\mu, \sigma), \\ \mathbb{E}(Z|\mathcal{F}(t)) &= -aR^*(t)\Delta t, \\ \mathbb{V}(Z|\mathcal{F}(t)) &= \sigma^2\Delta t, \end{aligned} \tag{6.5}$$

where the influence of higher order terms has been ignored. The spacing between the interest rates on the tree, denoted ΔR, are represented as

$$\Delta R = \sigma\sqrt{3\Delta t}, \tag{6.6}$$

in the cases where σ is constant [7]. As the lattice continues to grow, the strength of the mean reversion effects are proportional to $|R^*|$, and it is thus possible for the increments to become negative or arbitrarily large as emphasized in Eq 6.5 [9]. The solution is to implement a modified branching method, which inhibits the continued growth of the tree. In the case of a constant Δt, the tree becomes saturated and plateaus at a given time step t_i. The modified branching methods, denoted upward and downward branching, compliment the standard branching and ensure the nodes can only transition across (no change), upward or downward at the tree saturation points. This process is illustrated in Fig 6.1.

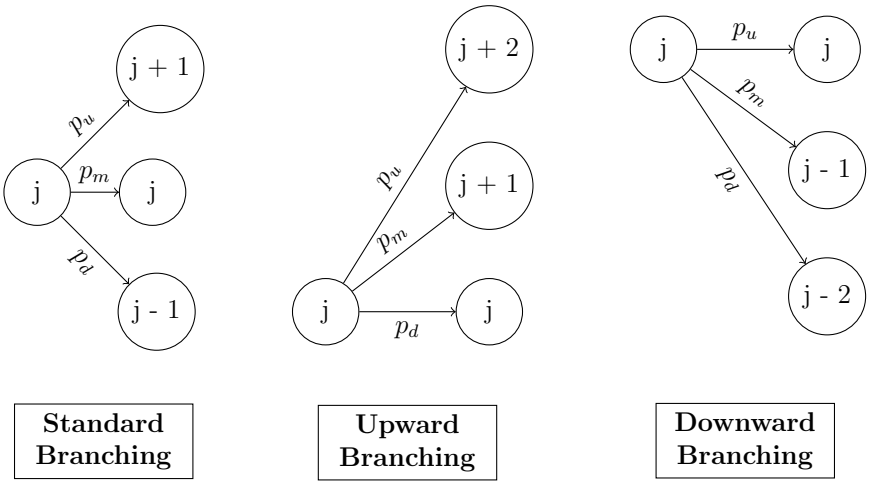

Figure 6.1: Illustration of the branching methods in the Hull-White model to ensure mean reversion.

Once the skeleton of the trinomial tree has been established, the branching probabilities are determined at each node. This is achieved by equating the moments obtained from this discrete time tree to those obtained under a continuous process. Additionally, a third equation is introduced to ensure the probabilities sum up to one. Let ΔR_u, ΔR_m and ΔR_d denote the value of R^* at node (i, j). Thus,

$$\begin{aligned} \mathbb{E}\left(R^{*n+1} - R^{*n}\right) &= p_u\Delta R_u + p_m\Delta R_m + p_d\Delta R_d = -aR_j^{*n}\Delta t, \\ \mathbb{E}\left(\left(R^{*n+1} - R^{*n}\right)^2\right) &= p_u\Delta R_u^2 + p_m\Delta R_m^2 + p_d\Delta R_d^2 = \sigma^2\Delta t + a^2(R_j^{*n})^2\Delta t^2, \\ p_u + p_m + p_d &= 1. \end{aligned} \tag{6.7}$$

By solving Eq 6.7 in conjugation with Eq 6.11, the branching probabilities for each time step can be obtained. By changing the branching at the first possible node, the algorithm proves to be the most computationally efficient. Let $\delta = aj\Delta t$, where j represents the width or "thickness" of the tree, relative to the origin $j = 0$. The probabilities for the three branching methods can then be determined as:

Table 6.1: Branching probabilities for trinomial 2D-short rate tree.

	Upward	**Standard**	**Downward**
p_u	$\frac{1}{6} + \frac{1}{2}(\delta^2 + \delta)$	$\frac{1}{6} + \frac{1}{2}(\delta^2 - \delta)$	$\frac{7}{6} + \frac{1}{2}(\delta^2 - 3\delta)$
p_m	$-\frac{1}{3} - \delta^2 - 2\delta$	$\frac{2}{3} - \delta^2$	$-\frac{1}{3} - \delta^2 + 2\delta$
p_d	$\frac{7}{6} + \frac{1}{2}(\delta^2 + 3\delta)$	$\frac{1}{6} + \frac{1}{2}(\delta^2 + \delta)$	$\frac{1}{6} + \frac{1}{2}(\delta^2 - \delta)$

where $p_{u,m,d}$ represent the probabilities to transition "upward", "across" or "downward" from a given node at time t_i to nodes at time t_{i+1}. It is possible to generalise the probability structure to fit a range of models and this is discussed in Section 7. The transition probabilities can be modified accordingly to yield the same expectation and variance and for more information, one refers the reader to [10]. Note also, that the transition probabilities are merely dependent on a, j and Δt and are independent of σ, which affects the spacing between the nodes. Let $t = m\Delta t$ denote the number of time-steps. To ensure the transition probabilities are strictly positive for j, the boundary conditions for each branching form can be derived as:

$$\begin{aligned} -\frac{\sqrt{2/3}}{a\Delta t} <& j < \frac{\sqrt{2/3}}{a\Delta t}, & j \in B_n \\ -\frac{-1-\sqrt{2/3}}{a\Delta t} <& j < \frac{-1+\sqrt{2/3}}{a\Delta t}, & j \in B_u \\ -\frac{1-\sqrt{2/3}}{a\Delta t} <& j < \frac{1+\sqrt{2/3}}{a\Delta t}, & j \in B_d. \end{aligned} \tag{6.8}$$

Let j_{max} and j_{min} represent the regions where, for a value of j, it is necessary to switch from standard branching to downward and upward branching. Let j_{max} represent the smallest integer at which this statement is satisfied. By Eq 6.8, normal branching is utilised whereby $j_{min} < j < j_{max}$ and upward/downward branching is used at the extreme regions once the tree has reached saturation point. Thus,

$$\begin{aligned} \frac{0.184}{a\Delta t} \leq & j_{max} \leq \frac{0.816}{a\Delta t}, \\ & j_{min} = -j_{max}. \end{aligned} \tag{6.9}$$

As it is desirable to switch branching process at the first possible opportunity, let

$$j_{max} = \left\lfloor \frac{0.184}{a\Delta t} \right\rfloor. \tag{6.10}$$

The tree for R^* can now be constructed. Using Eq 6.6, set the values of R^* at each node for each time step as:

$$R^*(i,j) = R^* = j\Delta R. \tag{6.11}$$

6.1.2 Calibrating the Lattice

The un-calibrated R^* tree is converted to that of R by displacing the nodes of the tree so as to exactly match the term structure of interest rates at each given time step. Define this shift as:

$$\alpha_t = R_t - R_t^*. \tag{6.12}$$

Additionally, define $Q_{i,j}$, the Arrow-Debreu price, as the present value of the security which has a payoff of \$1 if node (i, j) is reached and zero otherwise. Note that the value of the root node, $Q_{0,0} = 1$. More formally, suppose that $Q_{i,j}$ has been determined for $i \leq m$ $(m \geq 0)$. The price of a zero coupon bond maturing at time $(m+1)\Delta t$ is defined as:

$$\begin{aligned} P_{m+1} &= \sum_{j=-n_m}^{n_m} Q_{m,j} \exp[-R_m \Delta t] \\ &= \sum_{j=-n_m}^{n_m} Q_{m,j} \exp\big[-(\alpha_m + R_j^*)\Delta t\big] \\ &= \sum_{j=-n_m}^{n_m} Q_{m,j} \exp[-(\alpha_m + j\Delta R)\Delta t], \end{aligned} \tag{6.13}$$

where n_m is the number of adjacent nodes to the central node at the time $m\Delta t$. Under the Hull-White model, this equation can be solved analytically as:

$$\alpha_m = \frac{\log\left(\sum_{j=-n_m}^{n_m} Q_{m,j} \exp[-j\Delta R \Delta t]\right) - \log P_{m+1}}{\Delta t}, \tag{6.14}$$

which now provides the correction factor at each time step [7]. It is important to note, that the initial $\alpha_0 = r(0)$ must be chosen such that P_1 is priced correctly. Moreover, this is illustrated as:

$$P_1 = e^{-r_0 \Delta t}. \tag{6.15}$$

Note also, that it is in fact possible to analytically determine α_m without the need for forward induction via:

$$\alpha_t = F(0,t) + \frac{\sigma^2}{2a^2}\left(1 - e^{-2at}\right)^2. \tag{6.16}$$

This implementation is not desireable as the constructed tree does not provide an exact fit to the term structure. This is due to the fact that the underlying follows a continuous stochastic process and the tree is a discrete representation. Thus, forward induction provides a means of exactly matching the initial term structure and is the method proposed for tree construction [11]. These α's are calculated to give the right price of a ZCB maturing at time $2\Delta t$. Thus, to determine P_{m+1}, the trinomial tree is calibrated to an associating default free interest rate term structure. This can be achieved by means of a suitable interpolation method. This thesis chooses a linear interpolation scheme. Once the α's have been calculated for that given time step, it is possible to determine $Q_{i,j}$ for the next time step such that:

$$Q_{m+1,j} = \sum_k Q_{m,k} q(k,j) \exp[-(\alpha_m + k\Delta R)\Delta t], \tag{6.17}$$

where $q(k, j)$ is the probability of moving from node (m, k) to node $(m+1, j)$ and the summation is taken over all values of k for which this is nonzero [1]. An example of the constructed un-calibrated and calibrated trees are illustrated in Fig 6.2. It is now possible to price zero-coupon-bonds under the Hull-White Model. An example of this pricing method using data from Appendix A, as well as extensions to include coupon payments and optionality are illustrated in Tab 6.4.

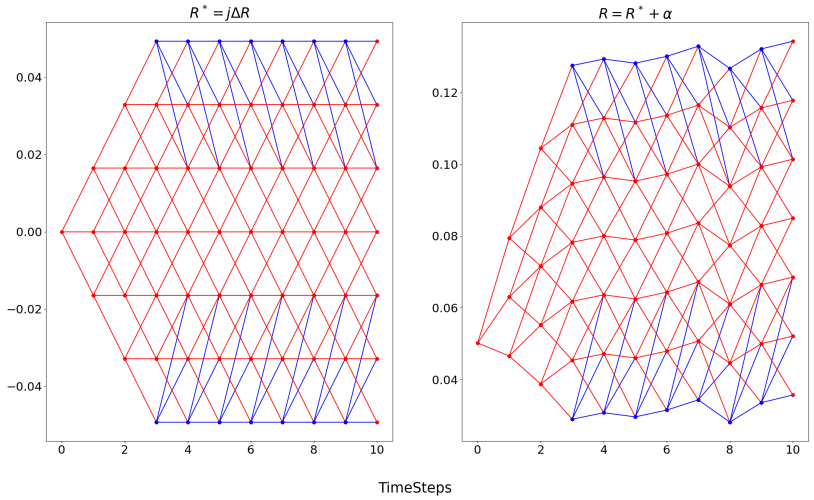

Figure 6.2: Illustration of the constructed trinomial tree for R^* (left) and the short-rate process r (right) for n=10 time steps, where red and blue branches signify standard and upward/downward branching respectively.

6.2 Analytical Solution of Affine Term Structure Models

Affine term structure models have a number of useful properties. One of the major features is the ability to analytical tractability. This means that it is possible to circumvent the modeling of the bond and instead construct a tree which models the price of the underlying option. This procedure only applies to European zero-coupon call and put options. In an affine term structure, bond prices are of the following form

$$P(t,T) = e^{A(t,T)-B(t,T)r_t}. \tag{6.18}$$

This analytic tractability is an attractive feature of affine term-structure models and the analytic solutions are not limited to the Hull-White Model. In fact, if one considers the general term-structure equation [12]

$$F_t + (\mu - \lambda\sigma)F_r + \frac{\sigma^2}{2}F_{rr} - rF = 0, \tag{6.19}$$

$$F(T,r) = \phi(r), \tag{6.20}$$

where $\phi(r)$ is some real-valued function and a short-rate process which follows:

$$dr_t = \mu(t,r_t)dt + \sigma(t,r_t)dW_t, \tag{6.21}$$

one can compute the partial derivatives of F in Eq 6.19 yielding:

$$A_t(t,T) - (1 + B_t(t,T))\, r - \mu(t,r)B(t,T) + \frac{\sigma^2}{2}B^2(t,T) = 0, \tag{6.22}$$

where one assumes

$$\begin{aligned} \mu(t,r) &= \alpha(t)r + \beta(t), \\ \sigma(t,r) &= \sqrt{\gamma(t)r + \delta(t)}. \end{aligned} \tag{6.23}$$

Under this assumption, the model satisfies an affine term structure whereby

$$\begin{aligned} B(T,T) &= A(T,T) = 0, \\ A_t(t,T) &= \beta(t)B(t,T) - \frac{\delta(t)}{2}B^2(t,T), \\ B_t(t,T) &+ \alpha(t)B(t,T) - \frac{\gamma(t)}{2}B^2(t,T) = -1, \end{aligned} \tag{6.24}$$

and is thus possible to provide an analytical solution to a range of affine term structure models.

6.2.1 Modelling Option Expiry Analytically using the Hull-White model

In the case of the Hull-White model, the boundary conditions of the parameters $A(\cdot)$ and $B(\cdot)$ are given by:

$$\begin{aligned} A(T,T) &= B(T,T) = 0, \\ B_t(t,T) &= aB(t,T) - 1, \\ A_t(t,T) &= \theta(t)B(t,T) - \frac{1}{2}\sigma^2 B^2(t,T). \end{aligned} \tag{6.25}$$

Solving these equations yield:

$$\begin{aligned} B(t,T) &= \frac{1}{a}\left(1 - e^{-a(T-t)}\right), \\ A(t,T) &= \int_t^T \left\{\frac{\sigma^2}{2}B^2(s,T) - \theta(s)B(s,T)\right\} ds. \end{aligned} \tag{6.26}$$

The next step is to be able to fit the theoretical observed bond prices to the observed prices and this is possible by making use of the forward rates and fitting these observed rates to the theoretical curve. This is possible due to the one-to-one relationship between forward rates and bond prices. The forward rates in an affine term structure model are given by:

$$F(0,T) = B_T(0,T)r_0 - A_T(0,T). \tag{6.27}$$

By substituting this expression into Eq 6.26 yield:

$$F(0,T) = e^{-aT}r_0 + \int_0^T e^{-a(T-s)}\theta(s)ds - \frac{\sigma^2}{2a^2}\left(1 - e^{-aT}\right)^2. \tag{6.28}$$

This equation can be solved $\forall T > 0$ by using the substitution:

$$F(0,T) = x(T) - g(T), \tag{6.29}$$

where $x(T)$, $g(T)$ are given by:

$$\begin{aligned} x'(T) &= -ax(t) + \theta(t), \quad x(0) = r(0) \\ g(t) &= \frac{\sigma^2}{2a^2}\left(1 - e^{-at}\right)^2 = \frac{\sigma^2}{2}B^2(0,t). \end{aligned} \tag{6.30}$$

This yields an expression for $\theta(T)$:

$$\theta(T) = F_T(0,T) + g_T(T) + a\left(F(0,T) + g(T)\right), \tag{6.31}$$

which by substitution and re-arrangement of formulae yields

$$\theta(T) = F_T(0,T) + aF(0,T) + \frac{\sigma^2}{2a}\left(1 - e^{-2aT}\right). \tag{6.32}$$

The equation in Eq 6.32 is of particular importance, being a suitable candidate to calibrate a default intensity term structure and is discussed in further detail in Section 9.5. By defining θ in this manner under a fixed a and σ, it is possible to obtain the bond prices under the Hull-White model as [12]:

$$P(t,T) = \frac{P^*(0,T)}{P^*(0,t)} \exp\left\{B(t,T)F(0,T) - \frac{\sigma^2}{4a}B(0,T)^2\left(1 - e^{-2at}\right) - B(t,T)r_t\right\}, \tag{6.33}$$

where $P^*(\cdot)$ corresponds to the risk-free bond prices. Moreover, a more formal derivation of Eq 6.33 is outlined in [13]. Most importantly, this provides a framework for constructing a

tree modelling the expiry of the underlying option. The end nodes of this tree can be priced analytically and one should use Eq 6.34.

$$\begin{aligned}
\hat{P}(t,T) &= \hat{A}(t,T)e^{-\hat{B}(t,T)R}, \\
\hat{B}(t,T) &= \frac{B(t,T)}{B(t,t+\Delta t)}\Delta t, \\
\ln \hat{A}(t,T) &= \ln \frac{P(0,T)}{P(0,t)} - \frac{B(t,T)}{B(t,t+\Delta t)} \ln \frac{P(0,t+\Delta t)}{P(0,t)}, \\
&\quad - \frac{\sigma^2}{4a}\left(1-e^{-2at}\right) B(t,T)[B(t,T)-B(t,t+\Delta t)].
\end{aligned} \tag{6.34}$$

Eq 6.34 provides the framework for pricing the nodes of the embedded European option at option expiry.

6.2.2 Closed-Form Solution

There is one further analytical solution available when pricing European options on zero-coupon bonds. Call (Π_c) and put (Π_p) options with a maturity T, on a zero-coupon bond maturing at time s, where $s > T$ can be expressed as:

$$\Pi^B = \begin{cases} LP(0,s)N(h) - KP(0,T)N(h-\sigma_p), & \Pi_c \\ KP(0,T)N(-h+\sigma_p) - LP(0,s)N(-h), & \Pi_p, \end{cases} \tag{6.35}$$

where L, K are the principal and strike price, and $N(\cdot)$ is a standard normal distribution respectively. Additionally, h and σ_p under the Hull-White one-factor model can be represented as:

$$\begin{aligned}
h &= \frac{1}{\sigma_p} \ln\left(\frac{LP(0,s)}{P(0,T)K}\right) + \frac{\sigma_p}{2}, \\
\sigma_p &= \frac{\sigma}{a}\left[1-e^{-a(s-T)}\right]\sqrt{\frac{1-e^{-2aT}}{2a}}, \quad s > T.
\end{aligned} \tag{6.36}$$

It is thus possible to price European options in Zero-Coupon Bonds in three different ways: analytically using Eq 6.35, by creating a tree which matures at option expiry and setting the end nodes using the analytical expression in Eq 6.34 or finally to create a tree maturing at the bonds expiry, to set the price of the end nodes to par, to discount through the tree and to update the payoff of the nodes at the relevant strike date. This procedure is illustrated in Fig 6.3.

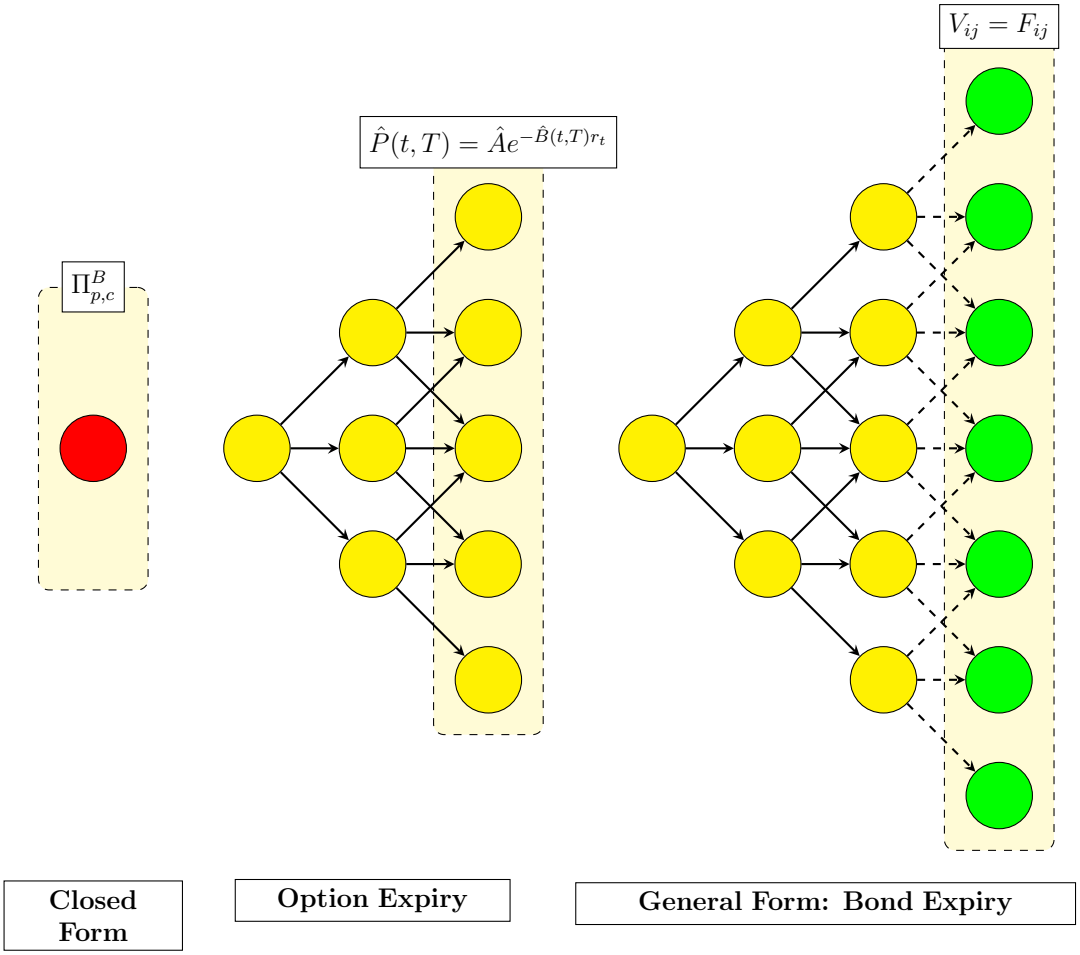

Figure 6.3: Illustration of pricing possibilities in European Zero-coupon bonds.

The third case is the most general and is necessary when pricing American options, where no closed form solution is available. The three methods were implemented and the results are illustrated in Tab 6.2.

Table 6.2: Analytical calculations and estimations based on the three available pricing mechanisms available in pricing of European Options under the Hull-White model.

	Call			**Put**		
Steps	Closed Form	Option Expiry	Bond Expiry	Closed Form	Option Expiry	Bond Expiry
10	1.0537	1.1166	0.8045	1.8093	1.8658	2.7750
50	1.0537	1.0550	0.8868	1.8093	1.8093	2.1309
100	1.0537	1.0595	1.0103	1.8093	1.8144	1.8883
200	1.0537	1.0545	1.0109	1.8093	1.8097	1.8888
500	1.0537	1.0538	1.0356	1.8092	1.8092	1.8401
1000	1.0537	1.0542	1.0505	1.8093	1.8097	1.8183

As can be seen, the closed form expression is independent of the number of steps. As the number of steps increases ($\Delta t \to 0$), both the option and bond expiry converge to the theoretical closed form expression, in the case of European Call/Put options on zero-coupon bonds. It is interesting to note that the option expiry based tree converges faster than the bond expiry counterpart. That being said, the time complexity of both trees is minimal in the one-factor short rate model. The relative error, between the theoretical closed form solution and the tree estimates are illustrated in Fig 6.4.

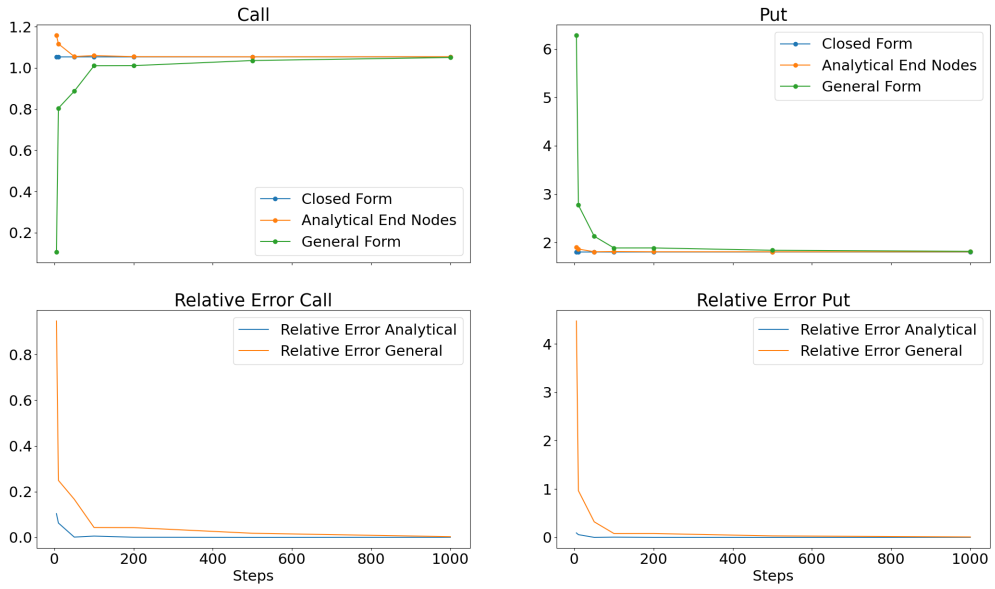

Figure 6.4: Convergence relations of pricing a European Call/Put bond option using the three available pricing methods.

An example tree, modeling the price of option expiry based on the data provided in Appendix A is illustrated for 10 time steps in Fig 6.5.

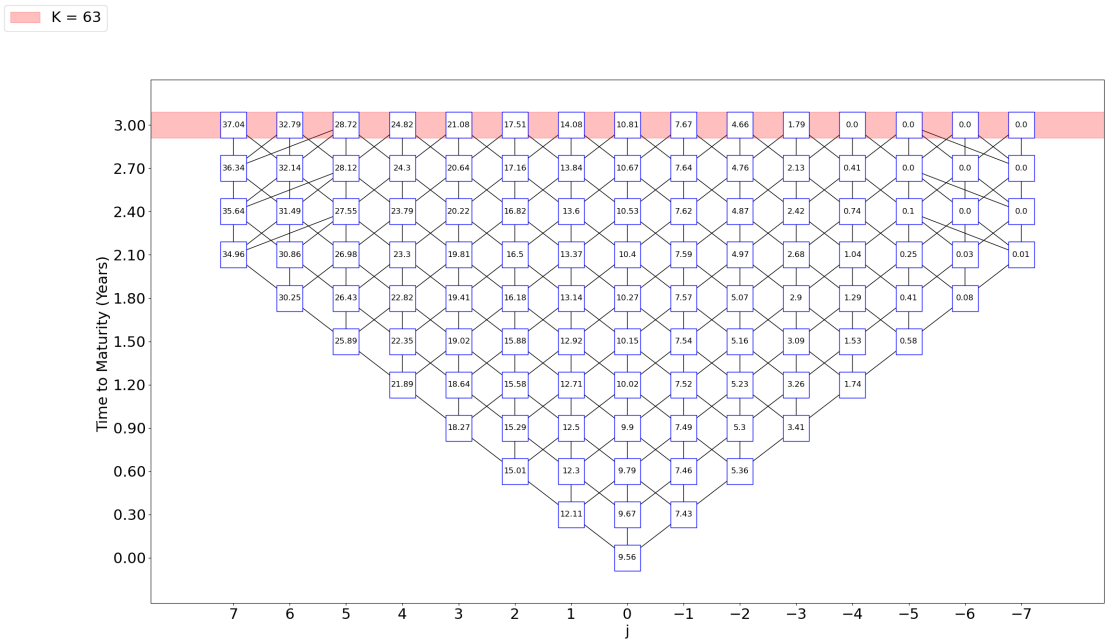

Figure 6.5: Analysis of analytical Prices from Hull-White one-factor short rate model.

6.3 Coupon Bearing Bonds

Now that it has been established on how to price zero-coupon bonds with various procedures, the goal becomes to extend these models to incorporate both coupons and payoffs from exercising options in a more general setting. This can be achieved using any of the aforementioned procedures. Though it is possible to build a tree for each of the option expiry's, it is preferable

to make use of the closed form solution in Eq 6.35 or by using the general form and modeling a tree expiring at bond maturity.

6.3.1 Jamshidian Procedure

The first solution is of theoretical importance. To start, one considers a coupon-bearing bond with an embedded European call option with strike price K and maturity T. Furthermore, assume there are a total of N payable cash flows after the expiration of the option. Consider one of these cash flows, denoted c_i at time s_i, where $s_i \geq T$ and $1 \leq i \leq N$. Additionally, let r_K denote the short rate r of the coupon-bearing bond equaling the strike price K at time T and K_i the value of a zero-coupon bond paying \$1 at time s_i, maturing at time T. The payoff of this embedded option can be expressed as:

$$\max \left[0, \sum_{i=1}^{n} c_i P(T, s_i) - K \right], \tag{6.37}$$

where $P(T, s_i)$ corresponds to the price of a zero-coupon bond at time T, paying \$1 at time s_i [14]. Due to the inverse relationship between rates and bond prices, increasing functions of r lead to a decrease in bond prices. As a result, a coupon-bearing bond will be worth more than K at time T and be exercised, iff $r < r_K$. Additionally, an analogous statement holds true for the zero-coupon bond maturity at time s_i, which is similarly worth more than $c_i K_i$ at time T. Thus, the payoff of the option in Eq 6.37 can be expressed as:

$$\sum_{i=1}^{N} c_i \max \left[0, P(T, s_i) - K_i \right], \tag{6.38}$$

which is denoted the Jamshidian procedure [14]. Thus, the European coupon bearing option can be considered as the sum of N options on underlying zero-coupon bonds. The procedure can be summarized by first determining r_k using popular root solving algorithms such as Newton-Raphson as illustrated in Eq 6.39 and adding up the prices of the associated zero-coupon bonds. This same procedure is not unique to the Hull-White model but can be applied to similar one-factor short rate models such as Ho-Lee, Vasicek and Cox-Ingersoll-Ross (CIR). Of particular note is the pricing of swaptions, where the Jamshidian procedure is similarly applicable and is discussed in more detail in Section 9.2. The interest rate r_k can be determined as:

$$r_k = \sum_{i=1}^{N} L_i \hat{P}(t, t_i), \tag{6.39}$$

where L_i is the coupon payment and/or principal payable at time i. This procedure was implemented for the data provided in Appendix A and the results are illustrated in Tab 6.3.

Table 6.3: Pricing of a European Coupon Bearing Bond using the Jamshidian procedure as a linear combination of N coupon-bearing bonds.

Jamshidian Option Procedure								
$r_k = 0.1634$								
K_i	$\boldsymbol{t}$	$\boldsymbol{t}_i$	$\boldsymbol{L}_i$	$\hat{\boldsymbol{A}}(0,t_i)$	$\mathbf{B}(0,t_i)$	$\boldsymbol{\sigma}_p$	$\boldsymbol{h}$	**price**
4.2694	3	4	5	0.9976	0.9516	0.0142	7.5600	0.4189
3.6826	3	5	5	0.9904	1.8127	0.0272	7.5730	0.7243
3.2057	3	6	5	0.9793	2.5918	0.0389	7.5847	0.9449
2.8139	3	7	5	0.9645	3.2968	0.0495	7.5953	1.1015
2.4887	3	8	5	0.9468	3.9347	0.0591	7.6049	1.2096
46.5397	3	9	105	0.9265	4.5119	0.0678	7.6135	26.8939
							Total	**31.2931**

6.3.2 Backward Branching

In an alternative procedure to incorporating coupons, one makes use of the aforementioned general form lattice tree. In this method, one must simply update the prices of the nodes on coupon payment dates. This can be achieved by manipulating Eq 6.40 to obtain the following:

$$V(i,j) = \sum_{j}^{v} q(k,j)[V(i+1,j) + \mathbb{1}_C(C_i)]e^{-r(i,j)\Delta t}, \quad v = \min(i, 2j_{max}+1), \tag{6.40}$$

where $\mathbb{1}_C(C_i)$ represent the coupons during time-steps where a coupon is payable. From a practical point of view, for coupons and/or strike prices, it may be difficult to ensure that the discretized time points fall exactly on the payment/strike dates when Δt is high. In the case of coupons, this can be rectified by minimising the euclidean distance between the generated date/index and the true coupon date, i.e. by choosing the $\hat{t}_c$ which is the closest to the true date and to add the coupon to that date instead (Fig 6.6). Naturally, as one increases the number of time steps, the estimated coupon time $\hat{t}_c$ will converge to the true value t_c.

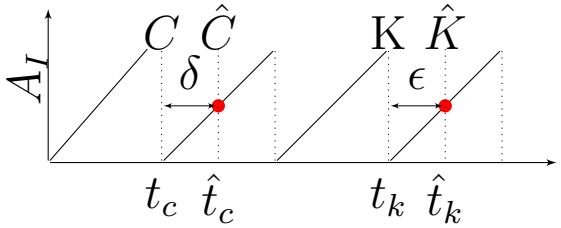

Figure 6.6: Incorporating coupons and strike prices into the tree pricing procedure.

The strike prices are more complicated due to the accrued interest which needs to be taken into account when modeling coupon bearing bonds. To compensate for this, as in the case of coupon dates, one selects the strike date ($K_{\hat{t}}$) which is closest to the true strike date (K_t). Additionally, one must calculate the accrued interest (I_A) and add it to the quoted strike price where $\hat{K} = K + I_A(n\Delta t)$. This is true in general if strike dates do not fall on coupon payment dates. It is of course possible to include the accrued interest to the coupon payment dates for

additional accuracy. This procedure can be circumvented to match exact payment/strike dates by constructing trees discussed in Section 7.2.

6.4 Early Exercise

In the case of European or American options, one must take into account the value of early exercise when back-propagating through the nodes. This can be achieved in a number of ways. One method is to value a non-callable bond from maturity until the price date. Then, one identifies the last possible time point/index where early exercise is possible and to re-iterate from this index to the root node (or last possible exercise date). In the case of European call options, the value of early exercise at a given time step for a particular set of nodes is simply

$$V(i,j) = \max(V(i,j) - K, 0). \tag{6.41}$$

American options are more complicated and require an additional step. As before, one must first calculate the value of early exercise on strike dates. In addition to this, it is at the discretion of the issuer of the bond to exercise their right to call/put the option. The issuer, in an attempt to maximise their value, will hope to wait until the optimal date to exercise this right. Let $C^{t_i}(V_{i,j})$ and $h^{t_i}(V_{i,j})$ denote the value of holding on to the option and the payoff at time t_i. Additionally, let t^* denote the optimal stopping time within the interval $[t_{i+1}, .., t_N]$. This value of continuation, denoted the continuation value can thus be expressed as:

$$C^{t_i}(V_{i,j}) = E^Q\left[e^{-r(t^*-t)}h(\cdot)\middle|V_{i,j}^{t_i}\right]. \tag{6.42}$$

Thus, the payoffs from early exercise for each respective nodes must be compared to the continuation value and the maximum is chosen as illustrated in Eq 6.43.

$$V^t(i,j) = \max\left(C^t(V(i,j)), \max\left(V^t(i,j) - K_t, 0\right)\right). \tag{6.43}$$

For the sake of completeness, Bermudan options are a more constrained form of their American counterpart and must similarly be priced under these conditions. It is now possible to price a variety of credit derivatives with European, Bermudan and American optionality features using a one-factor trinomial tree. A summary of the entire process is illustrated in Fig 6.7.

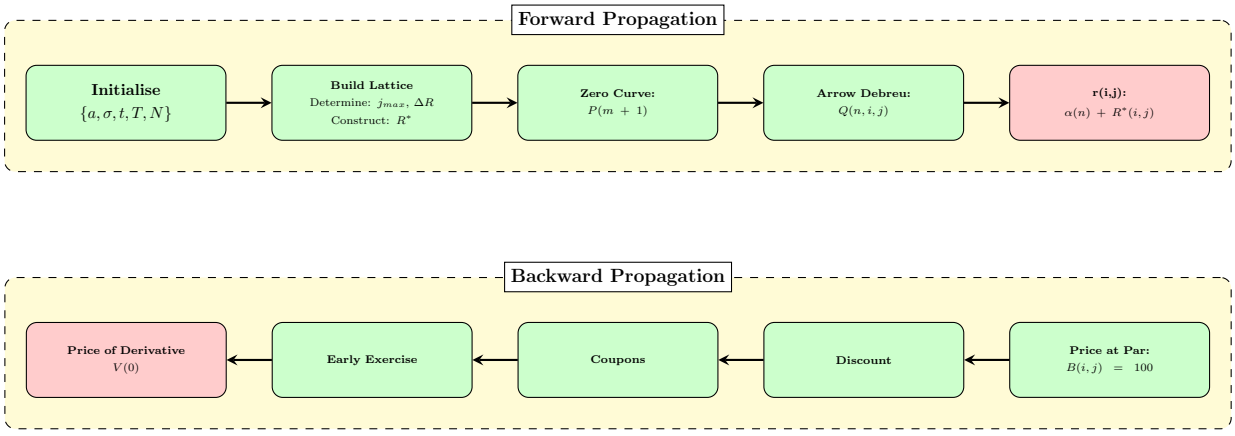

Figure 6.7: Illustration of the Forward and Backward propagation steps in the one-factor Hull-White model to price coupon bearing callable bonds.

6.4.1 Implementation

Now that the possible pricing strategies have been outlined, the one-factor trinomial tree can be fully implemented for a range of chosen time steps. Using the provided reference data from Appendix A, the general form tree is constructed and the results are illustrated in Tab 6.4.

Table 6.4: Pricing of chosen option types for a range of time steps. The Bermudan example had strike prices and strike dates at $K_i = [63, 64, 65]$ at $t_i = [3, 2, 1]$ years.

Steps	ZCB	European	Bermudan	American
10	63.7628	31.9154	31.9154	37.4906
50	63.7628	31.2640	31.264	39.1195
100	63.7628	31.3539	31.3539	39.0029
200	63.7628	31.2775	31.2775	39.0732
500	63.7628	31.2900	31.2900	39.1686

It is noted that the zero-coupon-bond is stable throughout the number of time steps, as it can be calculated numerically using Eq 2.1. Furthermore, the American, European and Bermudan options converge with a relatively few number of time steps.

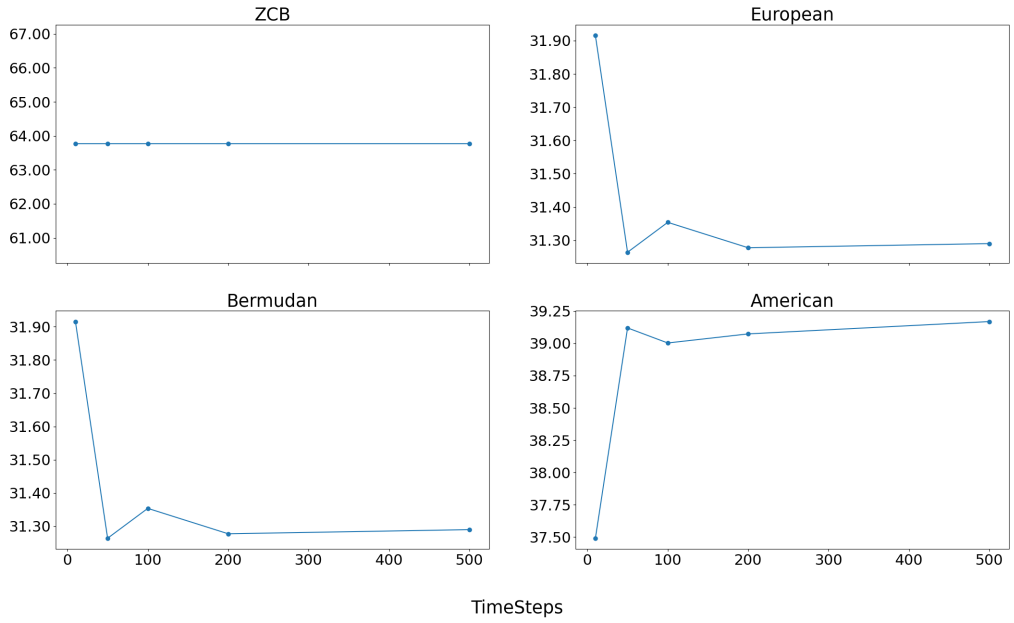

Figure 6.8: Convergence relations between the pricing of various credit derivative instruments using a two-dimensional trinomial tree.

6.4.2 Parameter Sensitivity

As it has been established how to price derivatives using a generalised trinomial tree framework under the Hull-White model, one must now contend with the influence of the calibration parameters which are required as input to the model. A calibration procedure is outlined in Section 9.2. A series of trees were constructed for pricing European and American options, freeing one parameter with the other held fixed. Moreover, a surface freeing both parameters is constructed and illustrated in Fig 6.10.

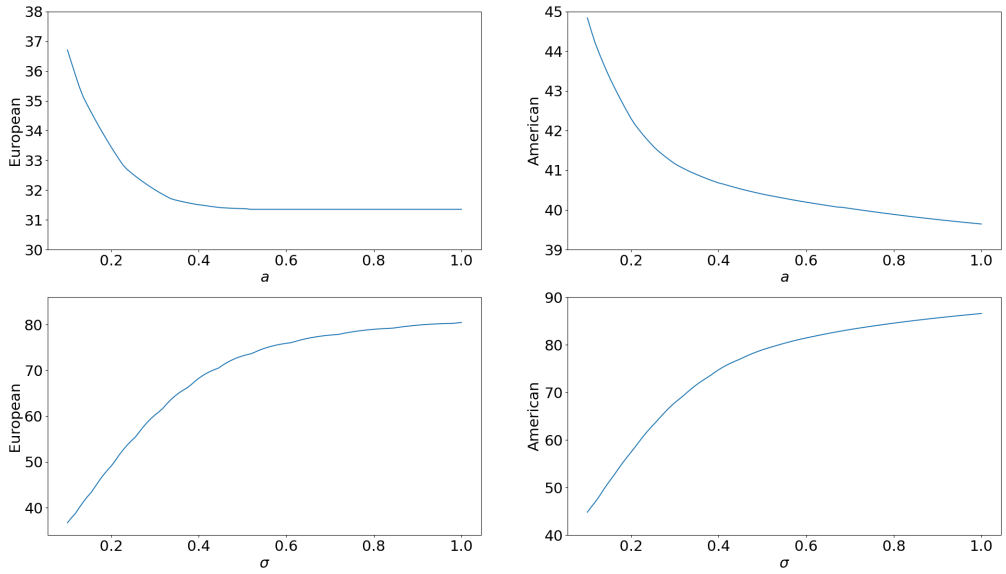

Figure 6.9: Sensitivity of the Hull-White One-Factor model bond prices to variations in the calibration parameters constructing a tree consisting of 50 time steps. When σ is varying, $a = 0.1$ and $\sigma = 0.01$ when a is varying.

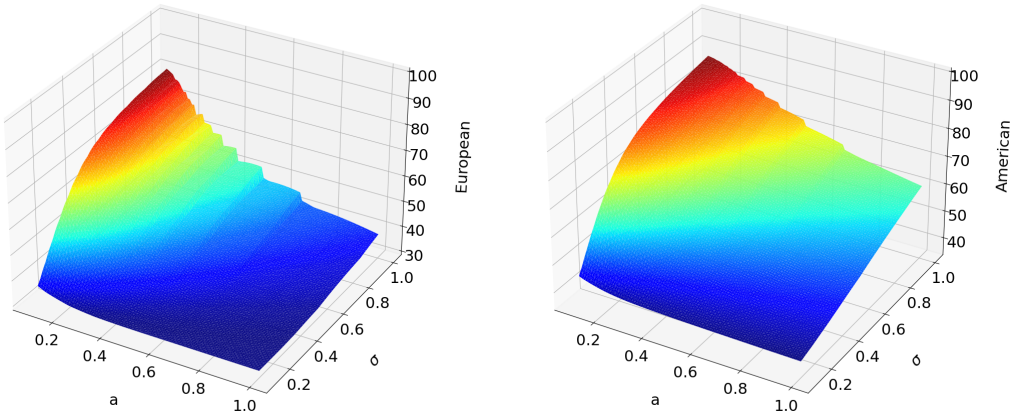

Figure 6.10: Sensitivity of European and American option prices to variation of the calibration parameters over 50 time steps.

7 One-Factor Model Extensions

In this family of affine term-structure models, the following sections will showcase the large amount of freedom one has to tweak the modeling framework based on the modelers' needs. The methodology is starkly similar, where one needs to ensure that the probability branching matches the correct moments. In doing so, tree construction is possible and not limited to pricing of embedded bonds and is particularly feasible for the matching of volatilities. Each proposed model comes with practical considerations, both from a mathematical as well as implementation perspective.

7.1 Black-Karasinski Model

To start, the proposed model can be generalised to include different functions of the short rate. This is the simplest extension whose process is almost identical to the implementation procedure in construction of the Hull-White model. This can be expressed as:

$$df(r) = [\theta(t) - a(t)f(r)]dt + \sigma(t)dW_t. \tag{7.1}$$

The original Hull-White model is returned when $f(r) = r$, and a and σ are constant [7]. The Black-Karasinski model is another historically popular model of choice where $f(r) = \ln(r)$, due to the model prohibiting the ability of the short-rate to become negative. The forward propagation procedure is analagous to it's Hull-White relative, apart from one notable exception, the shift α_m required in Eq 6.14 to match the term structure needs to be solved numerically. Let $x = f(r)$ and $g = f^{-1}(r) = e^x$. In this case, the short rate can be expressed as:

$$dx = [\theta(t) - a(t)x]dt + \sigma(t)dW_t. \tag{7.2}$$

Additionally, the bond prices can be illustrated as:

$$P_{m+1} = \sum_{j=-n_m}^{n_m} Q_{m,j} \exp[-g\left(\alpha_m + j\Delta r\right)\Delta t]. \tag{7.3}$$

The desired α_m can thus be determined numerically using a desired root solving algorithm by solving:

$$h(\alpha) = P_{m+1}\left(\alpha\right) - P^*_{m+1} = 0, \tag{7.4}$$

where P^* denotes the bond prices obtained from the chosen term structure. This procedure is not limited to the Black-Karasinski model and is applicable to a host of affine term structure models. One notable exception is the extended-CIR model, whose $\sigma\sqrt{r}$ leads to imaginary volatilities when r is small [15].

7.2 General Hull-White Model with Non-constant Δt

It is possible to take the methodology a few steps further. In a more general case, one begins by defining a function g which satisfies the following equation:

$$dg = [\theta(t) - a(t)g(t)]dt. \tag{7.5}$$

Additionally, let $x(r, t)$:

$$x(r, t) = f(r) - g(t). \tag{7.6}$$

As before, the diffusion process for $x(\cdot)$ is analagous to that of R^* in Eq 6.4 where,

$$\begin{aligned} dx &= [\theta(t) - a(t)f(r)]\,dt + \sigma(t)dW_t - [\theta(t) - a(t)g(t)]\,dt \\ &= -a(t)\left[f(r) - g(t)\right]dt + \sigma(t)dW_t \\ &= -a(t)xdt + \sigma(t)dW_t. \end{aligned} \tag{7.7}$$

Choose g such that $x(r, 0) = 0$. In doing so, the process is mean reverting to zero, where the unconditional expected value of $\mathbb{E}(x(\cdot)) = 0\ \forall t > 0$ [10]. The tree can now be constructed under similar procedures as outlined in the previous sections. This is an apt opportunity to introduce the spacing of tree nodes in the time dimension. These spacings may be arbitrary and at the discretion of the user, as long as the following constraint is satisfied:

$$\Delta x_i = \sigma(t_{i-1})\sqrt{3(\Delta t_i)}, \quad \Delta t_i = t_i - t_{i-1}. \tag{7.8}$$

By varying the node relations as in Eq 7.8, the branching probabilities for this process $x(\cdot)$ will need to be updated accordingly. As before, the branching probabilities will need to be matched to the expectation and variance. Consider a particular node $j\Delta x_i$, at time step i. Let

$$\begin{aligned} p_u &= (k+1)\Delta x_{i+1}, \\ p_m &= k\Delta x_{i+1}, \\ p_d &= (k-1)\Delta x_{i+1}, \end{aligned} \tag{7.9}$$

denote the probabilities of branching to the nodes upward, standard and downward at time $i+1$ for an integer k. Let

$$\begin{aligned} \mathbb{E}(dx) &= M, \\ \mathbb{E}(dx^2) &= V + M^2. \end{aligned} \tag{7.10}$$

The probabilities are matched as

$$\begin{aligned} j\Delta x_i + M &= k\Delta x_{i+1} + (p_u - p_d)\Delta x_{i+1}, \\ V + (j\Delta x_i + M)^2 &= k^2(\Delta x_{i+1})^2 + 2k(p_u - p_d)(\Delta x_{i+1})^2 + (p_u - p_d)k^2(\Delta x_{i+1})^2. \end{aligned} \tag{7.11}$$

The solution to these equations yield:

$$\begin{aligned} p_u &= \frac{V}{2\Delta x_{i+1}^2} + \frac{\epsilon^2 + \epsilon}{2} \\ p_m &= 1 - \frac{V}{\Delta x_{i+1}^2} - \epsilon^2 \\ p_d &= \frac{V}{2\Delta x_{i+1}^2} + \frac{\epsilon^2 - \epsilon}{2}, \end{aligned} \tag{7.12}$$

where ϵ can be considered as the distance between the expected value of x and the central branching node and is illustrated as:

$$\epsilon = \frac{j\Delta x_i + M - k\Delta x_{i+1}}{\Delta x_{i+1}}. \tag{7.13}$$

By defining

$$\begin{aligned} V &= \sigma^2(t_i)\left(t_{i+1} - t_i\right), \\ M &= -a(t_i)(t_{i+1} - t_i), \\ \Delta x_{i+1} &= \sigma(t_i)\sqrt{3(t_{i+1} - t_i)}, \end{aligned} \tag{7.14}$$

the branching probabilities will be non-negative if the boundary condition of $-\sqrt{\frac{2}{3}} < \epsilon < \sqrt{\frac{2}{3}}$ is satisfied [10]. Note that under this construction, one would require an additional time step beyond the region of interest. It seems reasonable to base this additional Δt_i as a function of the coupon payment frequency. Furthermore, in this setting it is desirable to choose the central node of the successive nodes such that the chosen node is within $\sqrt{\frac{2}{3}}\Delta x_{i+1}$ of the expected outcome. In doing so, this criteria can be satisfied by choosing a k (to the nearest integer) whereby:

$$k = \left[\frac{j\Delta x_i + M}{\Delta x_{i+1}}\right]. \tag{7.15}$$

Defining k in this manner ensures that we are always within $\Delta x_{i+1}/2$ of the expected outcome and non-negative probabilities are ensured. By defining the procedure in this manner, it is also

possible to prune the tree at every time step. In contrast to the constant Δt approach, the time varying tree does not converge in the same manner, yet can grow and shrink at each time step. The size of the tree at the next iteration $(i+1)$ is dependent on the extreme nodes of the previous time step i. The size of the tree is thus depicted as

$$\begin{aligned} j_{min}(i+1) &= \min_j(k_j) - 1, \\ j_{max}(i+1) &= \max_j(k_j) + 1. \end{aligned} \tag{7.16}$$

To illustrate this, let us consider a basic example provided in Tab 7.1. One starts by defining the time steps of interest. From here, the construction procedure follows Fig 7.1.

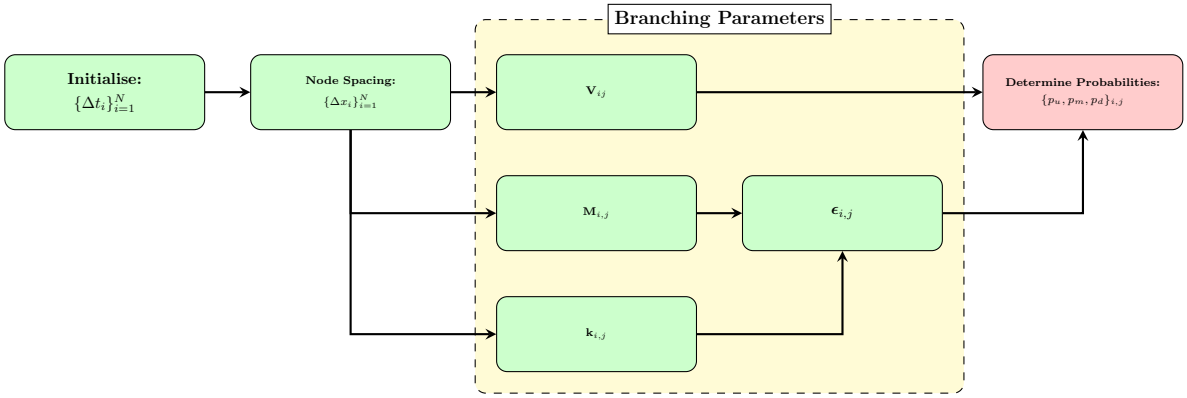

Figure 7.1: Illustration of the probability determination procedure for a non-constant Δt.

Table 7.1: Tree branching parameters obtained for the pre-selected chosen time steps.

t_i	0	1.5	1.6	2
Δx_i	-	0.6364	0.1643	0.3286

Under these specifications, the tree-branching calculations can be performed whereby $a = 1$ and $\sigma = 0.3$. The results are illustrated in Tab 7.2.

Table 7.2: Determination of Branching Parameters based on a selection of chosen time steps.

t	**x**	**M**	**V**	**k**	ϵ	p_u	p_m	p_d
0	0	0	0.135	0	0	0.1667	0.6667	0.1667
1.5	0.6364	-0.0636	0.009	3	0.4857	0.5275	0.4308	0.0418
1.5	0	0	0.009	0	0	0.1667	0.6667	0.1667
1.5	-0.6364	0.0636	0.009	-3	-0.4857	0.0418	0.4308	0.5275
1.6	0.6573	-0.2629	0.036	1	0.2	0.2867	0.6267	0.0867
1.6	0.493	-0.1972	0.036	1	-0.1	0.1217	0.6567	0.2217
1.6	0.3286	-0.1315	0.036	1	-0.4	0.0467	0.5067	0.4467
1.6	0.1643	-0.0657	0.036	0	0.3	0.3617	0.5767	0.0617
1.6	0	0	0.036	0	0	0.1667	0.6667	0.1667
1.6	-0.1643	0.0657	0.036	0	-0.3	0.0617	0.5767	0.3617
1.6	-0.3286	0.1315	0.036	-1	0.4	0.4467	0.5067	0.0467
1.6	-0.493	0.1972	0.036	-1	0.1	0.2217	0.6567	0.1217
1.6	-0.6573	0.2629	0.036	-1	-0.2	0.0867	0.6267	0.2867

Additionally, Fig 7.2 illustrates the schematic of a trinomial tree with unequal time steps. Note that the provided example is designed under extreme conditions, though the construction under these specifications remains to hold.

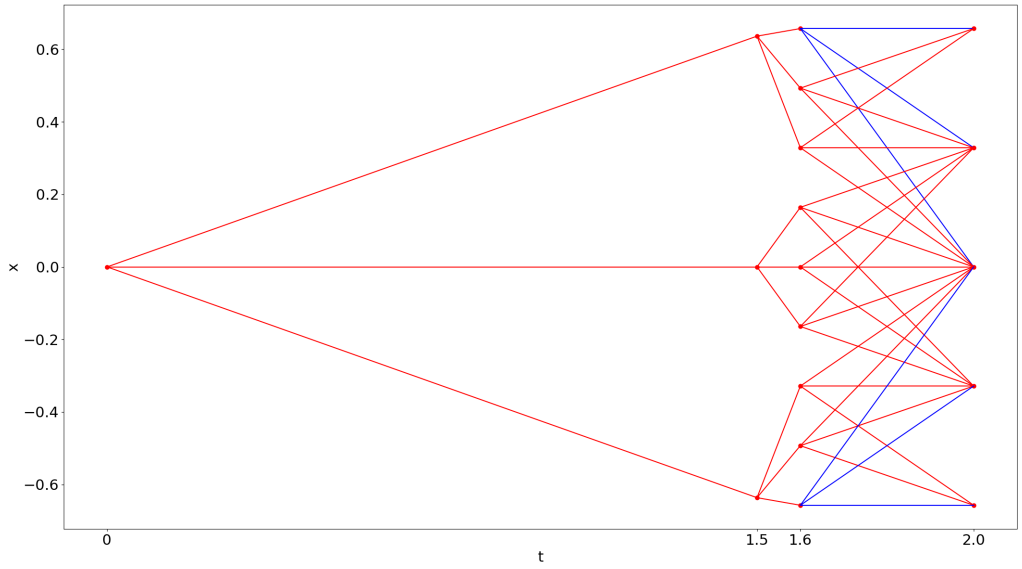

Figure 7.2: Constructing a short-rate tree for varying time steps Δt_i.

The final step in this generalization procedure involves the determination of the function $g(t)$. Note that $g(t)$ is a function of $\theta(t)$ and is attempting to correctly price discounted bonds at different maturities, by fitting the term structure. Thus, $g(t)$ is obtained by computing and matching the values obtained by matching the following

$$\begin{aligned} P_{i+1} &= \sum_j Q_{i,j} \exp[-r_{i,j}\Delta t_i] \\ &= \sum_j Q_{i,j} \exp\left[-f^{-1}\left(x_{i,j} + g_i\right)\Delta t_i\right], \end{aligned} \tag{7.17}$$

to the discount bond prices obtained from the term structure. This involves a Newton-Raphson (or alternative root solving) process. Under the example provided $g(t)$ can be evaluated for each time step as:

Table 7.3: Determination the calibration component required for the calculation of the short rate r.

g(t)	-2.9957	-2.7851	-2.8956	-2.9364

Analogous to the calculation of $\alpha(t)$, the short rate $r_{i,j}$ can be determined for each node by solving:

$$r_{i,j} = f^{-1}\left(x_{i,j} + g(i)\right). \tag{7.18}$$

7.3 Generalising the Drift: A robust compromise

There a number of ways the drift and volatility structures can be modified, and a one-factor short rate tree can be constructed. The generalisation procedures are outlined in the coming

sections. The most recent Hull paper [10] defines a process of the form:

$$dx = [\theta(t) + G(x,t)]dt + \sigma dW_t, \tag{7.19}$$

where $x = f(r)$. This procedure may be a better alternative to the proposal outlined in Section 7.4, especially if equations are of the form in Eq 7.19. This is due to the fact that this process is more robust and easier to implement than the proposal suggested. In contrast, the modeling procedure outlined therein is less general and not applicable to certain frameworks. In either case, it does bode a suitable alternative based on a modelers needs. As in the modelling procedure of other tree based methods, it is necessary to determine the branching procedure for any node (i, j). Denote the root of the tree $x_{0,0} = f(R_0)$, the Δt period rate at time zero. In contrast to alternative models, the reversion rate is not constant in this structure. As a result, the tree is not necessary symmetrical about it's center. Let ϕ_i be the expected value of x at time $i\Delta t$ conditional of having been at node $i-1, 0$ at the previous time step $(i-1)\Delta t$. Thus,

$$x_{i,j} = \phi_i + j\Delta x. \tag{7.20}$$

In contrast to the conventional models, constructing this tree is a two-step procedure. One assumes the center of the tree at the next iteration is the same as the tree in the previous iteration. In doing so, the branching pattern can be determined. As one assumes that $\theta(i\Delta t) = -G_{i,0}$, the conditional expectation of x can be expressed as:

$$E_{i,j} = \phi_i + j\Delta x + (G_{i,j} - G_{i,0})\Delta t. \tag{7.21}$$

Denote the index of the center of these nodes, with corresponding branching probabilities at time i as $k_{i,j}$. These k-values are chosen to ensure they are closest to the expected value $E_{i,j}$. With this minimisation, k can be expressed as:

$$k_{i,j} = \left\lfloor j + \frac{(G_{i,j} - G_{i,0})\,\Delta t}{\Delta x} + \frac{1}{2} \right\rfloor. \tag{7.22}$$

Furthermore let,

$$y_{i,j} = \left\lfloor j + \frac{(G_{i,j} - G_{i,0})\,\Delta t}{\Delta x} - k_{i,j} \right\rfloor. \tag{7.23}$$

It is now possible to construct the branching probabilities with the desired mean and variance of $E_{i,j}$ and $\sigma^2\Delta t$, respectively. The probabilities are thus expressed as:

$$\begin{aligned} p_u &= \frac{1}{6} + \frac{1}{2}\left(y^2 + y\right), \\ p_m &= \frac{2}{3} - y^2, \\ p_d &= \frac{1}{6} + \frac{1}{2}\left(y^2 - y\right). \end{aligned} \tag{7.24}$$

Once $k_{i,j}$ has been determined, the size of the tree at the next iteration can be determined. Based on the specification that one wants to ensure the center of the tree is as close to the expected value as possible, choose:

$$\begin{aligned} j_{min}(i+1) &= \min_j(k_j) - 1, \\ j_{max}(i+1) &= \max_j(k_j) - 1. \end{aligned} \tag{7.25}$$

In practice, and in the examples that follow, it is possible that there are multiple maxima or minima when performing these calculations. When this occurs, determine the index of the

center of the tree and from the k index minima/maxima, choose the k value whose index is closest to that value. This completes the first stage. As before, the second stage involves the shifting of the nodes at time $(i+1)\Delta t$ to match the price of a bond at $(i+2)\Delta t$. This is achieved in the conventional manner, by first determining the Arrow-Debreu prices for each of the nodes and shifting the nodes at each time step by a value α_i. In the case of the normal mode, where $x = r$, it is possible to value α_{i+1} analytically as illustrated in Eq 7.27. More complex models require a numerical procedure. The tree is initialised by setting:

$$\begin{aligned} Q_{0,0} &= 1, \\ \alpha_0 &= \phi_0 = f^{-1}(R_0), \\ j_{min}(0) &= j_{max}(0) = 0. \end{aligned} \tag{7.26}$$

Note that $\phi_{i+1} = \phi_i + \alpha_{i+1}$. The updating equations are provided below:

$$\begin{aligned} Q_{i+1,k} &= \sum_j Q_{i,j} p(j,k) \exp\left(-f^{-1}\left(\phi_i + j\Delta x\right)\Delta t\right), \\ P_{i+2} &= \sum_j Q_{i+1,j} \exp\left(-f^{-1}\left(\phi_i + j\Delta x + \alpha_{i+1}\right)\Delta t\right), \\ \alpha_{i+1} &= \frac{1}{\Delta t}\left(\ln\left(\sum_{j=j_{min}(i+1)}^{j_{max}(i+1)} Q_{i+1,j} e^{-j\Delta x \Delta t}\right) - \ln P_{i+2}\right) - \phi_i. \end{aligned} \tag{7.27}$$

7.3.1 Implementation: Thoughts and Advantages

The following sections in Section 7.3.2 and Section 7.3.3 attempt to illustrate the tree implementation over a set of functions G. The parameters utilised, as well as a more challenging term structure in the sections below are provided in Appendix C. Moreover, this allows the implementation of a time varying reversion factor, which may be suitable based on a complicated term structure. Additionally, it outlines the importance of choosing a suitable drift function and how it can be used to tackle the presence of negative interest rates. Furthermore, the outlined methodology outlines how with a single tree, one can convert the risk-neutral probabilities to real-world probabilities with a market price of risk adjustment. This is of particular importance due to increased regulations on financial institutions, where it is often necessary to consider processes in both the risk neutral and real world [10]. A summary of the methodology is illustrated in Fig 7.3.

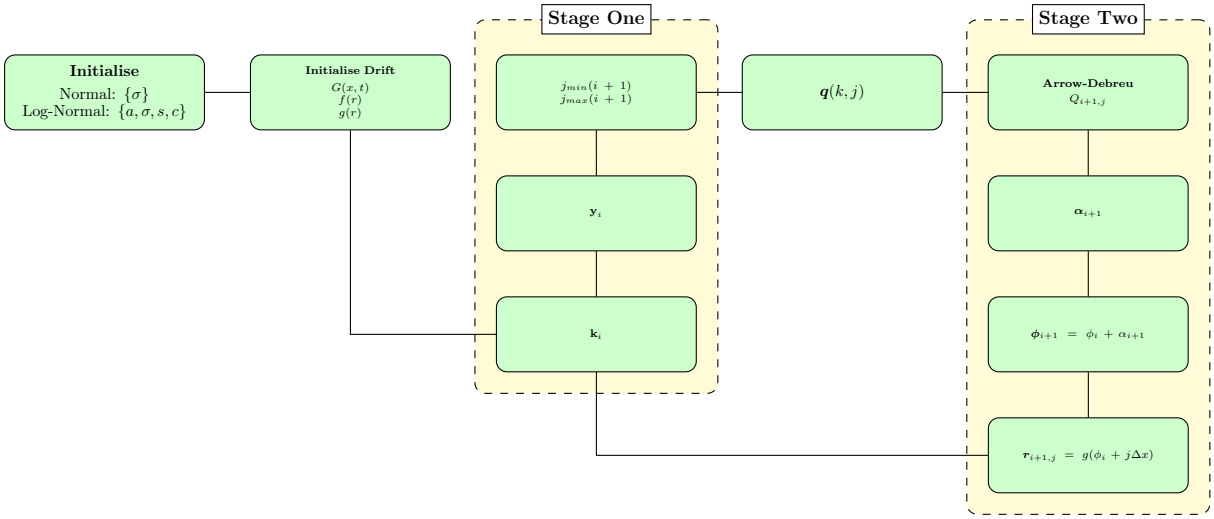

Figure 7.3: Summary of the updating procedure for constructing a tree from a diffusion process containing a generalised drift.

7.3.2 Normal Model

Let $x = f(r) = r$. Set G as in Eq 7.28 and $g = f^{-1}(r) = r$. With this setup, we ensure that interest rates are prohibited to go below -1%. The data provided consists of a term structure of interest rates in Euro from 01/03/2016. The full term structure is provided in Appendix C. The tree was implemented and the tree structure is visualisable in Fig 7.4. Additionally, the construction and evaluation of the first nodes in the tree is illustrated in Tab 7.4.

$$G(x,t) = \begin{cases} 0.02 & x < -0.01 \\ 0 & x \geq 0.01. \end{cases} \tag{7.28}$$

Table 7.4: Tree Generation for first three time steps of the Normal Model.

Normal Model								
i	**0**	**1**			**2**			
j	**0**	**-1**	**0**	**1**	**-1**	**0**	**1**	**2**
k	0	0	0	1	0	0	1	2
y	0	-0.4227	0	0	-0.4227	0	0	0
$\boldsymbol{p}_u$	0.1667	0.0447	0.1667	0.1667	0.0447	0.1667	0.166667	0.1667
$\boldsymbol{p}_m$	0.6667	0.4880	0.6667	0.6667	0.4880	0.6667	0.666667	0.6667
$\boldsymbol{p}_d$	0.1667	0.4673	0.1667	0.1667	0.4673	0.1667	0.1667	0.1667
Q	1	0.1668	0.6673	0.1668	0.1895	0.5548	0.2299	0.0278
$\boldsymbol{\phi}$	-0.0035	-0.0045			-0.0054			
$\boldsymbol{\alpha}$	-0.0035	-0.0009			-0.0001			
r	-0.0035	-0.0131	-0.0045	0.0042	-0.0141	-0.0054	0.0032	0.0119

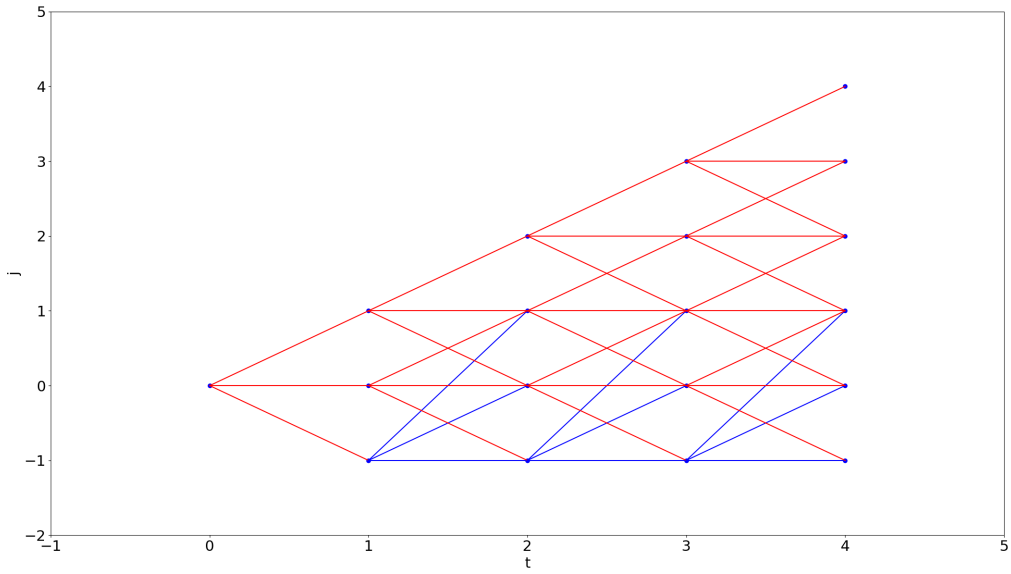

Figure 7.4: Constructing a short-rate tree for a normal model with parameter specifications as in Appendix C.

7.3.3 Lognormal Model

In a more practical setting, let $x = f(r) = \ln(r + s)$, for a fixed spread s. The addition of a constant spread allows for a lognormal model to be utilised in the presence of negative interest rates. The choice of spread is at the discretion of the user and for the purposes of this example is set to 2%. Set G as in Eq 7.29 and $g = e^r - s$. This tree was similarly implemented and visualised in Fig 7.5.

$$G(x,t) = \begin{cases} -\frac{acx}{e^x+c-s} & x < \ln(s) \\ -ax & x \geq \ln(s). \end{cases} \tag{7.29}$$

Table 7.5: Calculated parameters for the implementation of the Lognormal Model.

Lognormal Model									
i	**0**	**1**			**2**				
j	**0**	**-1**	**0**	**1**	**-2**	**-1**	**0**	**1**	**2**
k	0	-1	0	1	-1	-1	0	1	2
y	0	0.2769	0	-0.2435	-0.4137	0.2791	0	-0.246	-0.3222
$\boldsymbol{p}_u$	0.1667	0.3434	0.1667	0.0746	0.0454	0.3452	0.1667	0.0739	0.0575
$\boldsymbol{p}_m$	0.6667	0.5900	0.6667	0.6074	0.4956	0.5888	0.6667	0.6061	0.5629
$\boldsymbol{p}_d$	0.1667	0.0666	0.1667	0.3181	0.4591	0.0661	0.1667	0.3199	0.379668
Q	1	0.1668	0.6673	0.1668	0.0111	0.2100	0.5558	0.2127	0.01243
$\boldsymbol{\phi}$	-4.1062	-4.1749			-4.1934				
$\boldsymbol{\alpha}$	-0.0035	-0.0687			-0.0185				
r	-0.0035	-0.0081	-0.0046	-0.0001	-0.0110	-0.0084	-0.0049	-0.0004	0.00538

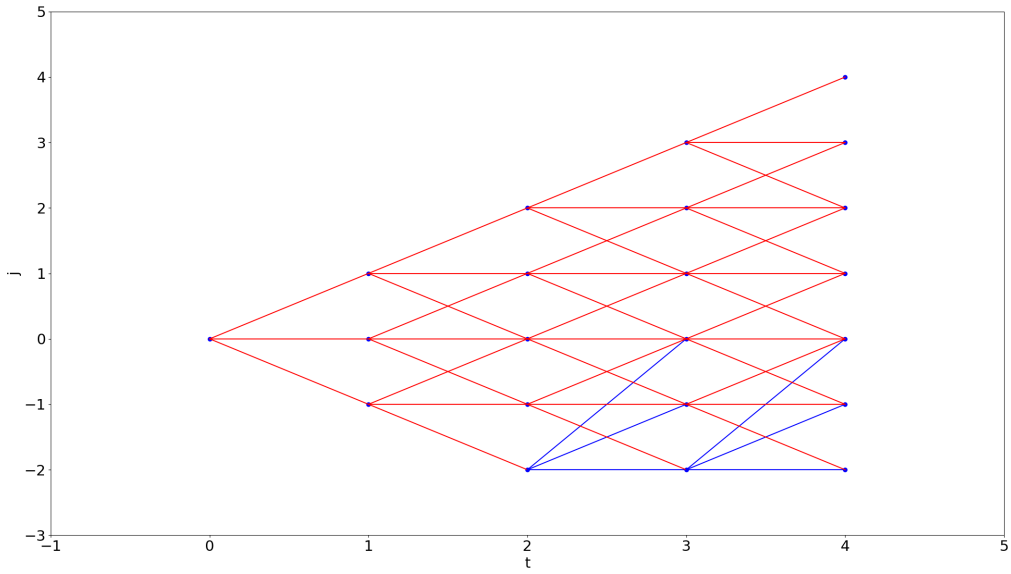

Figure 7.5: Constructing a short-rate tree for a log-normal model with parameter specifications as in Appendix C.

The construction of the drift function as in Eq 7.29 does bare some useful properties. This model can be used to determine the price of caps/floors or swaptions over different strike prices and maturities [10]. The standard market model can then be used to determine the implied volatilities associated with these prices. As stated in Section 9.2, the Black's model or Bachelier's model are suitable candidates. Note that in the presence of negative interest rates, the Black model requires the swap rate and the strike rate to be shifted by a spread s.

7.4 Generalized One-Factor Models

The following procedure outlines the most general form of one factor models illustrated in this thesis. After having dealt with a time varying drift, one can take this process a few steps further. Consider a process of the form:

$$dr = [\theta(t) + F(r)]dt + G(r)dW_t, \tag{7.30}$$

where $F(r), G(r)$ are functions which determine the drift and velocity of r respectively [4]. In this setup, $G(r)$ must be continuously differentiable whereby:

$$x = f(r) = \int \frac{dr}{G(r)}, \quad \frac{dx}{dr} = \frac{1}{G(r)}. \tag{7.31}$$

Let $H(x,t)$ be denoted as the drift of the process x, where x follows the process:

$$\begin{aligned} dx &= H(x,t)dt + dW_t, \\ H(x,t) &= \frac{\theta(t) + F(r)}{G(r)} - \frac{G'(r)}{2}, \\ r &= f^{-1}(x). \end{aligned} \tag{7.32}$$

As in all the proposals outlined previously, one begins by matching the first two moments which are denoted m_1 and m_2.

$$\begin{aligned} m_1 &= f\left(r_j + \left(\theta + F(r_j) - \frac{G(r_j)G'(r_j)}{2}\right)\Delta t\right), \\ m_2 &= \Delta t + m_1^2. \end{aligned} \tag{7.33}$$

Under this construction, it is noted that m_1 moment yields the correct first moment for x by performing a Taylor expansion of $f(r)$ in the expression for m_1 and evaluating the limit as Δt approaches zero. As m_2 is a function of m_1, the limit under this condition approaches Δt. Thus, as Δt approaches zero, the second moment is also matched. As in the previously outlined general expansions, we desire to choose a j^* which matches the central node as close as possible. Thus:

$$j^* = \left[\frac{m_1 - x_0}{\Delta x} + \frac{1}{2} \right], \tag{7.34}$$

where $\Delta x = \sqrt{3\Delta t}$. The obtained probabilities are non-negative under the following constraint:

$$m_1 - x_0 - j^* \Delta x \leq \frac{\Delta x}{2}. \tag{7.35}$$

This yields the following transition probabilities for a given node (i, j):

$$\begin{aligned} p_u &= \frac{\Delta t + (m_1 - x_0 - j^* \Delta x)^2}{2\Delta x^2} + \frac{m_1 - x_0 - j^* \Delta x}{2\Delta x}, \\ p_m &= 1 - p_u - p_d, \\ p_d &= \frac{\Delta t + (m_1 - x_0 - j^* \Delta x)^2}{2\Delta x^2} - \frac{m_1 - x_0 - j^* \Delta x}{2\Delta x}. \end{aligned} \tag{7.36}$$

As before, it is not possible to determine the short-rate analytically and requires numerical proceedings. The Arrow-Debreu prices can be obtained via:

$$\begin{aligned} Q_{i,j} &= \sum_{k=j_d(i-1)}^{j_u(i-1)} Q_{i-1,k} q(k,j) \exp(-r_k \Delta t), \\ r_k &= f^{-1}(x_0 + k\Delta x), \end{aligned} \tag{7.37}$$

where

$$P_{i+1} = \sum_{j=j_d(i)}^{j_u(i)} Q_{i-1,k} \exp(-r_j \Delta t), \tag{7.38}$$

matches the initial interest rate term structure [4]. Note that the procedure outlined assumes that the Δt is constant, but can similarly be extended using similar methodology as was previous outlined. Finally, Hull outlines that the entire procedure can be extended to models of the form:

$$dr = F(r,t)dt + G(r,t)dW_t, \tag{7.39}$$

where this dependence function $F(r,t)$ contains a suitable function to adequately fit the term structure. One ends this section by deducing that these class of models can be generalised and extended in a variety of ways to satisfy the users needs.

7.5 Hedging One-Factor Model

One concludes the discussion on two-dimensional trees by using the chosen and constructed Hull-White one-factor trinomial lattice tree to hedge a portfolio of interest rate derivatives. The sensitivity of the obtained option prices can be viewed through the lens of partial derivatives of the option prices denoted as The Greeks. The most common Greeks are Delta, Gamma, Vega, Theta and Rho and can be derived from the Black-Scholes equation illustrated in Eq 7.40.

$$\frac{\partial V}{\partial t} + \frac{1}{2}\sigma^2 S^2 \frac{\partial^2 V}{\partial S^2} + rS\frac{\partial V}{\partial S} - rV = 0, \tag{7.40}$$

where V, S, t, r correspond to the price of the option and the price of the underlying at time t, the annualised risk-free interest rate and the volatility, respectively. It is possible to solve this equation, yielding two solutions for put and call options as in Eq 7.41.

$$\Pi_{p,c} = \begin{cases} C(S_t,t) &= \overbrace{N(d_1)S_t}^{\text{Stock Position}} - \overbrace{N(d_2)Ke^{-r(T-t)}}^{\text{Bond Position}}, \\ P(S_t,t) &= \underbrace{N(-d_2)Ke^{-r(T-t)}}_{\text{Bond Position}} - \underbrace{N(-d_1)S_t}_{\text{Stock Position}}, \end{cases} \tag{7.41}$$

where d_1 and d_2 can be defined as follows:

$$\begin{aligned} d_1 &= \frac{1}{\sigma\sqrt{T-t}}\left[\log\left(\frac{S_t}{K}\right) + \left(r + \frac{\sigma^2}{2}(T-t)\right)\right], \\ d_2 &= d_1 - \sigma\sqrt{T-t}. \end{aligned} \tag{7.42}$$

At expiry the payoff of the call $C(\cdot)$ and put $P(\cdot)$ options can be expressed in Eq 7.43, where K and P correspond to the strike price and premium of the option at time τ.

$$\begin{aligned} C(S_\tau,\tau) &= \max(S_\tau - K, 0) - P, \\ P(S_\tau,\tau) &= \max(K - S_\tau, 0) - P, \end{aligned} \tag{7.43}$$

In addition, $N(\cdot)$ is the cumulative distribution function of the standard normal distribution, $\tau = T - t$ is the time to maturity in years [16]. It is possible to generalize the Black-Scholes equation to include dividends (q), reaching the following set of equations Eq 7.44 - 7.45:

$$\Pi_{p,c} = \begin{cases} C(S_t,t,q) &= S_t e^{-q\tau}N(d_1) - N(d_2)Ke^{-r\tau}, \\ P(S_t,t,q) &= Ke^{-r\tau}N(-d_2) - S_t e^{-q\tau}N(-d_1), \end{cases} \tag{7.44}$$

where d_1 and d_2 can be defined as follows:

$$\begin{aligned} d_1 &= \frac{1}{\sigma\sqrt{\tau}}\left[\log\left(\frac{S_t}{K}\right) + \left(r - q + \frac{\sigma^2}{2}\tau\right)\right], \\ d_2 &= d_1 - \sigma\sqrt{\tau}. \end{aligned} \tag{7.45}$$

Formally the Greeks, derivatives of the Black-Scholes equation are illustrated in Tab 7.6 [16].

Table 7.6: The analytical solution to the Black-Scholes formula for the chosen Greeks.

Greek	**Derivative**	**Call**	**Put**
Delta (Δ)	$\frac{\mathrm{d}\Pi_{p,c}}{\mathrm{d}S}$	$N(d_1)$	$N(d_1) - 1$
Gamma (Γ)	$\frac{\mathrm{d}^2\Pi_{p,c}}{\mathrm{d}S^2}$	$\frac{N'(d_1)}{S\sigma\sqrt{\tau}}$	
Vega (ν)	$\frac{\mathrm{d}\Pi_{p,c}}{\mathrm{d}\sigma}$	$SN'(d_1)\sqrt{\tau}$	
Theta (θ)	$\frac{\mathrm{d}\Pi_{p,c}}{\mathrm{d}t}$	$-\frac{SN'(d_1)\sigma}{2\sqrt{\tau}} - rKe^{-r\tau}N(d_2)$	$-\frac{SN'(d_1)\sigma}{2\sqrt{\tau}} + rKe^{-r\tau}N(-d_2)$
Rho (ρ)	$\frac{\mathrm{d}\Pi_{p,c}}{\mathrm{d}r}$	$K\tau e^{-r\tau}N(d_2)$	$-K\tau e^{-r\tau}N(-d_2)$

These second order finite difference approximations of the Greeks can be extended such that they can be extracted from the trinomial tree [17]. This can be achieved in the following way:

$$\begin{aligned}
\Delta &= \frac{V(0+\delta r) - V(0-\delta r)}{2\Delta r}, \\
\Gamma &= \frac{V(0+\delta r) + V(0-\delta r) - 2V(0)}{\Delta r^2}, \\
\nu &= V(0+\delta\sigma) - V(0), \\
\Theta &= V(0) - V(0+\delta t),
\end{aligned} \tag{7.46}$$

where $V(0)$ corresponds to the price of the option at the root node, δt, $\delta\sigma$ and δr correspond to a shift in parameter values and are defined as:

$$\delta r = 0.0001, \tag{7.47}$$

$$\delta\sigma = 0.01, \tag{7.48}$$

$$\delta t = \frac{1}{365}. \tag{7.49}$$

This entails the construction of a separate tree for each parameter shift, and comparing the results from both trees. The Greeks were determined for a given set of bond parameter values from Appendix.A and illustrated in Tab 7.7. Note that DV01 is common market parlance of the Greek Δ, standing for dollar variation of one percent.

Table 7.7: Determination of Greeks of a Call option from the Calibrated 2-dimensional trinomial short rate tree.

Steps	**Option Price**	**DV01**	**Gamma**	**Vega**	**Theta**
10	0.8045	-0.0009	0.0101	104.5627	0.0002
50	0.8868	-0.0140	0.1639	141.0503	0.0031
100	1.0104	-0.0107	0.1242	137.1375	0.0023
200	1.0109	-0.0124	0.1457	137.0894	0.0027
500	1.0356	-0.0140	0.1651	138.5228	0.0031
1000	1.0505	-0.0135	0.1591	137.8669	0.0030

8 Intensity Model

When attempting to price defaultable corporate bonds, one requires a measurement for the defaultability of the derivative. This manifests itself in the form of an intensity or credit term structure. The modeling procedure follows the same protocol as was discussed in the aforementioned sections, yet one does not have the same luxury of a risk-free term structure to calibrate the model. Schönbucher provides some alternatives to this thesis [9].

Given historical market data, it is possible to develop a term structure for high-yield corporate bonds. One can map the yields, credit spreads (I-spread, OAS, etc) or hazard rates to a suitable term structure which can be used in the 3D-lattice tree to price derivatives, analagous to utilising the risk-free government treasury curves in calibrating the short rate. Prior to modeling, there are a number of apparent issues which need to be addressed during implementation. To start, when modeling spreads, it is pertinent to define a suitable choice of risk-free term structure as a benchmark. As was previously discussed, there are several candidates which have been proposed and are used in practice; the government curve and the LIBOR curve and OIS rates. The answer is far from trivial especially considering given these curves could differ by 100bp [9].

8.1 Government Bonds

To start, government bonds seem like the most appropriate candidate, under the assumption that the issuing government is reliable and unlikely to default. Given the trader were to be investigating bonds originating from European and American sources, this assumption holds true. That being said, the spread between these treasury bonds and the highest rated AAA-rated investment grade bonds is far too large to be explained by one single variable, especially default risk. Naturally, there are other factors such as risk premia, liquidity and taxation effects which may in part explain these observations, it has been speculated that the true risk-free term structure lies somewhat above the treasury rate. Thus using government issued treasury bonds as a benchmark term structure leads to a heightened measure of the implied default risk [9].

8.2 LIBOR / STIBOR

The alternative approach to using LIBOR rates (or any other inter-bank offered rate) lead to similar issues. First and foremost, LIBOR rates are not considered to be default-free. These rates are defined as the interbank offered refinancing rate of AA-rated banks in London and can often yield a negative spread. A negative spread would imply a negative default risk, which is similarly unreasonable. Given the large number of credit derivatives available, a general rule of thumb is to select the default-free rate based on the defaultable obligor's assets [9]. These are the repo rates and swap curve for high and low rated obligors, respectively. That being said, for ease of availability and convenience, it was decided to use government treasury bonds as the risk-free term structure.

8.3 OIS

The final approach is using OIS (overnight indexed swap) rates, which have become particularly popular after the 2008 credit crisis [18]. Prior to 2008, the spread between these two curves was approximately 10bp, which has since seen a dramatic increase. As derivatives should be valued by estimating expected cash flows in a risk-neutral world and then discounting them using a risk-free rate, the OIS is a more suitable alternative to that of LIBOR. Additionally, OIS rates are longer-term rates stemming and derived from the overnight rates offered by the inter-bank.

That being said, as many derivative payoffs are dependent on LIBOR rates, one must now keep track of multiple term structures. Practitioners tend to assume that the spread between OIS and LIBOR rates are constant or deterministic, yet Hull proposes a model for relaxing this assumption by modeling using a two-factor trinomial tree. For full details, we refer the reader to Hull [18].

8.4 Modeling Process

The process of modeling the defaultable term structure is two fold. Given a time series of defaultable bond yields with varying times to maturity, group the bonds into a suitable category such as industry or credit rating when applicable. When modeling spreads, the spread can be determined by subtracting the observed bond yield to a corresponding risk-free alternative with a similar time to maturity. This term structure is then processed by removing extreme values and abnormalities using a relevant metric (IQR, mean, median etc). This thesis utilised inter-quartile ranges (IQR) to remove extreme values present in the upper and lower whiskers. Following on from this, the resulting term structure is bucketed into a suitable choice of tenors and the median value is chosen. This replicates a term structure, analogous to that of the risk-free treasury curves. Once smoothed, these curves can be interpolated by a suitable method such as cubic splines, bootstrapping, Nelson-Siegel (NS) or Nelson-Siegel-Svensson (NSS) [9]. For the purposes of this paper, and to minimise the complexity and reduce the number of calibration parameters, Nelson-Siegel (NS) is utilised. The final step in this procedure is to obtain the required calibration parameters $(\bar{a}, \bar{\sigma})$ from the fitted curves for pricing derivatives. As the functional form of the Hull-White one-factor model can be solved analytically, this function can be fitted to the smoothed NS-curve and the calibration parameters can be optimized from algorithms such as Nelder-Mead or COBYLA.

8.5 Data Processing

The Hull-White extended two-factor model, represented by a 3D-trinomial tree models the default intensity $\lambda(t)$ as an input to the pricing model. It is naturally possible to utilise spreads, yields or alternatives based on the credit derivative being modeled, and the methods outlined would apply in a general case. Denote the chosen input as the credit intensity. When using yield spreads, it is import to distinguish between the various options at ones disposal. Callable bonds can be notably viewed from a yield-to-call (YTC), yield-to-worst (YTW) or yield-to-maturity (YTM) perspective.

The resulting data requires further processing. The goal is to achieve a smooth term structure which is applicable to each bond within a chosen industry. Naturally, it must be noted that by doing so, it is possible that the resulting term-structure will not adequately represent the inherent default risk within particular bonds.

To start, it was necessary to remove any negative credit intensities. These data-points are deemed dis-interesting as they imply that the treasury bond is both risk-less and more profitable. Though this may occur in the market, it would merely disrupt the smoothing of the term structure. Likewise when modeling spreads, any intensities exceeding 500bp, or with a maturity greater than 10 years were also removed. Finally, due to the nature of the variant fluctuations of these curves, the data was further filtered by using inter-quartile ranges (IQR), where intensities outside the lower and upper whisker were also removed. In order to adequately map and provide a benchmark curve to each bond, a term structure was created for their representative industry. Similarly, as before, outliers were removed based on an industry by industry basis based on the aforementioned methods.

8.6 Default Intensity λ

There is one important additional factor to consider. When default occurs, the bond or credit derivative still has some underlying value. This value is depicted by the implied default and survival probabilities, as well as the recovery rate of the underlying and is an important factor to consider when calibrating the spread curve.

8.6.1 Hazard Rates

The collection of these variables can be expressed as the Hazard rate using Poisson processes. Consider the stopping time as the time point τ_i of a particular event. The point process is then the collection of stopping times up until a time point t. Furthermore, it must be assumed that each of these stopping times are unique, in ascending order and that there only a finite number of them over a given time interval. By doing so, this provides a suitable framework in timing the risk of events, most notably default. This collection of events can thus be viewed as a stochastic process where:

$$N(t) = \sum_i \mathbb{1}_{\tau_i \leq t}, \tag{8.1}$$

where $N(t)$ are the number of time points before time t [9]. Thus, if one lets τ be a stopping time with $F(T) = \mathcal{P}(\tau \leq T)$ be it's distribution function with density $f(T)$, the hazard rate $h(T)$ can be defined as:

$$h(T) = \frac{f(T)}{1 - F(T)}. \tag{8.2}$$

One must also assume that $F(T) < 1, \forall T$. For later time points $\tau > t, t > 0$, the conditional hazard rate is expressed as:

$$h(t,T) = \frac{f(t,T)}{1 - F(t,T)}, \quad F(t,T) = \mathcal{P}\left(\tau \leq T | \mathcal{F}_t\right). \tag{8.3}$$

Note that in this case, the distribution function is the conditional distribution of τ, with the information provided at time t. Thus, the hazard rate is interpreted as the local arrival probability of the stopping time at time t. This can be expressed as:

$$h(t) = \lim_{\Delta t \to 0} \frac{1}{\Delta t} \mathcal{P}\left(\tau \leq t + \Delta t | \tau > t\right). \tag{8.4}$$

With this information it is possible to construct the underlying distributions,

$$F(t) = 1 - e^{-\int_0^t h(s)ds}, \quad F(t,T) = 1 - e^{-\int_t^T h(t,s)ds}. \tag{8.5}$$

It is clear that the hazard rate and survival probability are closely affiliated with the Poisson process $N(t)$. The default intensity can thus be expressed as:

$$\lambda(t) = h(t,t). \tag{8.6}$$

It is conventional for authors to refer to these events as "default intensity" or "hazard rates" as synonyms. There is one fundamental difference, that the hazard rates are defined for future dates but for the purposes of this paper, unless otherwise stated, the definitions will be analagous. Note that when constructing the trinomial tree, the survival and default probabilities are expressed as:

$$P_s(t) = e^{-\lambda(t)\Delta t}, \quad P_d(t) = 1 - e^{-\lambda(t)\Delta t}. \tag{8.7}$$

8.6.2 Recovery Rates

The concept of which recovery rate is discussed in more detail in Section 12.1, yet this section will provide a brief interlude. When a bond defaults, the bond still has some inherent value. Thus, an investor is at least expected to recover a fraction of their investment. This metric is denoted the recovery rate π. Furthermore, one can measure the default risk of a corporate bond by means of the spread between the risk-free interest rate and the corporate bonds of the same maturity. Denote this measurement as the yield spread, $y(t)$. The relationship between this spread and the recovery rate is denoted the default intensity or hazard rate. The relationship is expressed as

$$\lambda(t) = \frac{y(t)}{1-\pi} = \frac{y(t)}{q}, \tag{8.8}$$

where q is the loss quota of the bond. Recovery rate can be modelled in a number of ways, yet this thesis decided to incorporate bond seniority as the descriptive factor. The relationship between recovery rate and bond seniority was obtainable from a chosen ratings provider. In the case of this thesis, the source is Moody's. Moreover, a market convention is to estimate the recovery rate at 40%, which is echoed by the data provided in Fig 8.1. In addition to modelling the recovery rate, one must choose a recovery convention when pricing derivatives. This can include recovery of market value, recovery of treasury etc and is discussed in more detail in Section 12.1.

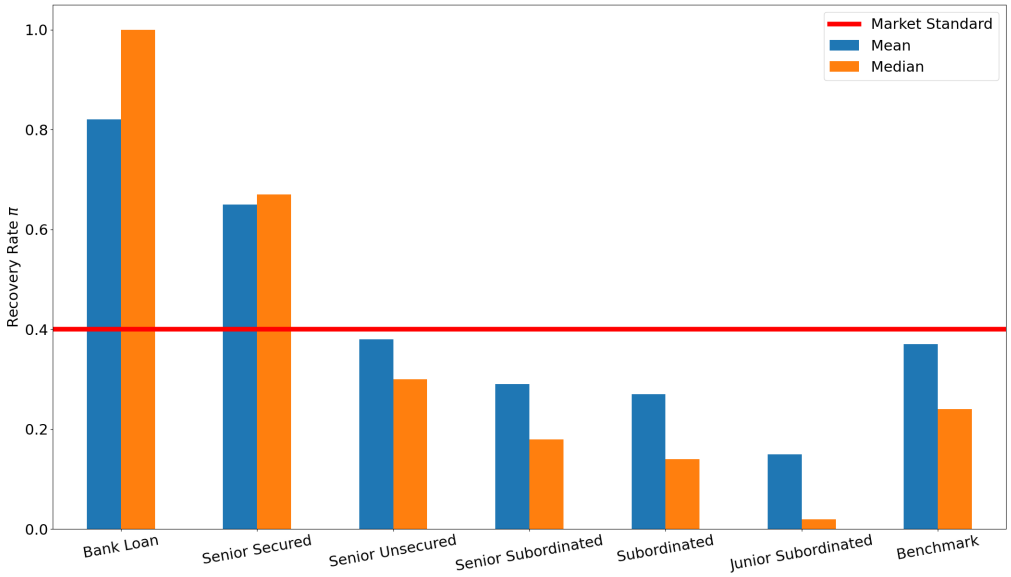

Figure 8.1: Recovery Rates for selected bonds as obtained from Moodys [6].

8.7 Clustering

Once a satisfactory time series of credit intensities were obtained, it was decided to discretize the data into suitable buckets, based on their time to maturity. The median value within these buckets was chosen. When choosing these buckets, one must consider a number of factors including suitable spacing between the tenors, a suitable number of tenors, a sufficient number of data points within each bucket and the co-linearity which is induced by the tenors on the beta coefficients to the fitted Nelson-Siegel model [19]. This can be determined by a number of

suitable approaches, such as a heuristic option, by quantiles, using a binned statistic and the Jenks-Fischer algorithm. The Jenks-Fischer algorithm is a clustering technique designed to find the natural breaks within the classes by minimising the variance within classes and maximising the variance between classes. For the purposes of this paper, ten buckets were chosen for the clustering process. The various clustering procedures are outlined in Fig 8.2. On the basis of this, the Jenks-Fischer algorithm was chosen.

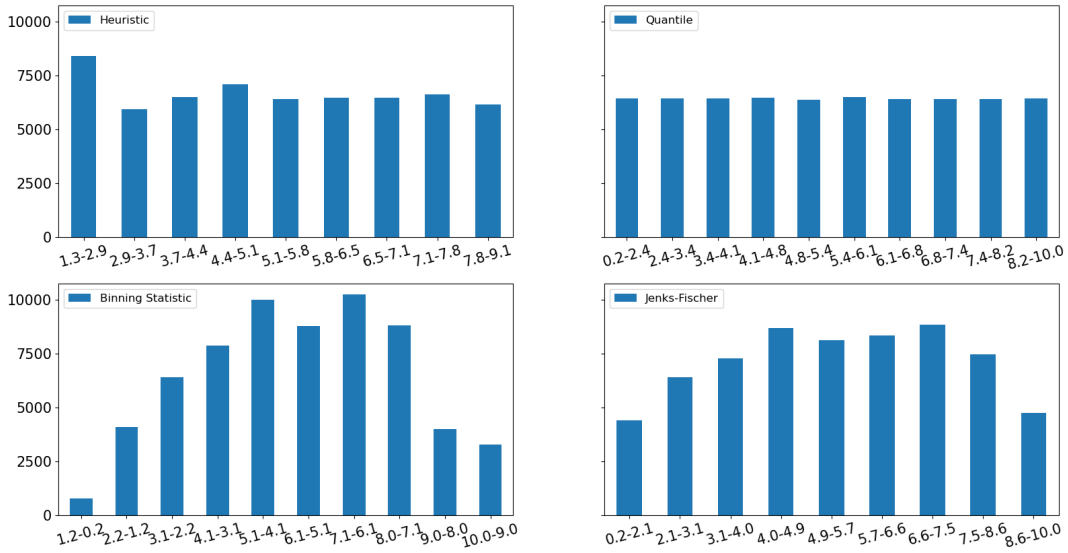

Figure 8.2: Distribution of credit intensities across tenor buckets based on the chosen clustering algorithm. The x-axis corresponds to the time to maturity and the y-axis refers to the number of data points present in that cluster.

The Jenks-Fischer was applied to the entire dataset, so each industry received the same clustering. To ensure this method was satisfactory, the algorithm was applied to each individual industry and a confusion matrix was generated between the global and individual discretisations. Additionally, the distribution of the credit intensities were analysed for the entire time series to heuristically determine whether the bucketing was reasonable as illustrated in Fig 8.3.

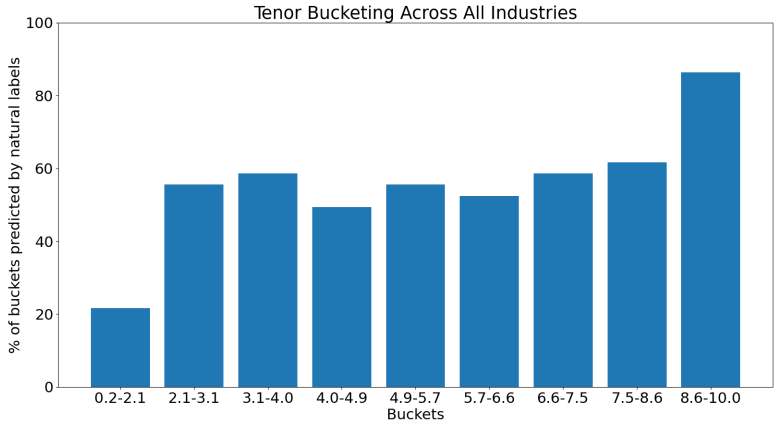

Figure 8.3: Example distribution of credit intensities across one possible tenor bucketing using the JF-algorithm.

Though it is clear that bonds closer to expiry were not necessarily accurately represented by

the choice of tenor, relative to bond specific clustering, one must only keep track of one set of clusters and it was decided that the results were satisfactory.

8.8 Interpolating the Term Structure

Now that the term structures of each individual industry were suitably discretised, it was necessary to be able to interpolate any point on these curves. The Nelson-Siegel model provided an apt choice, with C^∞ smooth properties which will prove useful in determining suitable approximation of calibration parameters required for the calibration of the stochastic two-factor model.

8.8.1 Nelson-Siegel (NS)

For a conventional risk-free interest rate term structure, the Nelson-Siegel (NS) model can be described as:

$$r(\tau) = \beta_0 + \beta_1 \left(\frac{\lambda}{\tau} \left(1 - e^{-\tau/\lambda} \right) \right) + \beta_2 \left(\frac{\lambda}{\tau} \left(1 - e^{-\tau/\lambda} \right) - e^{-\tau/\lambda} \right), \tag{8.9}$$

where β_i correspond to the yield term level, slope and curvature for a given term structure respectively. This can similarly be applied to the credit spread or hazard rate curves. For the sake of completeness, an alternative option is that of the Nelson-Siegel-Svensson (NSS) [20], whose original model as illustrated as:

$$r(\tau) = \beta_0 + \beta_1 \left(\frac{1 - e^{-\tau/\lambda_1}}{\frac{\tau}{\lambda_1}} \right) + \beta_2 \left(\frac{1 - e^{-\tau/\lambda_1}}{\frac{\tau}{\lambda_1}} - e^{-\tau/\lambda_1} \right) + \beta_3 \left(\frac{1 - e^{-\tau/\lambda_2}}{\frac{\tau}{\lambda_2}} - e^{-\tau/\lambda_2} \right). \tag{8.10}$$

The additional terms in the NSS-model provide an additional hump structure which may be useful for certain term structures. That being said, it is desired to require the calibration of as few terms as possible and given the shape and structure of the generated term structures is unlikely to require the additional coefficients. Thus, the more conventional NS approach will be utilised.

8.8.2 Properties of Nelson-Siegel

Additionally, the NS model provides a few additional benefits due to the nature of the factor loadings which correspond to the level, slope and curvature components of a spot rate or intensity curve.

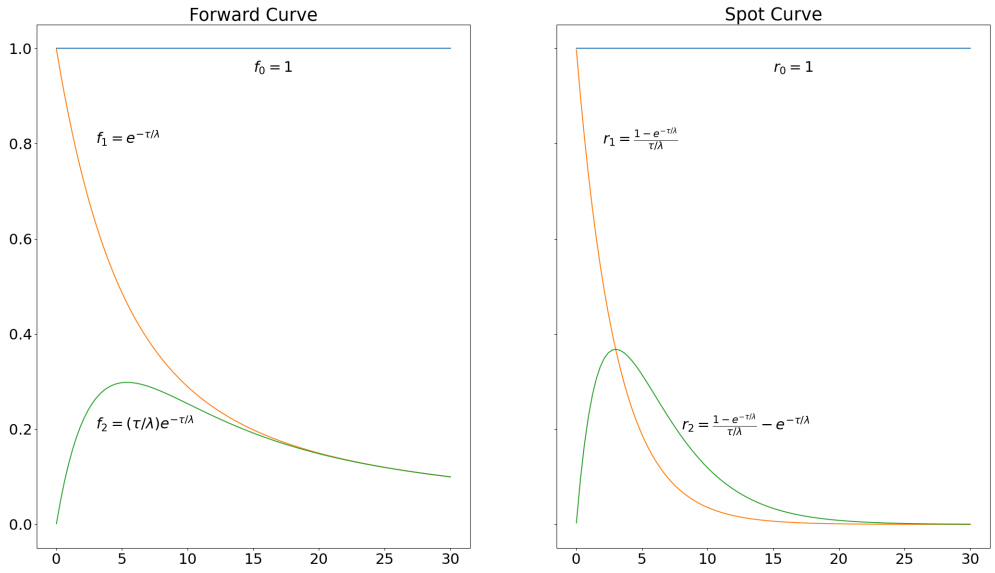

Figure 8.4: Illustration of the behavior of the forward and spot curves of the Nelson-Siegel factor loadings over a range of τ values.

Each of the above components serve the purpose of providing a limiting behaviour as a function of the time to maturity. As $t \to \infty$ the intensity converges to a constant rate of β_0 which is assumed to be non-negative. In contrast, as $t \to 0$ the process converges to $\beta_0 + \beta_1$. These boundary conditions are of particular importance and are required during the calibration process. The β_1 or slope component parameter can thus be positive or negative. In addition, the β_2 parameters controls the rate of decay to which the slope and curvature component decay to zero. In conjunction with λ, who controls the shape and location of the curvature component, it is possible to calibrate NS to a suitable term structure. This can be achieved using two possible methods, the first is to maximise the curvature component and location of the hump/trough to determine λ. The alternative is to force the location of the hump/trough at a given time to maturity [19]. In the modeling of interest rates, the latter is the preferred method and is the method chosen for this thesis where $\lambda = 1$. Both methods linearalize the resulting optimisation process, which is a desirable feature.

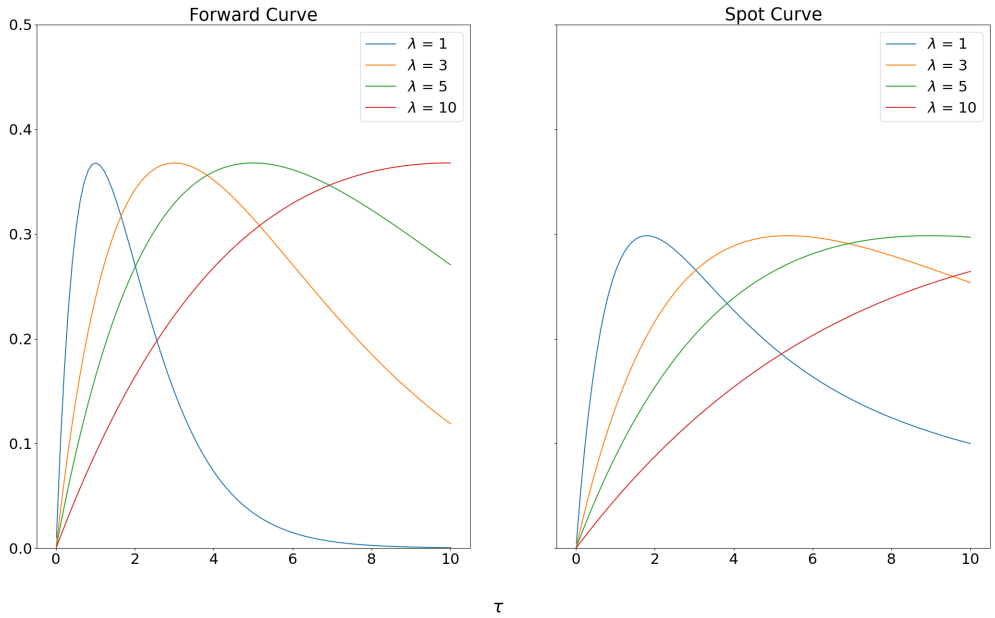

Figure 8.5: Behavior of the forward and spot rate curves of the Nelson-Siegel model over a variety of λ values. The forward curve reaches its maximum at $\tau = \lambda$ and the spot curve reaches maximum for $\tau > \lambda$.

As can be seen in Fig 8.5, the curvature component is maximised in the forward curve when $\tau = \lambda$ yet reaches its maximum when $\tau > \lambda$ for the spot curve.

8.8.3 Fitting the Nelson-Siegel Model

As outlined in the section prior, one starts by fixing λ and freeing the β coefficients. An arbitrary starting point is chosen. It must be noted that a conventional ordinary-least squares (OLS) approach will lead to a large co-linearity between the obtained β parameters. There are ways of dealing with this such as using a ridged-regression approach in conjugation with variance-inflation-factor (VIF) to measure co-linearity [19]. For the purposes of this paper, a constrained optimization by linear approximation (COBYLA) numerical optimisation technique is used to determine the optimal β coefficients for each curve, in conjunction with mean-squared-error (MSE) as an objective function. Moreover, it is now possible to interpolate these curves with the obtained coefficients for an in-sample selection of tenors. As was previous discussed, the contribution of each of the β and λ parameters leads to the following constraints:

$$\beta_0 > 0 \quad \beta_0 + \beta_1 > 0 \quad \lambda > 0. \tag{8.11}$$

As an example of this process, two functions are used to generate data and the optimisation algorithm is applied to determine the optimum beta coefficients mapping the function. The first, is a Nelson-Siegel model with known parameters and the second is a subset of the Nelson-Siegel, a popular function used to interpolate yield curves in the 1990's. The results are shown in Fig 8.6 and Tab 8.1.

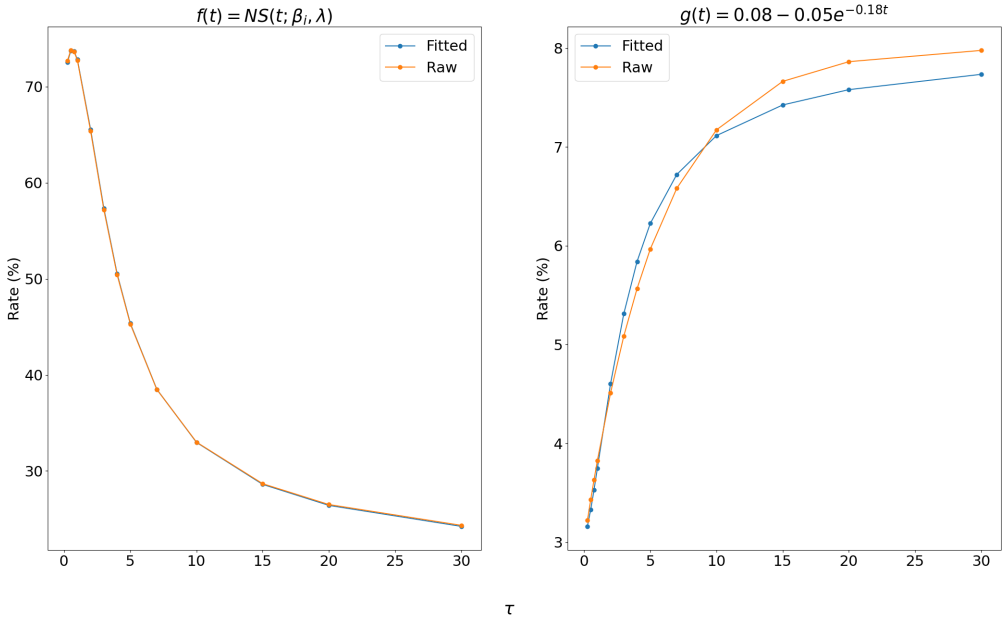

Figure 8.6: Performance of the optimisation procedure for fitting the Nelson-Siegel model to a chosen term-structure.

Table 8.1: Obtained β parameters from performing the optimisation procedure using COBYLA with $\lambda = 1$.

	$f(t) = NS(t; \beta_i, \lambda)$	$g(t) = 0.08 - 0.05e^{-0.18t}$	$f(t)$ Initialised Params
β_0	0.1983	0.0819	0.2
β_1	0.4981	-0.0489	0.5
β_2	0.8138	-0.0528	0.8

As can be seen, the fit is exact for $f(t)$, though the β parameters obtained do show some variation. This is to be expected, as the optimization algorithm need not obtain a unique solution. Furthermore, in the case of $g(t)$, the obtained β parameters show some issues in modeling the long-end of the yield curve. This process must be repeated for each day in the time series data provided, yielding a rate surface. In addition, it is reasonable to assume that due to the large number of bonds provided, that their distributions do not align for varying industries, grades and/or senorities. On that basis, it is decided to filter each bond by their industry sector before fitting an NS curve to their term structures.

9 Calibration

It has now been established how to construct both a short-rate and credit intensity tree under the Hull-White model. Additionally, a methodology has been outlined in how to obtain the term structures for both models. This leads to the final obstacle which needs to be addressed, calibrating the models to suitable calibration parameters $\{a, \sigma, \bar{a}, \bar{\sigma}, \rho\}$. Conventionally, the short-rate is calibrated to swaption volatilities or caps/floors. The intensity model is less conventional, where this thesis suggests fitting the functional form of the Hull-White model to the intensity curve and calibrating it to obtain the relevant parameters. When modeling the three-dimensional lattice, a primitive pairwise correlation is proposed between the two term-structures. Let us begin with the short-rate.

9.1 Swaps

Swaps are interest rate derivatives whereby there is an agreement between two parties to exchange cash flows in the future. The cashflows within these contracts usually entail the future value of an interest rate, exchange rate or other market variable, whose payment dates are defined within the agreement. In contrast to other derivatives such as forward contracts, swaps rely on the exchange of cash flows between two parties. In addition, these contracts require a risk-risk discount rate for cash flows. Prior to the financial crisis in 2008, LIBOR rates were utilised though nowadays OIS rates are preferred. For the purposes of this thesis, the aforementioned government treasury curves will be assumed to be risk-free. The underlying swaptions provide a suitable reference to calibrate the required parameters for the Hull-White model.

9.2 Swaptions

Swaptions, or swap option contracts are similar to stock options, where the owner has the right but not the obligation to enter into an agreement at a pre-determined time in the future. In the case of swaptions, this can be cateogrized into payer and receiver swaptions. A payer swaption allows the owner to enter into an interest rate swap where they pay a fixed interest rate and receive a floating interest rate. In contrast, owners of receiver swaptions pay a floating interest rate and receive a fixed interest rate. Due to the nature of swaps, a payer swaption can be viewed as a put option on a fixed rate bond with the strike price equal to the face value of the bond [21]. Similarly, receiver swaptions operate in the same way, viewed as a call option on a fixed rate bond with the strike price equal to the face value of the bond.

As in the case of stock options, the strike dates of these agreements can be categorized into Bermudan, European and American swaptions but are primarily traded over-the-counter (OTC). These contracts are particularly attractive as they allow financial institutions to hedge against future interest rate risks.

9.3 Black Model

The Black model or Black-76 is a simple two-factor model and widely accepted standard market model (SMM) for the pricing of swaptions. The reasons are two-fold, the price is theoretically correct under the assumption of a log-normally distributed short-rate and the implied volatility input can be calculated from market data. Consider a payer swaption paying a fixed interest rate s_k, receiving LIBOR on a swap which lasts n years starting in T years with m payments per year and principal L. The value of the payer swaption under Blacks formula can be expressed as:

$$S_{pay} = \frac{L}{m} \sum_{i=1}^{mn} P(0, T_i)(s_0 N(d_1) - s_k N(d_2), \tag{9.1}$$

where

$$\begin{aligned} d_1 &= \frac{\ln\left(\frac{s_0}{s_k}\right) + \sigma^2 \frac{T}{2}}{\sigma\sqrt{T}}, \\ d_2 &= d_1 - \sigma\sqrt{T}. \end{aligned} \tag{9.2}$$

For the purposes of calibration, the swap rate s_0 is considered to be at-the-money (ATM). Let A denote the discounted payoffs as:

$$A = \frac{1}{n} \sum_{i=1}^{mn} P(0, T_i). \tag{9.3}$$

The swaptions under the Black model are thus defined as:

$$\begin{aligned} S_{pay} &= LA\left(s_0 N(d_1) - s_k N(d_2)\right), \\ S_{rec} &= LA\left(s_k N(-d_2) - s_0 N(-d_1)\right). \end{aligned} \tag{9.4}$$

In addition, the swap rate at time T for a swap starting at time T_0 and ending at time T_N can thus be expressed as:

$$S(T, T_0, T_N) = \frac{P(t, T_0) - P(t, T_n)}{\sum_{i=1}^{n} \delta\left(T_{i-1}, T_i\right) P(t, T_i)}, \quad T < T_0 < T_N. \tag{9.5}$$

For the sake of completeness, not that it is possible to determine an approximation for the swap rate as mentioned in [22], by noting that the ratio of bond prices follows a log-normal distribution. Under this assumption, the true swap rate can be approximated as:

$$\tilde{S}(T, T_0, T_N) = \frac{P(0, T_n)}{\sum_{i=1}^{n} \delta\left(T_{i-1}, T_i\right) P(0, T_i)} \left(\frac{P(t, T_0)}{P(t, T_n)} - 1\right), \quad T < T_0 < T_N. \tag{9.6}$$

9.3.1 Hull White Model Prices

As was discussed in Section refsec.jamshidianProcedure in the analytic extension of pricing European options, it is possible to view a swaption as the sum of n zero-coupon bonds. The payer swaption is thus merely a put option on these zero-coupon bonds and can be priced using Eq 6.35. In this setting, the Jamshidian procedure can be applied in conjugation with the following formulae:

$$\begin{aligned} P_s(K, T_0, T_P) &= \sum_{i=1}^{n} P_p(T_0, T_i, X_i), \\ c_i &= \begin{cases} K\delta(T_{i-1}, T_i), & i = 1, ..., n-1 \\ L + K\delta(T_{n-1}, T_n), & i = n \end{cases} \\ X_i &= \exp\left(A(T_0, T_i) - B(T_0, T_i) r^*\right), \end{aligned} \tag{9.7}$$

where $\delta(\cdot)$ is a function of the time between payment dates. Additionally, r^* satisfies the following equation:

$$\sum_{i=1}^{n} c_i \exp\left(A(T_0, T_i) - B(T_0, T_i) r^*\right) = 1. \tag{9.8}$$

It is thus possible to apply the Jamshidian procedure to obtain model prices for a chosen a and σ.

9.4 Calibration of Short Rate Parameters

Given the volatility implied swaption prices and the jamshidian option pricing procedure implied Hull-White model prices, one must now determine the optimal calibration parameters for the one-factor and two-factor models. There are a number of ways to achieve this. To start, since a and σ are constant, one could limit the number of parameters required for calibration. In an alternative case, where either a, σ or both are functions of time, the required measures increase. Hull provides a notable example. Let

$$\sigma(t) = \begin{cases} \sigma_0, & t \leq t_1 \\ \sigma_i, & t_i < t \leq t_{i+1} \\ \sigma_n, & t > t_n. \end{cases} \tag{9.9}$$

To ensure the calibration parameters are well behaved, penalty functions can be applied to obtain a suitable objective function to minimise. Using the example provided, one suitable objective function is:

$$\theta = \sum_{i=1}^{n}(U_i - V_i)^2 + \sum_{i=1}^{n} w_{1,i}(\sigma_i - \sigma_{i-1})^2 + \sum_{i=1}^{n-1} w_{2,i}(\sigma_{i-1} + \sigma_{i+1} - 2\sigma_i)^2, \tag{9.10}$$

where the weights $w_{1,i}$ and $w_{2,i}$ are at the discretion of the user. An alternative procedure is to calibrate to all available instruments to obtain the global best-fit parameters. In this setting, one can fix either calibration parameter and find the other corresponding optima or to free both parameters. This thesis opts for the latter. Let U, V denote the market prices obtained from the Black-76 model and Hull-White model, respectively. As the relative difference is of more interest than the absolute difference, a suitable objective function can be defined as:

$$\theta(a, \sigma) = \sum_{\substack{1 \le i \le n_m \\ 1 \le j \le n_t - 1}} w_{i,j} \left(\frac{V_{i,j}(a, \sigma)}{U_{ij}} - 1 \right)^2, \tag{9.11}$$

where $w_{1,i}$ is a suitable weighting for each of the lengths and swaption expiry's [22]. A commonly used minimisation procedure in these markets is Levenberg-Marquadt. Naturally, under this construction it is possible to determine any linear combination of measures to calibrate the parameters. This is considered the global measure for calibrating the instruments. Regardless of choice, the calibration volatilities should be chosen such that they match the credit instrument being valued. Thus, one possible solution is to set the weights of instruments with similar expiry's to 1 and zero otherwise. If one were to use these setups in practice, it becomes necessary to have a different set of calibration parameters for every option and every type of option [10]. As an example, consider the following ATM swaption volatilities obtained from Bloomberg in Tab 9.1 and the obtained volatility surface in Fig 9.1.

Table 9.1: Swaption Volatilities for the Euro on 23/05/2013.

		Maturity					
		1Yr	2Yr	3Yr	4Yr	5Yr	6Yr
Expiry	1Mo	29.18	36.98	41.39	46.92	48.90	51.34
	3Mo	28.60	36.79	42.11	48.07	51.53	53.77
	6Mo	30.36	40.30	45.41	49.82	53.75	55.65
	9Mo	33.15	41.07	47.21	51.69	56.14	57.69
	1Yr	36.27	41.59	48.72	53.27	58.32	59.59
	2Yr	46.96	52.07	56.78	60.64	63.14	64.66
	3Yr	57.65	63.03	66.81	68.27	70.49	70.95
	4Yr	68.08	70.78	70.62	71.80	73.15	73.02
	5Yr	72.62	72.58	73.22	73.75	74.10	74.13
	6Yr	70.83	72.20	73.58	73.88	74.23	73.81
	7Yr	72.29	72.75	72.60	73.08	72.66	72.22

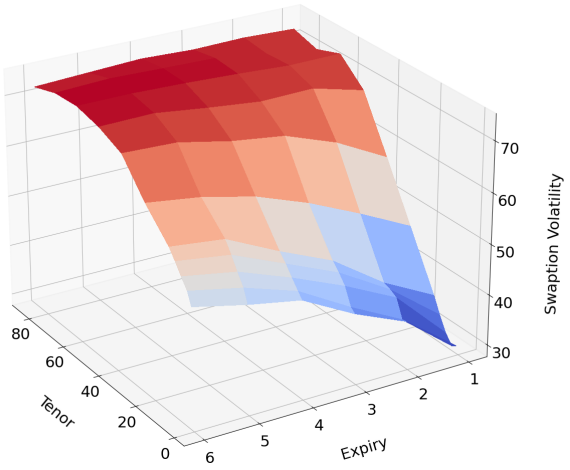

Figure 9.1: Three-dimensional surface representation of the swaption volatilities based on Tenor and Expiry.

Note that the swaption volatilities are quoted in basis points (bp) and the input to both the Black-76 and Hull-White models are expressed in percentage fractions. The global calibration objective function as in Eq 9.11 is applied to yield the optimal a and σ on that particular day. Recall that this procedure could be modified based on the credit derivative being priced. In addition note that payment dates can vary between the maturity and expiry of the swaption. This thesis used the Jamshidian procedure with a payment date every six months. The obtained market and model prices are displayed in Tab 9.2 and Tab 9.3.

Table 9.2: Implied Market Prices using the Black-76 Model.

		Maturity					
		1Yr	2Yr	3Yr	4Yr	5Yr	6Yr
Expiry	1Mo	0.01	0.05	0.09	0.14	0.18	0.21
	3Mo	0.04	0.14	0.28	0.42	0.54	0.63
	6Mo	0.10	0.31	0.59	0.86	1.11	1.30
	9Mo	0.17	0.50	0.92	1.34	1.70	1.98
	1Yr	0.25	0.72	1.29	1.85	2.32	2.69
	2Yr	0.96	2.00	3.13	4.17	5.01	5.63
	3Yr	2.25	3.85	5.46	6.86	7.95	8.71
	4Yr	4.09	6.17	8.15	9.80	11.03	11.83
	5Yr	6.42	8.86	11.08	12.87	14.15	14.92
	6Yr	9.11	11.80	14.16	16.00	17.25	17.94
	7Yr	12.05	14.88	17.28	19.09	20.26	20.83

To illustrate this, consider the following example swaption volatilites as in Tab 9.1. The market prices are obtained using the black model, yielding:

Table 9.3: Implied Model Prices using the Hull-White Model with optimal parameters a and σ.

		Maturity					
		1Yr	2Yr	3Yr	4Yr	5Yr	6Yr
Expiry	1Mo	0.87	1.21	1.43	1.59	1.71	1.80
	3Mo	0.87	1.21	1.44	1.60	1.72	1.81
	6Mo	0.87	1.21	1.45	1.62	1.74	1.83
	9Mo	1.72	2.39	2.85	3.18	3.41	3.59
	1Yr	1.72	2.40	2.87	3.20	3.44	3.62
	2Yr	3.39	4.70	5.59	6.23	6.70	7.04
	3Yr	4.98	6.89	8.18	9.10	9.77	10.26
	4Yr	6.49	8.95	10.61	11.80	12.66	13.30
	5Yr	7.91	10.90	12.91	14.34	15.38	16.15
	6Yr	9.25	12.73	15.07	16.73	17.94	18.82
	7Yr	10.51	14.46	17.10	18.98	20.33	21.32

9.4.1 Day Count Conventions

If one were interested in higher degrees of precision, day count conventions could be implemented to the chosen model. As the fixed rate of the swap of the underlying swap option is usually expressed as actual/365 or 30/360, the annuity A in Eq 9.3 can be modified as:

$$A = \sum_{i=1}^{mn} a_i P(0, T_i), \quad a_i \in [T_{i-1}, T_i], \tag{9.12}$$

where a_i is the accrual fraction within the time interval $[T_{i-1}, T_i]$.

9.4.2 Negative Interest Rates

Due to the current nature of negative interest rates, the primary valuation methods of pricing swaptions has changed. This leaves the trader with a number of modeling options. The first is to shift the values by a factor α. The strike rate s_k thus becomes $\tilde{s}_k = s_k + \alpha$. An alternative approach is to use the Bachelier normal model as in Eq 9.13 and leaves the implementation to the discretion of the reader. It is also possible to implement a custom drift structure in accordance with either of these models as was proposed in Section 7.

$$\begin{aligned} S_{pay} &= LA\left[(s_0 - s_k)N(d) + \sigma^*\sqrt{T}N'(d)\right] \\ S_{rec} &= LA\left[(s_k - s_0)N(-d) + \sigma^*\sqrt{T}N'(d)\right], \end{aligned} \tag{9.13}$$

where $\sigma^*\sqrt{T}$ is the standard deviation of s_T and

$$d = \frac{s_0 - s_k}{\sigma^*\sqrt{T}}. \tag{9.14}$$

9.4.3 Hedging Swaptions

As with the pricing of stock options, one can perform a sensitivity analysis on swaption prices. The Greeks for swaption prices under the Black-76 model can thus be defined in Tab 9.4.

Table 9.4: Hedging of Interest Rate Swap Options using Black-76 model.

Hedging: Swaptions			
Greek	**Derivative**	**Payer**	**Receiver**
Delta (Δ)	$\frac{\mathrm{d}S_{pay,rec}}{\mathrm{d}s_0}$	$\mathrm{LA}N(d_1)$	$\mathrm{LA}(N(d_1)-1)$
Gamma (Γ)	$\frac{\mathrm{d}S^2_{pay,rec}}{\mathrm{d}s_0^2}$	$\frac{LAN'(d_1)}{\sqrt{T}s_0\sigma_F}$	
Vega (ν)	$\frac{\mathrm{d}S_{pay,rec}}{\mathrm{d}\sigma}$	$SLAN'(d_1)\sqrt{T}$	
Theta (θ)	$\frac{\mathrm{d}S_{pay,rec}}{\mathrm{d}T}$	$-\frac{SLAN'(d_1)\sigma_F}{2\sqrt{\tau}} - rs_k e^{-r\tau}N(d_2)$	$-\frac{SLAN'(d_1)\sigma_F}{2\sqrt{\tau}} + rs_k e^{-r\tau}N(-d_2)$

9.5 Calibration of Intensity Parameters

As in the case of the short-rate models and their accompanying term structure, it is necessary to outline a method for calibrating the model parameters in the intensity space. This thesis proposes fitting the functional form of the Hull-White model to the suitable term structure and calibrating this fit by means of a suitable metric to obtain the calibration parameters.

9.5.1 Fitting the Hull-White Functional Form

As was stated in Section 6.2.1, Eq.6.32 can be used to calibrate the default intensity term structure, through a noteworthy and useful property. For an arbitrary twice differentiable bond curve $\{p^*(0,T); T > 0\}$ w.r.t T, a suitable θ can be chosen from Eq.6.32 to produce a term structure whereby $p(0,T) = p^*(0,T)\ \forall T > 0$ [12]. This is where the choice of fitting the observed bond prices to a Nelson-Siegel model becomes relevant, as the NS model satisfies these requirements. By differentiating Eq.8.9, one has an expression for the instantaneous forward rate $F(0,T)$ and its derivative $F_T(0,T)$ as:

$$\begin{aligned} f(\tau) = F(\tau) &= \beta_0 + \beta_1 e^{-\frac{\tau}{\lambda}} + \beta_2 \frac{\tau}{\lambda} e^{-\frac{\tau}{\lambda}}, \\ f'(\tau) = F_T(0,T) &= \frac{\beta_1}{\lambda}\left(-e^{-\frac{\tau}{\lambda}}\right) + \frac{\beta_2}{\lambda} e^{-\frac{\tau}{\lambda}}\left(1 - e^{-\frac{\tau}{\lambda}}\right). \end{aligned} \tag{9.15}$$

where $f'(\tau)$ and $f'(\tau)$ correspond to the instantaneous forward rate of the credit spreads and its derivative, respectively. It is now possible to find an analytical expression for $\theta(T)$ and obtain the relevant calibration parameters required as inputs to the 3D model. As in the case of obtaining the β parameters in fitting the NS curve, the COBYLA algorithm is utilised using arbitrary $\bar{a}$ and $\bar{\sigma}$ values as a starting point, with MSE as a performance metric. The calibration parameters $\bar{a}, \bar{\sigma}$ must also abide by the following constraints:

$$\begin{aligned} 0 < &\bar{a} \leq 1, \\ 0 < &\bar{\sigma} \leq 1. \end{aligned} \tag{9.16}$$

This process is repeated for each industry, for each day, yielding a time series of interpolated term structures and Hull-White calibration parameters. When applied to the entire time series, it leads to the following illustration:

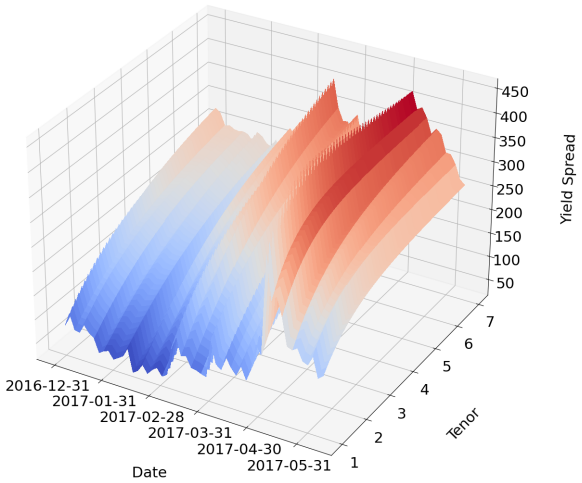

Figure 9.2: Illustration of fitting Nelson-Siegel and the Hull-White functional form to the entire time series of an intensity credit curve denoted by the yield spread, for bonds categorised as Basic Industry.

Using the intensity curve obtained in Tab 8.1 and the aforementioned COBYLA algorithm, the calibrated mean reversion and volatility parameters are illustrated in Tab 9.5.

Table 9.5: Obtained β parameters from performing the optimisation procedure using COBYLA with $\lambda = 1$.

	$f(t) = NS(t; \beta_i, \lambda)$	$g(t) = 0.08 - 0.05e^{-0.18t}$
$\bar{\alpha}$	0.6744	0.1296
$\bar{\sigma}$	0.5572	0.1314

9.6 Correlation

The final parameter to be calibrated is the correlation between the two processes, denoted by ρ. This is achieved using historical data consisting of risk-free treasury curves and the aforementioned intensity term structures. A time series of correlations must be obtained for each industry, country and date respectively. This is achieved using pairwise correlation between the term structures. It is interesting to note the behavior of the bond prices at different times to maturity for each of the two curves, as well as between them. An example correlation between the the times to maturity of the term structures is illustrated in Fig 9.3.

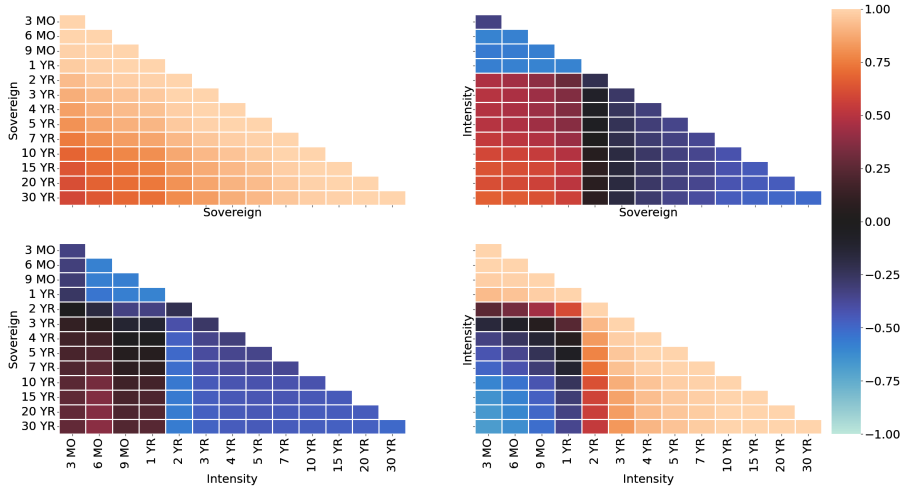

Figure 9.3: Inter correlation between a US Sovereign curve and a constructed intensity term structure.

The calibration parameter ρ is obtained by means of pairwise correlation. This is to ensure that the model can have the highest predictive power with the fewest number of features as possible. For the purposes of this thesis, the Pearson correlation is utilised, yielding a time series of correlations for each respective industry (or credit grade) and treasury curve combination as in Fig 9.4.

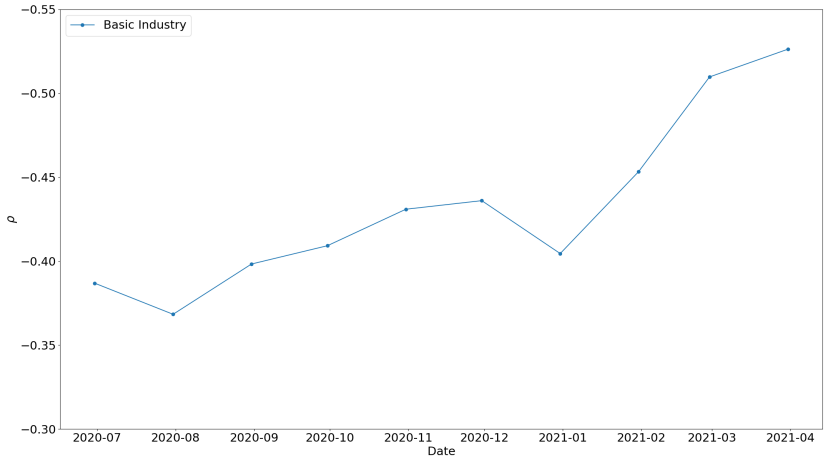

Figure 9.4: Correlation time series for a selection of fixed rate and callable bonds between a US treasury curve and corporations categorised as basic industry.

10 Multi-curve Modelling using Trees

There is one additional caveat that is noteworthy. As was mentioned in Sec.8 the choice of benchmark risk-free curve is far from trivial. LIBOR rates or OIS rates remain popular candidates and a modeling framework is proposed in Hull [18]. Additionally, certain credit derivatives such as diff swaps or diff swap options require the yield curves from two countries to be modelled simultaneously [23]. One can even generalise this one step further by viewing the price of a derivative with respect to a third country [24]. This is may be of particular consideration when pricing derivatives from exotic countries, where one would desire to express the single or two-way cash flows with respect to the home currency.

10.1 Analytical Solution to Two-Factor Model

The former is discussed in detail in Hull [18], thus let us consider the latter.The two-factor approach can be similarly subset into two further categories. One can either model two correlated processes by choosing from a family of one-factor models with a term structure for each process or one implements a two factor model on a single term structure. Of course, the choice is dependent on what one wants to model. Let us begin with the former.

10.2 Two One-factor Models

To model a credit derivative such as a diff swap, one constructs a tree for each of the currencies independently, from the viewpoint of a risk-neutral investor in their respective country [25]. Let x_1 and x_2 denote the processes for r_1 and r_2, the short rates from these currencies respectively. These processes are analagous to that of Eq 6.4. That being said, one needs a process of the

short rate of r_1 from the viewpoint of an r_2 investor or vice-versa. This can be achieved by reducing the drift of one of the processes by a scaling factor. This yields

$$dx_2^* = [\theta_2(t) - \rho_x \sigma_2 \sigma_x - a_2 x_2^*]dt + \sigma_2 dz_2, \tag{10.1}$$

where ρ_x, σ_x are the instantaneous coefficient of correlation between the exchange date and the interest rate of r_2 and the volatility of the exchange rate, respectively. The effect of shifting between risk-neutral worlds means that one of the trees nodes must be reduced by

$$\psi(n) = \frac{\rho_x \sigma_2 \sigma_x}{a_2} \left(1 - e^{-a_2 n \Delta t}\right), \tag{10.2}$$

for each time step $0 \leq n \leq N$. The three-dimensional tree can thus be constructed with the calibration parameters $(a_1, \sigma_1, a_2, \sigma_2, \rho)$. Note that ρ is the correlation between the two interest rates and ρ_x is the correlation between the exchange rate and the r_2 rate. It is noteworthy that it is possible to value these differential swaps analytically [23].

10.3 One Two-Factor Model

Two-factor models abide the user the opportunity to monitor a richer pattern of term structure movements and volatility structures, in contrast to its one-factor relative. The two-factor models can be expressed in the form [25]:

$$df(r) = [\theta(t) + u - af(r)]dt + \sigma_1 dz_1, \tag{10.3}$$

where u is a stochastic process with initial value zero and follows the process:

$$du = -budt + \sigma_2 dz_2, \tag{10.4}$$

and b is a constant and $a \neq b$. Under the assumption that $f(r) = r$ this setup has some attractive properties. First and foremost, the price of a zero-coupon bond can be represented as:

$$P(t,T) = A(t,T) \exp\left(-B(t,T)r - C(t,T)u\right). \tag{10.5}$$

where $C(\cdot)$, $B(\cdot)$ are defined in Eq 10.7. Under this construction the complete yield curve can be calculated analytically when $f(r) = r$ under the following constraints:

$$\begin{aligned} B_t - aB + 1 &= 0, \\ C_t - bC + B &= 0, \\ A_t - \theta(t)AB + \frac{1}{2}\sigma_1^2 AB^2 + \frac{1}{2}\sigma_2^2 AC^2 + \rho\sigma_1\sigma_2 ABC &= 0. \end{aligned} \tag{10.6}$$

For further details, we refer the reader to [25] but provide the solutions to the equations below, which yield

$$\begin{aligned} B(t,T) &= \frac{1}{a}\left(1 - e^{-a(T-t)}\right), \\ C(t,T) &= \frac{1}{a(a-b)} e^{-a(T-t)} - \frac{1}{b(a-b)} e^{-b(T-t)} + \frac{1}{ab}, \\ \ln A(t,T) &= \ln\left(\frac{P(0,T)}{P(0,t)}\right) + B(t,T)F(0,t) - \eta, \end{aligned} \tag{10.7}$$

where

$$\begin{aligned}\eta =&\frac{\sigma_1^2}{4a}\left(1-e^{-2at}\right)B(t,T)^2\\&-\rho\sigma_1\sigma_2\left(B(0,t)C(0,t)B(t,T)+\gamma_4-\gamma_2\right)\\&-\frac{1}{2}\sigma_2^2\left(C(0,t)^2B(t,T)+\gamma_6-\gamma_5\right),\end{aligned}\tag{10.8}$$

and

$$\begin{aligned}\gamma_1 &= \frac{e^{-(a+b)T}(e^{(a+b)t}-1)}{(a+b)(a-b)}-\frac{e^{-2aT}(e^{2at-1})}{2a(a-b)},\\ \gamma_2 &= \frac{1}{ab}\Bigg(\gamma_1+C(t,T)-C(0,T)\\&\quad+\frac{1}{2}B(t,T)^2-\frac{1}{2}B(0,T)^2+\frac{t}{a}-\frac{e^{-a(T-t)}-e^{-aT}}{a^2}\Bigg),\\ \gamma_3 &= -\frac{e^{-(a+b)t}-1}{(a-b)(a+b)}+\frac{e^{-2at}-1}{2a(a-b)},\\ \gamma_4 &= \frac{1}{ab}\left(\gamma_3-C(0,t)-\frac{1}{2}B(0,t)^2+\frac{t}{a}+\frac{e^{-at}-1}{a^2}\right),\\ \gamma_5 &= \frac{1}{b}\left(\frac{1}{2}C(t,T)^2-\frac{1}{2}C(0,T)^2+\gamma_2\right),\\ \gamma_6 &= \frac{1}{b}\left(\gamma_4-\frac{1}{2}C(0,t)^2\right).\end{aligned}\tag{10.9}$$

The functional form can similarly be expressed as:

$$\theta(t)=F_t(0,t)+aF(0,t)+\phi_t(0,t)+a\phi(0,t),\tag{10.10}$$

where

$$\phi(t,T)=\frac{1}{2}\sigma_1^2B(t,T)^2+\frac{1}{2}\sigma_2^2C(t,T)^2+\rho\sigma_1\sigma_2B(t,T)C(t,T)[26].\tag{10.11}$$

The price of a European option can be similarly constructed as in Eq 6.35 where h is given by:

$$h=\frac{1}{\sigma_p}N(h)-KP(t,T)N(h-\sigma_p).\tag{10.12}$$

The volatility function σ_p is more complex than it's one-factor relative.

$$\begin{aligned}\sigma_p^2=\int_0^t\Big[&\sigma_1^2\left(B(,T)-B(\tau,t)\right)^2\\&+\sigma_2^2\left(C(\tau,T)-C(\tau,t)\right)^2\\&+2\rho\sigma_1\sigma_2\left(B(\tau,T)-B(\tau,t)\right)\left(C(\tau,T)-C(\tau,t)\right)\Big]d\tau.\end{aligned}\tag{10.13}$$

This equation can be simplified by letting

$$\begin{aligned}U&=\frac{1}{a(a-b)}\left(e^{-aT}-e^{-at}\right),\\V&=\frac{1}{b(a-b)}\left(e^{-bT}-e^{-bt}\right).\end{aligned}\tag{10.14}$$

The solution to this equation can thus be illustrated as:

$$\sigma_p^2 = W_1 + W_2 + W_3, \tag{10.15}$$

where

$$\begin{aligned}
W_1 &= \frac{\sigma_1^2}{2a} B(t,T)^2 \left(1 - e^{-2at}\right), \\
W_2 &= \sigma_2^2 \left(\frac{U^2}{2a} \left(e^{2at} - 1\right) + \frac{V^2}{2b} \left(e^{2bt} - 1\right) - \frac{2UV}{a+b} \left(e^{(a+b)t} - 1\right) \right), \\
W_3 &= \frac{2\rho\sigma_1\sigma_2}{a} \left(e^{-at} - e^{-aT}\right) \left[\frac{U}{2a} \left(e^{2at} - 1\right) - \frac{V}{a+b} \left(e^{(a+b)t} - 1\right) \right].
\end{aligned} \tag{10.16}$$

It must be noted that the Jamshidian decomposition procedure cannot be used to extend these formulae to price coupon-bearing bonds yet it is possible to price European zero-coupon bonds under the three modeling methods as described in Section 6.2.

10.3.1 Constructing the Two-Factor Tree

The dependence on the first stochastic variable on the second can be removed by some clever manipulation. Let

$$y = x + \frac{u}{b-a}. \tag{10.17}$$

The underlying stochastic processes can thus be described as:

$$\begin{aligned}
dy &= [\theta(t) - ay]dt + \sigma_3 dz_3, \\
du &= -budt + \sigma_2 dz_2,
\end{aligned} \tag{10.18}$$

where

$$\sigma_3^2 = \sigma_1^2 + \frac{\sigma_2^2}{(b-a)^2} + \frac{2\rho\sigma_1\sigma_2}{b-a}. \tag{10.19}$$

Furthermore, the correlation between the processes dz_2, dz_3 is

$$\tilde{\rho} = \frac{\rho\sigma_1 + \sigma_2/(b-a)}{\sigma_3}. \tag{10.20}$$

The tree building follows a similar procedure to all the previous methodology. This highlights the flexibility of modeling these credit derivatives with the use of trinomial trees. The update functions under this construction are illustrated in Eq 10.21.

$$\begin{aligned}
r &= f^{-1}\left(j\Delta y - \frac{k\Delta u}{b-a}\right), \\
P_{m+1} &= \sum_{j,k} Q_{m,j,k} \exp\left(-f^{-1}\left(\alpha_m + j\Delta y - \frac{k\Delta u}{b-a}\right)\Delta t\right), \\
Q_{m+1,j,k} &= \sum_{j,k} Q_{m,j^*,k^*} \exp\left(-f^{-1}\left(\alpha_m + j^*\Delta y - \frac{k^*\Delta u}{b-a}\right)\Delta t\right),
\end{aligned} \tag{10.21}$$

where k^*, j^* are all the possible pairs of combinations at time $m\Delta t$. The shift required at each time step α_m can thus be described as

$$\alpha_m = \frac{1}{\Delta t}\left(\sum_{j,k} Q_{m,j,k} \exp\left(j\Delta y - \frac{k\Delta u}{b-a}\right) - \ln P_{m+1}\right). \tag{10.22}$$

The transition probability matrices are constructed in the same manner as outlined in Sec.11.1.

10.3.2 Two-Additive-Factor Gaussian model

Furthermore, it can be shown that the two-factor Hull-White model can be written as a Two-Additive-Factor Gaussian model by means of a suitable transformation. This property could bode useful when attempting to calibrate the model parameters. For the sake of completion, the G2++ model is briefly outlined below and the calibration transformation parameters are provided. For full details and a more formal proof, we refer the reader to [8]. In the G2++ framework, the short rate is modelled as a function of two stochastic variables $x(t)$, $y(t)$ and a deterministic function $\Phi(t)$. Let $\bar{a}, \bar{b}, \sigma_1, \sigma_2, \bar{\rho}$ denote the factors of the Hull-White two-factor model. The analogy with the G2++ model can its calibration parameters can be shown as

$$\begin{aligned} a &= \bar{a}, \\ b &= \bar{b}, \\ \sigma &= \sqrt{\sigma_1^2 + \frac{\sigma_2^2}{(\bar{a}-\bar{b})^2}} + 2\bar{\rho}\frac{\sigma_1\sigma_2}{\bar{b}-\bar{a}}, \\ \eta &= \frac{\sigma_2}{\bar{a}-\bar{b}}, \\ \rho &= \frac{\sigma_1\bar{\rho}-\eta}{\sigma}, \\ \Phi(t) &= r_0 e^{-\bar{a}t} + \int_0^t \theta(\nu) e^{-\bar{a}(t-\nu)} d\nu. \end{aligned} \tag{10.23}$$

Of course, in an analogous manner it is possible to transform the G2++ model into the Hull-White model. We refer to reader to Blanchard for further details [27].

11 Constructing Two One-Factor Models

For the purposes of pricing the desired credit derivatives, it was decided to use the former approach, to construct two one-factor Hull-White trees and incorporate the correlation thereafter. One follows the suggested tree building procedure by Schönbucher [1]. The desired two-dimensional short rate model (and analogously a two-dimensional default intensity model) must also be extended to incorporate defaultability in order to price credit derivatives. The resulting 3D-lattice tree extends into 3-dimensions, consisting of $[\min(m, 2j^r_{max})] \times [\min(m, 2j^\lambda_{max})]$ number of nodes for each $m\Delta t$ time step. The possibility of a bond to default at any given time also allows incorporates the ability of the bond to recover. This can be expressed as the fractional and equivalent recovery models. For a more formal representation of these processes, one refers the reader to [1]. It is key to note that whichever specification is required, the model can easily be adapted to fit the modelers needs. For the purposes of the model construction as a 3D-lattice, it is assumed that defaults lie within the time period $[t, t + \Delta t]$. The general concept is to construct two independent 2D short-rate (r) and default intensity (λ) trees, to aptly combine and calibrate the resulting 3D-tree. More formally, the recipe for extending the 2D-model can be illustrated as follows:

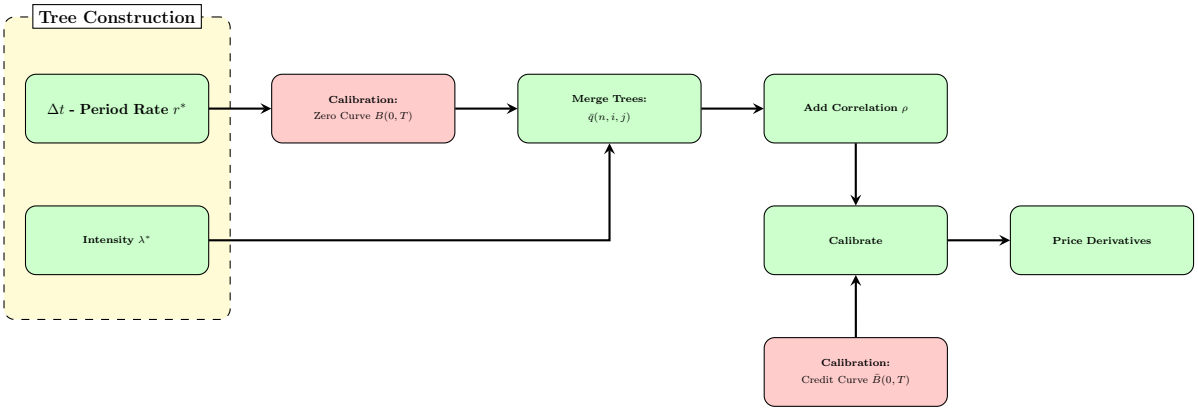

Figure 11.1: Illustration of the Three-dimensional Modelling Process.

Analogously to the 2D-tree, the calibration of the 3D-tree to enable credit derivative pricing requires both a forward and backward propagation step. Moreover, some additional intermediary steps are required to ensure the probability space remains within the desired bounds. Once established, the Arrow-Debreu prices and in turn, the default intensity are determinable, through calibration with a suitable credit term structure.

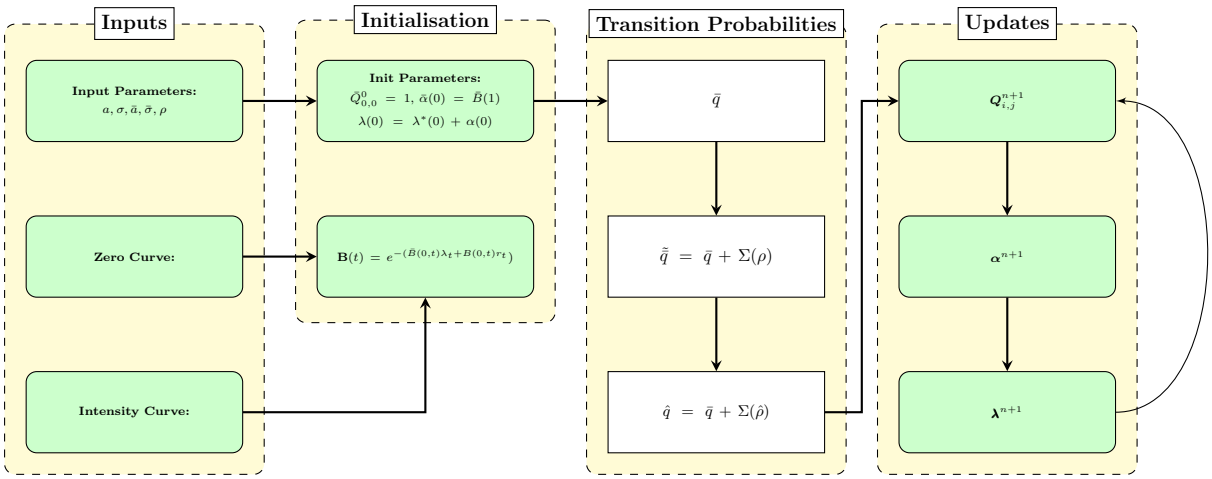

Figure 11.2: Illustration of the three-dimensional forward propagation procedure using the Hull-White model.

11.1 Transition Probabilities

When merging the two independent trees, the transition probabilities to the resulting nodes in $(r_u, r_m, r_d) \times (\lambda_u, \lambda_m, \lambda_d)$ space must also be adapted. This step introduces the correlation between the two Brownian processes. Let (p'_u, p'_m, p'_d) and (p_u, p_m, p_d) denote the marginal probabilities of the default intensity λ and short-rate r trees respectively. As before, the transition probabilities for both independent trees can be constructed as per Tab 6.1. The transition probabilities of the combined movements of the short-rate (r) and the intensity (λ) can be expressed as:

$$\bar{q}(n,i,j) = \begin{pmatrix} p'_u p_d & p'_u p_d & p'_u p_d \\ p'_u p_d & p'_u p_d & p'_u p_d \\ p'_u p_d & p'_u p_d & p'_u p_d \end{pmatrix} + \epsilon\Sigma, \tag{11.1}$$

where

$$\Sigma = \begin{cases} \begin{pmatrix} -1 & -4 & 5 \\ -4 & 8 & -4 \\ 5 & -4 & -1 \end{pmatrix} & \rho < 0 \\ \\ \begin{pmatrix} 5 & -4 & -1 \\ -4 & 8 & -4 \\ -1 & -4 & 5 \end{pmatrix} & \rho > 0, \end{cases} \tag{11.2}$$

where $p'_{u,m,d}$ and $p_{u,m,d}$ correspond to the marginal probabilities of the intensity and short-rate, respectively. Additionally, ϵ can be defined as:

$$\epsilon = \begin{cases} \frac{\rho}{36} & \rho > 0 \\ -\frac{\rho}{36}, & \rho < 0, \end{cases} \tag{11.3}$$

and ρ is the correlation between the two stochastic processes [9]. The sum of either the rows or columns will return the marginal probabilities of the two independent processes. Additionally, in the case of binomial trees, the correlation framework can be set as follows [18]:

$$\bar{q}(n,i,j) = \begin{pmatrix} p'_u p_u + \epsilon & p'_u p_d - \epsilon \\ p'_d p_u - \epsilon & p'_d p_d + \epsilon \end{pmatrix}, \tag{11.4}$$

where

$$\epsilon = \begin{cases} \frac{\rho}{4}, & \rho > 0, \\ -\frac{\rho}{4}, & \rho < 0. \end{cases} \tag{11.5}$$

It must be noted that the probability matrix $\bar{q}(n,i,j)$ corresponds to a tree consisting of non-defaultable nodes. Due to this construction, and for non-zero ρ, it is possible that these transition probabilities become negative for some time point $m \leq N$. Note that for extreme correlations the transition probabilities converge at $j = 0$ nodes to the following:

$$\begin{matrix} \lim\limits_{\rho \to -1} \bar{q} & \lim\limits_{\rho \to 1} \bar{q} \\ \begin{pmatrix} \frac{1}{3} & 0 & 0 \\ 0 & \frac{2}{3} & 0 \\ 0 & 0 & \frac{1}{3} \end{pmatrix} & \begin{pmatrix} 0 & 0 & \frac{1}{3} \\ 0 & \frac{2}{3} & 0 \\ \frac{1}{3} & 0 & 0 \end{pmatrix}. \end{matrix} \tag{11.6}$$

Naturally one can remedy the negative transition probabilities by increasing the number of time steps, though a suitable alternative presents itself. During each transition level t, one checks the nodes which yield negative transition probabilities. The chosen ρ is modified such that the maximum value of ρ which obtains the minimum non-negative transition probabilities. Note that once a node yields a negative transition probability, all nodes emanating from this will similarly yield negative probabilities. This procedure will induce a small bias into the correlation, though will disappear as $\lim \Delta t \to 0$ [25]. Fig 11.3 illustrates the obtained ρ matrix for each time step t for a given set of parameters.

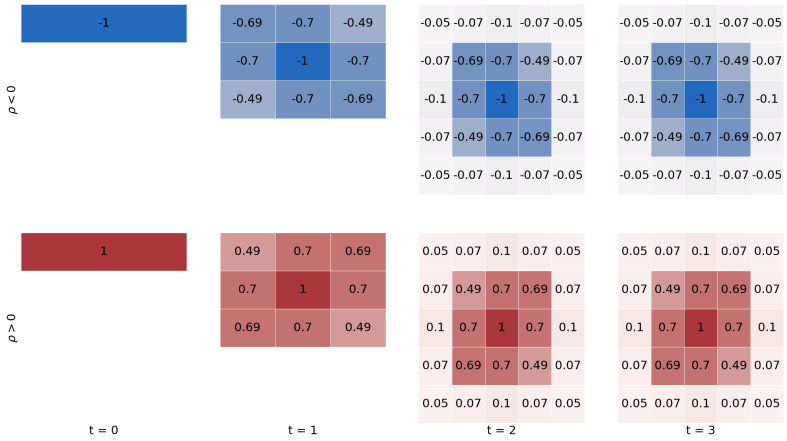

Figure 11.3: Optimized ρ parameters obtained for each node from an initial $\rho = -1$ transition probabilities for the layers 0.

11.2 Incorporating Default

Once the transition probabilities have been remedied, one must now incorporate the likelihood for a bond to default at any given time step. This adds an extra dimensionality to the three-dimensional space. The survival probability can be defined as:

$$1 - p = \mathbb{E}^Q \left[\exp\left(- \int_t^{t+\Delta t} \lambda_s ds \right) \middle| \mathscr{F}_t \right]. \tag{11.7}$$

It is assumed that the default intensity is constant over time $[t, t + \Delta t]$. Thus

$$1 - p = e^{-\lambda_t \Delta t}. \tag{11.8}$$

By allowing one default transition for each node between $[t, t + \Delta t]$, given that default happens at the beginning of an interval, a default branching transition can be illustrated as:

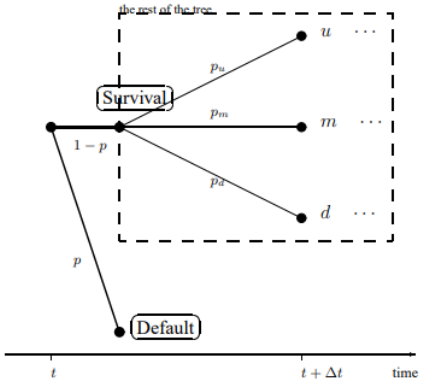

Figure 11.4: Illustration of survivability and defaultability at a particular node in the tree [1].

The full tree can similarly be displayed as:

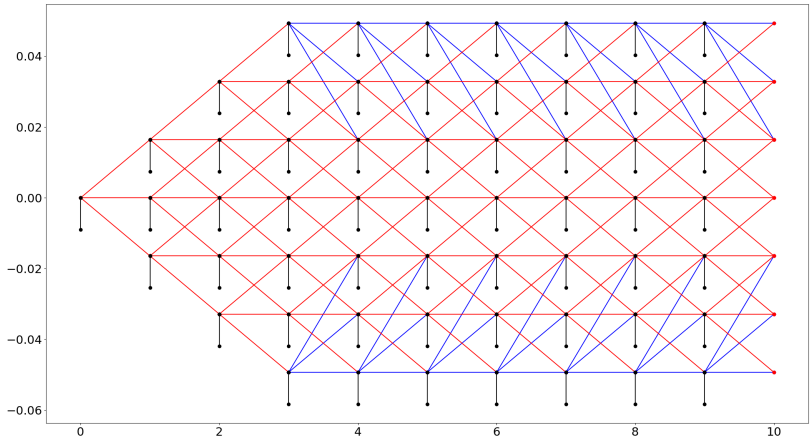

Figure 11.5: Illustration of a defaultable two-dimensional tree at any node.

By incorporating this additional dimension and the likelihood to default, the transition probabilities must similarly taken into account this amendment. By defining the default probability as p and survival as $1-p$, the marginal intensities must be scaled by:

$$p_u \to p_u(1-p), \quad p_u \to p_m(1-p), \quad p_d \to p_u(1-p), \tag{11.9}$$

where the tree would end at a default. Though it is possible to construct a separate default tree, one can compensate for the default branches during pricing. One can consider the transition probabilities $\bar{q}(\cdot)$ as the probability of transitioning from node (n-1, i, j) to (n, i, j) given survival. Given survival, the survival probability (as in Eq 11.7) is taken into account in Eq 12.2 in the calculation of $V_{ij}^{''n}$ and thus, the transition probability matrix need be amended.

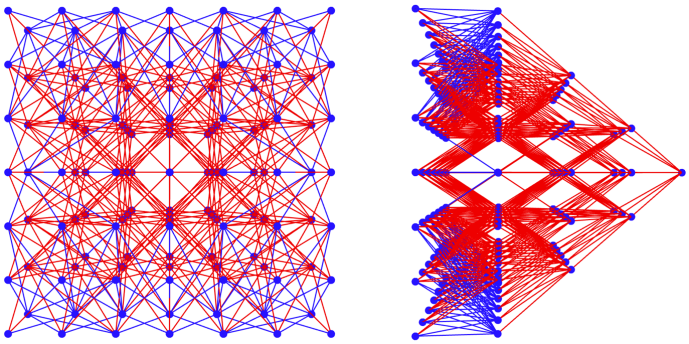

Figure 11.6: Illustration of an un-calibrated trinomial tree.

11.3 Fitting the combined tree

Once the trees for r and λ^* have been constructed, one must calibrate the combined tree to the default intensity λ. In doing so, one must not affect the calibration to r [1]. This is achieved by shifting the combined tree in only one-dimension, the intensity space. As in the short-rate case, this can be illustrated as:

$$\lambda_i^n = \lambda_i^{*n} + \alpha_\lambda^n. \tag{11.10}$$

By calibrating in this way, one only affects the realisations of the intensity at the nodes (n, i, j), while also not unsettling the dynamics of r and its calibration to the default free bond prices.

In contrast to the 2-dimensional case, this calibration method must take into account the full tree. Let $\bar{Q}^n_{i,j}$ denote the state price at node (n, i , j). As before, the root node survival state price is initialised as $\bar{Q}^0_{0,0} = 1$. Additionally, $\lambda^0_0 = \alpha_\lambda$ is chosen such that:

$$\bar{P}_1 = e^{-r^0_0 \Delta t} e^{-\lambda^0_0 \Delta t}, \tag{11.11}$$

where $\bar{P}_1$ are the defaultable bond prices. Thus:

$$\bar{\alpha}_0 = -\frac{1}{q\Delta t}\left(\ln\left(\bar{P}_1\right) - \ln\left(P_1\right)\right). \tag{11.12}$$

As in the two-dimensional case, the state prices must be updated via:

$$\bar{Q}^{n+1}_{i,j} = \sum_{k,l} \bar{Q}^n_{i,j}\bar{q}(k,l,i,j)\exp\left(-(r^n_l + q\lambda^n_k)\Delta t\right). \tag{11.13}$$

At this stage one must distinguish between using a fractional or equivalent recovery model. If one considers defaults to occur in a continuous time model in an interval $[t, t+\Delta t]$, the fractional recovery factor $e^{-q\Delta t}$ is required. In contrast, during equivalent recovery where defaults occur at the beginning at an interval, one replaces this factor with $1 - q(1 - e^{-\lambda\Delta t})$. Under this construction, this factor yields an expectation of 1 in the event of survival, and $(1 - q)$ in the event of default. For the purposes of this paper, fractional recovery will be used. Furthermore, in order to calibrate this model an expression for $\bar{\alpha}_{n+1}$ can be obtained via:

$$\begin{aligned}\bar{P}_{n+1} &= \sum_{k,l} \bar{Q}^{n+1}_{i,j}\exp\left(-(r^{n+1}_l + q\lambda^{n+1}_k)\Delta t\right) \\ &= \sum_{k,l} \bar{Q}^{n+1}_{i,j}\exp\left(-(r^{n+1}_l + q\lambda^{*n+1}_k)\Delta t\right)\exp\left(-\bar{\alpha}_{n+1}\Delta t\right).\end{aligned} \tag{11.14}$$

Re-arranging the above formula yields:

$$\bar{\alpha}_n = \frac{1}{\Delta t}\left(\ln\left(\sum_{i,j}\bar{Q}^n_{i,j}\exp\left(-(r^n_j + q\lambda^{*n}_i)\,\Delta t\right)\right) - \ln\bar{P}_{n+1}\right). \tag{11.15}$$

By iterating over the tree, the calibrated tree can be obtained, as illustrated in Fig 11.7.

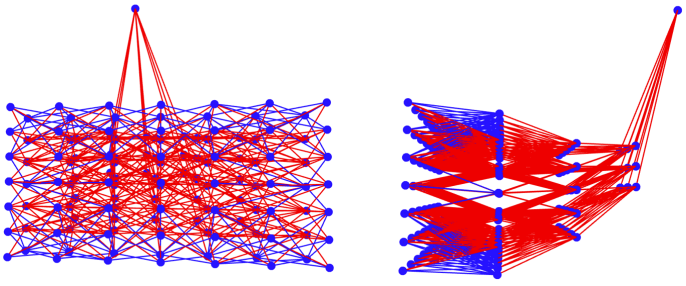

Figure 11.7: Illustration of a calibrated 3d Trinomial tree over 10 steps.

12 Pricing Credit Derivatives

Once the calibrated tree has been constructed, it is now possible to price various derivative securities. One benefit of the chosen model, is the diversity of derivatives which can be priced. The pricing is achieved in a similar method to the 2D counterpart, though one must take into account the characterisations of the derivative by its payoff in default, survival and early exercise features. Thus, in order to price specific credit derivatives, one must define the following variables at each node (n, i, j) whereby:

- f_{ij}^n - The payoff of the derivative at default
- F_{ij}^n - The payoff of the derivative given survival. This includes coupons, payments etc
- G_{ij}^n - The early exercise payoff

The sign of these payoffs is at the discretion of the user, yet in this thesis one views the pricing from the viewpoint of the issuer. Let V_{ij}^n denote the price of the credit derivative at node (n, i, j). The back-propagation procedure proceeds as before, by setting the end nodes of the tree to the value at final payoff.

$$V_{ij}^N = F_{ij}^N \tag{12.1}$$

One continues the backward induction by considering the survival nodes and discounting accordingly, as in the 2D case.

$$V_{ij}^{''n} = \sum_{k,l} p_{i,j}^n e^{-r_j^n \Delta t} V_{kl}^{n+1} \quad \forall n < N, \tag{12.2}$$

As the tree is constructed from the perspective that each node represents the payoff given survival, the defaultability is taken into account during back-propagation as:

$$V_{ij}^{'n} = e^{-\lambda_i^n \Delta t} V_{kl}^{''n} + (1 - e^{-\lambda_i^n \Delta t}) f_{ij}^n + F_{ij}^n \quad \forall n < N. \tag{12.3}$$

Finally, the early exercise payoff is taken into account, yielding the price of the credit derivative V_{ij}^n at node (i, j) for a given time step n.

$$V_{ij}^n = \max\left(V_{ij}^n, G_{ij}^n\right). \tag{12.4}$$

This procedure is repeated for each time step yielding the price of the credit derivative at the root node $V_{0,0}^0$. Due to the general nature of this tree setup, it is possible to price a range of different credit derivatives based on a few specifications [1].

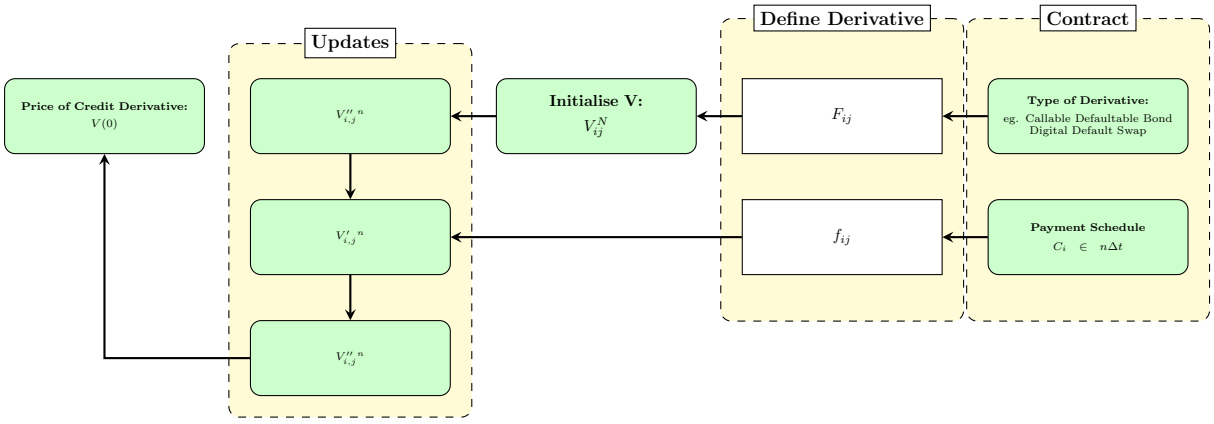

Figure 12.1: Illustration of the back-propagation procedure for the pricing of a credit derivative.

12.1 Modeling Recovery

As in the case of modeling the credit term structure, the defaultable bonds have an inherent value when default occurs. These defaultable claims can be modeled in a variety of ways, namely; zero-recovery (ZR), recovery of treasury (RT), multiple defaults (MD), recovery of market value denoted as fractional recovery (RMV) or recovery of par (RP). This is of particular importance

during backpropagation and pricing of particular credit derivatives. This thesis focuses on the pricing of defaultable bonds, so one begins by attempting to price a zero-coupon defaultable bond. The recovery of market-value approach or recovery of par seem to be the most apt choices. That being said, if one were to use (RP) in pricing bonds with a large time to maturity, it is likely that the value of a bond at default may exceed the value of the bond given survival. One potential remedy is to discount this constant value throughout the tree which would make the interpretation of the results more reasonable. Due to this, the recovery of market value was selected as a recovery pricing model for this thesis.

12.1.1 Defaultable zero-coupon bonds

Consider a defaultable zero-coupon bond which has survived up until time T. This bond is priced as:

$$\bar{B}(t,T) = \mathbb{E}\left[e^{-\int_t^T r(s)ds\mathbb{1}_{\tau>T}}\right]. \tag{12.5}$$

Let $\mathcal{G}$ be a subset of the filtration $\mathcal{F}_\infty$. Thus, the price of the zero-coupon bond can be expressed as the conditional expectation of the zero-coupon bond given the information up until time t. This equates as:

$$\begin{aligned}\bar{P}(0,T) &= \mathbb{E}\left[e^{-\int_0^T r(s)ds\mathbb{1}_{\tau>T}}\right] \\ &= \mathbb{E}\left[\mathbb{E}\left[e^{-\int_0^T r(s)ds\mathbb{1}_{\tau>T}}\right]|\mathbb{G}\right] \\ &= \mathbb{E}\left[e^{-\int_0^T r(s)ds}\mathbb{E}\left[\mathbb{1}_{\tau>T}\right]|\mathbb{G}\right] \\ &= \mathbb{E}\left[e^{-\int_0^T r(s)+\lambda(s)ds}\right]\end{aligned} \tag{12.6}$$

In the case where $\rho = 0$, and the two stochastic processes are independent, it is possible to factor out these integrals whereby:

$$\begin{aligned}\bar{P}(0,T) &= P(0,T)\mathbb{E}\left[e^{-\int_0^T \lambda(s)ds}\right] \\ &= P(0,T)P_s(0,T),\end{aligned} \tag{12.7}$$

where $P_s(0,T)$ is the implied survival probability at time T. Of course, these two processes are usually not independent and this de-coupling procedure will not apply.

12.1.2 Recovery of Market Value

Prior to pricing the chosen credit derivatives in the lattice model, it will be necessary to lay down the assumptions of the chosen recovery model in the event of default. Let τ and $\Phi(\tau)$ denote the time of default and value of the claim in the event of default. The value of the claim of the defaultable asset is thus:

$$\Phi(\tau) = (1-q)P(\tau-). \tag{12.8}$$

Under this construction, it is possible to determine the price of the pre-defaulted asset by means of recursion [9]. This is due to the fact that Eq 12.8 is proportional to the pre-default claim, which in itself is dependent on the recovery payoff. This leads to the following definition. Let X denote the payoff of the defaultable asset at time T. Consider the first jump of a point process $N(t)$ (with intensity $\lambda(t)$). Let τ be the time at which this first jump occurs. Finally, assume that the martingale

$$m(t) = e^{-\int_0^t q\lambda(s)ds}\mathbb{E}\left[e^{-\int_t^T r(s)+q\lambda(s)dsV}\middle|\mathcal{F}_t\right] \tag{12.9}$$

does not jump at this time τ. The price of the defaultable asset under the assumption of recovery market value is thus illustrated as:

$$P_{RMV}(t) = \mathbb{1}_{\tau>t}\mathbb{E}\left[e^{-\int_t^T r(s)+q\lambda(s)dsV}\middle|\mathcal{F}_t\right] + \mathbb{1}_{\tau=t}(1-q)P_{RMV}(t-) \tag{12.10}$$

12.2 Two-Factor Closed Form Solution

It is possible to specify the payoffs of a credit derivative at the end nodes, as in the case of the one-factor model. The price of a defaultable bond under these conditions is the solution to the equations illustrated in Eq 12.11 as

$$\begin{aligned} \bar{B}(t,T) &= B(t,T)e^{\bar{A}(t,T)-\bar{B}(t,T)r(t)}, \\ \bar{A}(t,T) &= \frac{1}{2}\int_t^T \bar{\sigma}^2(s)\bar{B}(t,s)^2 ds - \int_t^T \bar{B}(t,s)\tilde{k}(s)ds, \\ \tilde{k} &= \bar{k}(t) + \rho\bar{\sigma}(t)B(s,T). \end{aligned} \tag{12.11}$$

In doing so, it would be possible to construct a tree at the option expiry and analytically price defaultable European zero-coupon bonds at their end nodes based on the methods previously outlined [1].

12.3 Three-Dimensional Lattice Approach

The general form, modelling a tree representing the life of the bond is the chosen approach for this thesis. On that basis, this allows the user to price a range of credit derivatives under a suitable definition of F, f and G. A list of popular credit derivatives are illustrated in Tab 12.1. Note that based on which credit intensity one chooses, in the pricing of defaultable bonds it is possible to recoup the one-factor short rate results. This can be achieved by setting $q = 0$ or analagously a full recovery rate $\pi = 1$. Of course, the Eq 11.15 as well as it's initialisation need to be taken into consideration. As the variables $q\Lambda$ and Λ are linear combinations of one another, one could construct the tree for the defaultable bond yields and scale in the loss quota during back-propagation. Of course, under this setting it would be easier to simply construct the one-factor model.

Table 12.1: Pricing methodologies for various credit derivatives based on a fractional recovery model [1].

	Credit Derivative		
	Defaultable Bond	**Digital Default Swap**	**Default Swap**
F_{ij}^N	$\mathrm{L} + C_N$	1	1
F_{ij}^n	$\mathbb{1}\{C_i\}$	$\mathbb{1}\{-s\}$	$\mathbb{1}\{-s\}$
f_{ij}^n	$(1-q)V''^n$	1	$1-(1-q)\bar{B}_{i,j}^{*n}$
$G_{i,j}^n$	$-\infty$	$-\infty$	$-\infty$

13 Hedging 3-Dimensional Tree

The Greeks of the three-dimensional tree can be obtained by similar methods as outlined in Section 7.5 with some additional sensitivities relating to default and intensity [1]. Let Υ and

ζ denote the sensitivity to default and intensity respectively. These "Greeks" can thus be expressed as:

$$\begin{aligned} \Upsilon &= \frac{V^1_{1,0} - V^1_{-1,0}}{2\Delta\lambda}, \\ \zeta &= V^0_{0,0} - f^0_{0,0}, \end{aligned} \tag{13.1}$$

where $V^n_{i,j}$ correspond to the locations of nodes at the coordinates (n, i, j). Additionally $f^0_{0,0}$ corresponds to the implied default probability at the root node.

13.1 Implementation

The three-dimensional tree was constructed for a range of parameter values and the back-propagation procedure was implemented to price a corporate defaultable bond.

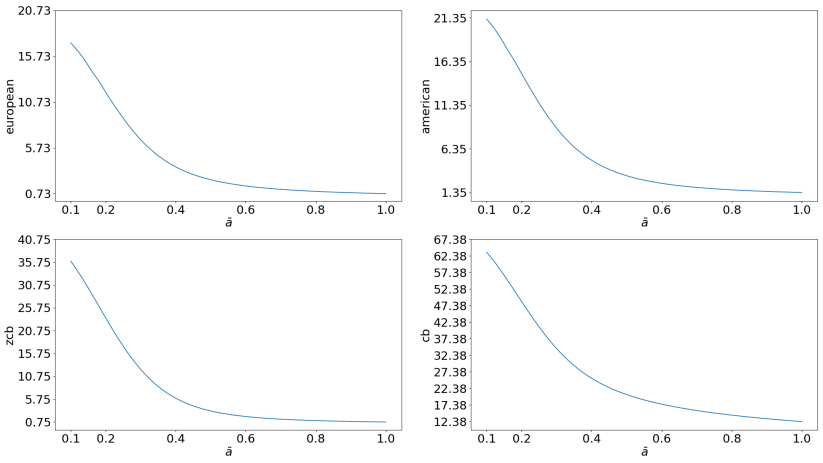

Figure 13.1: Illustration of the effect of $\bar{a}$ on the price of European and American coupon bearing bonds as well as their non-exercise counterparts.

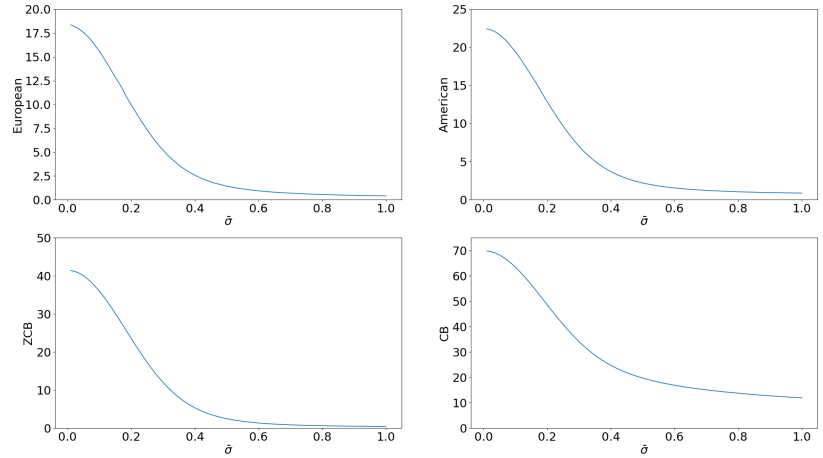

Figure 13.2: Illustration of the effect of $\bar{\sigma}$ on the price of European and American coupon bearing bonds as well as their non-exercise counterparts.

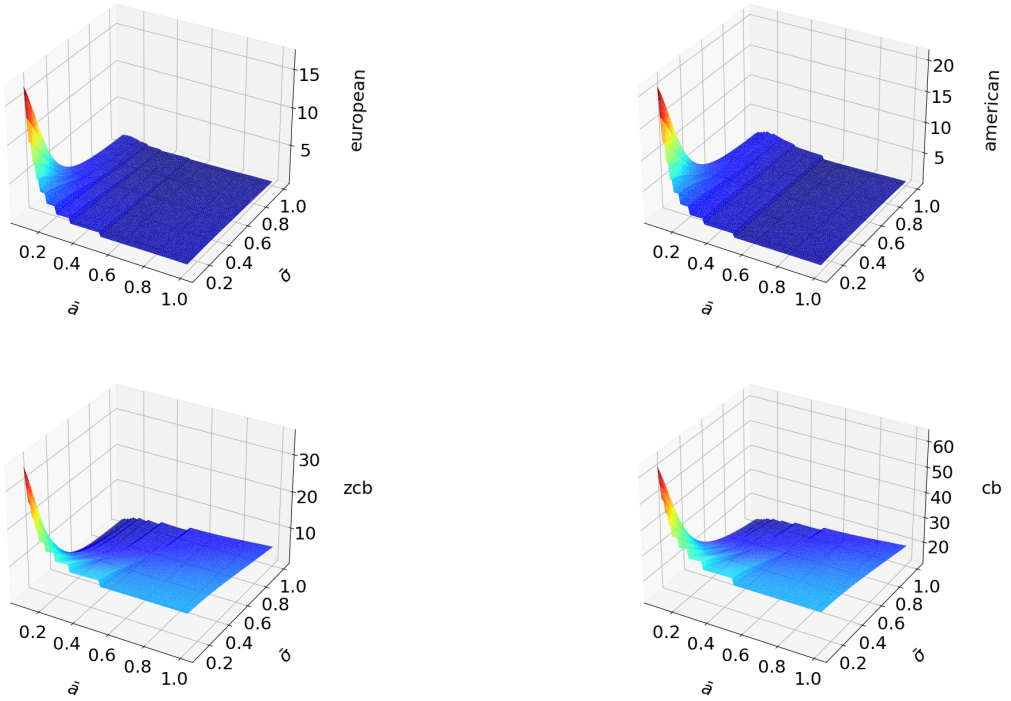

Figure 13.3: Surface representation of the combined effects of $\bar{a}$ and $\bar{\sigma}$ on the price of European, American, ZCB and CB bonds.

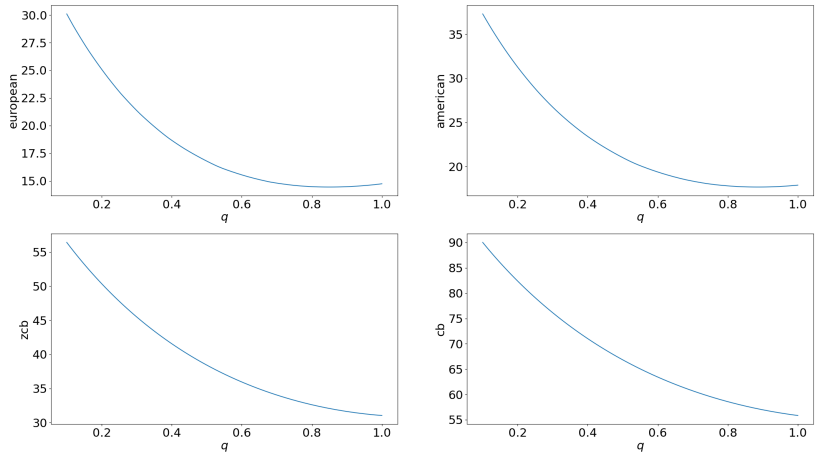

Figure 13.4: Illustration of the effect of the loss quota q on the price of European and American coupon bearing bonds as well as their non-exercise counterparts.

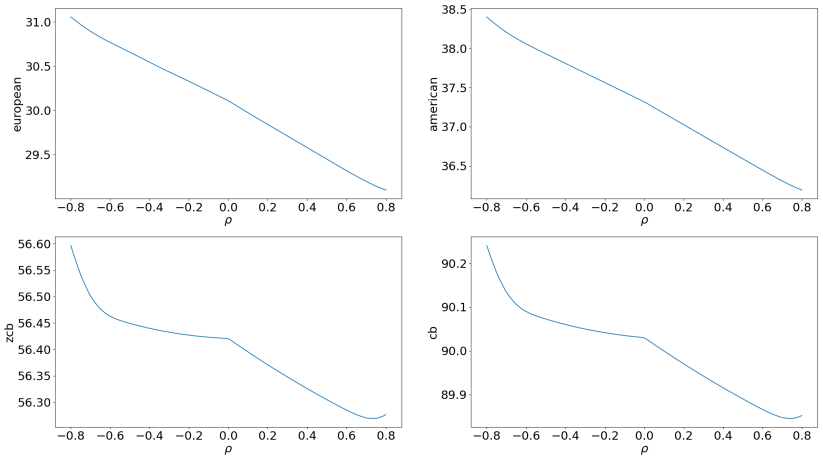

Figure 13.5: Illustration of the effect of ρ on the price of European and American coupon bearing bonds as well as their non-exercise counterparts.

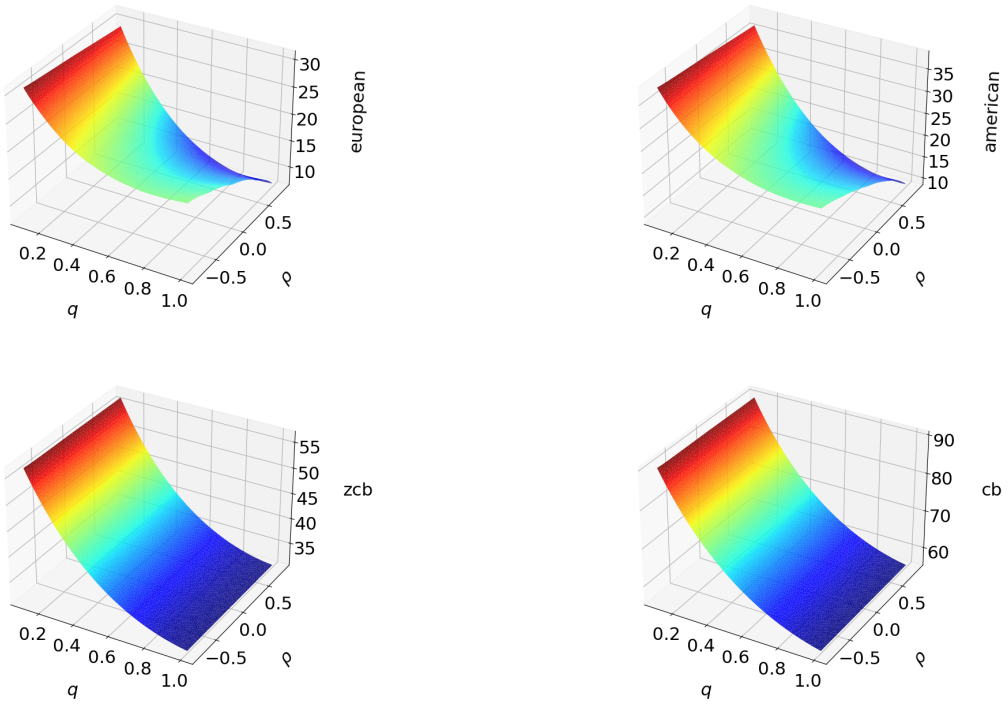

Figure 13.6: Surface representation of the combined effects of ρ and loss quota q on the price of European, American, ZCB and CB bonds.

14 Discussion & Conclusion

This thesis was able to replicate and implement the addition of default to the two-factor trinomial tree initially developed by Schönbucher [1]. There are a number of things to note. As can be seen in the model key Fig 4.1, there a number of features to consider when developing a two factor model, especially if one were to utilise it in practice. The model framework is heavily dependent on both the benchmark curves, as is to be expected. The choice of risk-free curve is not trivial, yet the data is publicly available and is "model ready". This means at least that any errors would be limited to the choice of risk-free curve and not be subject to any modelling errors, at least if the bond being modelled is in-sample (time to maturity) and lies within the term-structure bounds.

Of course, one still needs to tend to the choice of "risk-free" curve, where treasury curves, OIS and LIBOR rates are valiant competitors with a significant spread between them. As payoffs from interest rate derivatives usually depend on LIBOR, models have been developed to model the evolution between two different term structures. Hull outlines that a trinomial tree can be extended to jointly model the OIS and LIBOR rates simultaneously, without assuming the spread to be constant or deterministic [18].

In contrast, the credit curve construction can be developed in a number of ways, and these specifications will directly impact the obtained prices and thus, is a natural source of error. Due to the nature of these lattice trees, small deviations in specifications will compound throughout the nodes of the tree and yield significant variations in price. The sensitivity of the tree model can be analysed, through the use of the Greeks in both the 2d and 3d case, which would give a relative indication of the impact of each respective curve. Moreover, one possible alternative to the modelling approach is the use of CDS spreads to construct the curves. This would in one sense be ideal, though the data is expensive, potentially unreliable and unlikely to be available for each corporation on each pricing date within the data set.

Furthermore, the 3d model provides a lot of flexibility and diversity in modeling a range of credit derivatives. This is particularly attractive if one were to use this framework in practice. Additionally, the framework is not limited to the Hull-White model and can even be generalized to the entire class of affine term structure models as in Section 7. Similarly, it is not limited to probability distributions with three possible outcomes at each node, and will be applicable to both 2d and 3d lattice based modeling approaches.

Based on how the 3d model was constructed, there are some possible extensions and improvements which will have influence over the time and memory complexity of the model. The 3d model is particularly susceptible to memory and complexity issues when dealing with a larger number of time steps (> 100). The probabilities in particular, need only be stored for the $(2j^R_{max} + 1, 2j^C_{max} + 1, 9)$ combinations, as the tree will reach its saturation point. This thesis constructed the probability matrix for each time step, shifting each probability space for each node accordingly to showcase where each node could traverse. This is appealing from a matrix multiplication perspective though does incorporate a lot of zero values in large matrices. Naturally, sparse matrices can be used to rectify this issue. Additionally, due to the enforcement of non-negative transition probabilities, one can see that boundary nodes converge to independence ($\rho = 0$) between the two processes. In the two-dimensional case, this issue is also apparent though is rectified by the introduction of j_{max}. As a result, a similar implementation could be incorporated to trim the tree and reduce the dimensionality of the matrices and in-turn, the number of nodes. These nodes similarly contribute little to the overall price weighting, mainly due to these extreme events having a low transition probability. By this logic, as their relative

contribution is minimal, the trimming of the tree could be justified.

Based on the results illustrated in Section 13.1, the impact of correlation between the two stochastic processes has a low relative contribution to the price of the bond. The impact of $\bar{a}$ is analogous to the one-factor counterpart, yet $\bar{\sigma}$ shows an inverse relationship. The most notable variable to consider is the recovery rate π, expressed as a function of the loss quota q. Of course, this is in part due to the nature of the recovery of market value, which was chosen in the modeling framework. Never the less, in the case of the relevant contribution of modeling parameters and calibrating them, the impact of the loss quota is notable.

Relating further to the calibration parameters, the values are assumed to be constant at each time step. It is possible to extend the trees to include time-varying calibration parameters, though this would highly impact the complexity of the model which is not necessarily desirable. Section 7.3 provides a framework for implementing a time-varying drift and mean reversion parameter. Additionally, it provides a way of adding bounds to the value of the short rate at nodes in the tree. This could bode useful if the federal reserve or governing body would declare that interest rates would not breach a certain threshold. This gives the user a lot of freedom to manipulate the tree, though requires the specification of a suitable drift function which may not be entirely trivial.

One major factor which would influence the aid with the time complexity in the 3d case is the introduction of a time-varying Δt as was described in Section 7. In doing so, one could more intricately model the option pricing procedure by having a finer Δt close to exercise dates and more coarse Δt post option expiry. This could likely even increase the accuracy of the model, providing finer granularity in regions of interest as well as reducing the time and memory complexity. As the 3d model is constructed from the nesting of two two-dimensional models, this procedure would be implemented during the construction of the 2-dimensional trees. One further benefit of imposing a non-constant Δt, is the ability to exactly force the location of nodes on payment dates and exercise dates. In doing so, one can exactly match the term structure to these dates. That being said, if the number of time steps is less than the total number of coupon/exercise dates, the model will still yield dubious results. One possible solution to this is to stack the coupons on payment dates, so as certain node levels receive a linear combination of coupon payments. That being said, these implementations are considered superfluous, as the time and memory complexity of two-dimensional trees is low.

Of course, when calculating the relevant calibration parameters it is also possible to utilise different methods than the suggested Jamshidian procedure. The volatilities of caps/floors or swaptions can be matched to either the time-dependent a and σ using either the one factor or two-factor models, or alternative numerical methods. A notable alternative is the use of the G2++ model or the methods proposed in Section 7. Most importantly, based on Fig 13.5 and similarly emphasized by Schönbucher [1], the impact of correlation on the price of credit derivatives can be minor (he showed this by pricing digital default swaps), especially in relation to the other calibration parameters. A model has been proposed to calibrate each of these parameters, with one notable exception. The loss quota q, or analogously the recovery rate π has a significant impact on the pricing of the credit derivatives. In conjugation with the fact that even when recovery rate has been modelled, one must still choose a relevant recovery convention. This thesis chose recovery of market value, yet this is of course at the discretion of the user. This leads to the conclusion that specific emphasis should be taken when dealing with recovery.

Relating back to the model construction, due to the nature of default intensity as well as in-

terest rates, it is possible for both variables to become negative under the Hull-White model. Non-negativity is enforceable through a transformation of either variable using $\tilde{r} = e^r$ or $\tilde{\lambda} = e^{\lambda}$, though this will result in Eq.11.15 being no longer available in closed form. Thus, a root solving algorithm will need to be utilised to determine the α values at each time step. In the current market climate, modeling negative interest rates is in fact desirable, though negative intensities are a larger concern. As previously stated, default intensity as well as implied survival and default probabilities are heavily dependent on one another. Negative intensities could lead to negative survival/default probabilities which is most evident when using a small number of time steps. The model does not break down during these specifications, though a possible positive transformation would aid in the robustness and reliability of the model. Market practitioners have circumvented this issue by modelling the short-rate under the Hull-White model and the credit intensity using Black-Karasinski, enforcing the intensity to be non-negative without the need for a positive transformation at a later date. As the modelling framework is generalisable, this is a reasonable and easily implementable practical solution.

This thesis focused on implementing the conventional Hull-white model in the three dimensional framework. One major advancement would be the implementation of the generalisation of the transition probabilities to any affine term structure model. In doing so, one could not be limited to modeling under the Hull-White model, but in fact have access to any model which is a subclass of affine term-structure models. That being said, this generalisation does come with it's own inherent issues and is not just limited to transition probability generalisation.

References

[1] Philipp J.Schönbucher. "A Tree Implementation Of A Credit Spread Model For Credit Derivatives". In: *Available at SSRN 240868* (1999).

[2] Donatien Hainaut and Renaud MacGilchrist. "An interest rate tree driven by a Lévy process". In: *The Journal of Derivatives* 18.2 (2010), pp. 33–45.

[3] Natalia Beliaeva and Sanjay Nawalkha. "Pricing American interest rate options under the jump-extended constant-elasticity-of-variance short rate models". In: *Journal of Banking & Finance* 36.1 (2012), pp. 151–163.

[4] John C.Hull and Alan D.White. "A generalized procedure for building trees for the short rate and its application to determining market implied volatility functions". In: *Quantitative Finance* 15 (Mar. 2015). DOI: 10.1080/14697688.2014.961530.

[5] Dominic O'Kane and Saurav Sen. "Credit Spreads Explained". In: *Journal of Credit Risk* 1.2 (2005), pp. 61–78.

[6] Kenneth Emery. "Moody's Ultimate Recovery Database". In: *Moody's Special Comment* (Apr. 2007).

[7] John C.Hull and Sankarshan Basu. *Options, Futures and Other Derivatives*. tenth. Pearson, 2018.

[8] Diamano Brigo and Fabio Mercurio. *Interest Rate Models Theory and Practice*. Springer Finance. Springer Berlin Heidelberg, 2013. ISBN: 9783662045534. URL: https://books.google.se/books?id=USvrCAAAQBAJ.

[9] Philipp J.Schönbucher. *Credit Derivatives Pricing Models: Models, Pricing and Implementation*. The Wiley Finance Series. Wiley, 2003. ISBN: 9780470842911.

[10] John C.Hull and Alan D.White. "Interest Rate Trees: Extensions and Applications". In: *Quantitative Finance* 18.7 (2018), pp. 1199–1209. DOI: 10.1080/14697688.2017.1406131.

[11] John C.Hull. "Using Hull-White Interest Rate Trees". In: *The Journal of Derivatives* 3 (May 2000). DOI: 10.3905/jod.1996.407949.

[12] Tomas Björk. *Arbitrage Theory in Continuous Time*. Oxford university press Oxford, 2020.

[13] John C.Hull and Alan D.White. *Properties of Ho-Lee and Hull-White Interest Rate Models*. URL: http://www-2.rotman.utoronto.ca/~hull/TechnicalNotes/TechnicalNote31.pdf.

[14] John C.Hull and Alan D.White. *Valuing Options on Coupon-Bearing Bonds in a One-Factor Interest Rate Model*. URL: https://www-2.rotman.utoronto.ca/~hull/TechnicalNotes/TechnicalNote15.pdf.

[15] John C.Hull and Alan D.White. "Numerical Procedures for Implementing Term Structure Models I". In: *The Journal of Derivatives* 2.1 (1994), pp. 7–16. ISSN: 1074-1240. DOI: 10.3905/jod.1994.407902.

[16] Jan Müller. "Option Pricing using Artificial Neural Networks". Eng. BSc Thesis. Lund University, 2021.

[17] Victor Lopez. "Swaption pricing under the single Hull White model through the analytical formula and Finite Difference Methods". MA thesis. Mälardalen University, 2016.

[18] John C.Hull and Alan D.White. "Multi-curve Modelling Using Trees". In: *Innovations in Derivatives Markets*. Vol. 165. Springer, Cham, Dec. 2016, pp. 171–189. ISBN: 978-3-319-33445-5. DOI: 10.1007/978-3-319-33446-2_9.

[19] Jan Annaert et al. "Estimating the Yield Curve Using the Nelson-Siegel Model: A Ridge Regression Approach". In: *Capital Markets: Asset Pricing & Valuation eJournal* (2012).

[20] Lars E.O. Svensson. *Estimating and Interpreting Forward Interest Rates: Sweden 1992 - 1994*. Working Paper 4871. National Bureau of Economic Research, Sept. 1994. DOI: 10.3386/w4871.

[21] Wouter G. Tilgenkamp. "Swaption pricing under the Hull-White One Factor Model". BSc Thesis. Delft Institute of Applied Mathematics, 2014.

[22] Sebastien Gurrieri, Masaki Nakabayashi, and Tony Siu Tung Wong. "Calibration Methods of Hull-White Model". In: *Econometrics: Applied Econometrics & Modeling eJournal* (2009).

[23] Jason Z.Wei. "Valuing Differential Swaps". In: *Journal of Derivatives* 1.3 (1994).

[24] Chuang-Chang Chang, San-Lin Chung, and Min-Teh Yu. "Valuation and Hedging of Differential Swaps". In: *Journal of Futures Markets* 22 (Jan. 2002), pp. 73–94. DOI: 10.1002/fut.2208.

[25] John C.Hull and Alan D.White. "Numerical Procedures for Implementing Term Structure Models II". In: *The Journal of Derivatives* 2.2 (1994), pp. 37–48. ISSN: 1074-1240. DOI: 10.3905/jod.1994.407908.

[26] John C.Hull. *"The Hull–White Two Factor Model"*. URL: http://www-2.rotman.utoronto.ca/~hull/TechnicalNotes/TechnicalNote14.pdf.

[27] Arnaud Blanchard. "The Two-Factor Hull-White Model: Pricing and Calibration of Interest Rates Derivatives". MA thesis. KTH Royal Institute of Technology, 2020.

Appendices

A Reference Data: John C.Hull, Options, Futures and Other Derivatives

Table A.1: Data obtained from John C.Hull "Options, Futures & Other Derivatives" [7]. Note Δt is not an input parameter, illustrated only as a reference. It is calculated from the relevant day count convention and bond expiry.

Zero Rates	
Maturity (days)	**Rate (%)**
3	5.01772
31	4.92828
62	4.97234
94	4.96157
185	4.99058
367	5.09389
731	5.79733
1096	6.30595
1461	6.73464
1826	6.94816
2194	7.08807
2558	7.27527
2922	7.30852
3287	7.39790
3653	7.49015

Contract Information	
a	0.1
σ	0.01
Steps	100
Δt	0.09

Calibration Parameters	
t	3
T	9
K	63
Coupon (%)	5
Coupon Frequency	Annual
Day Count Convention	Annual/365 Fixed

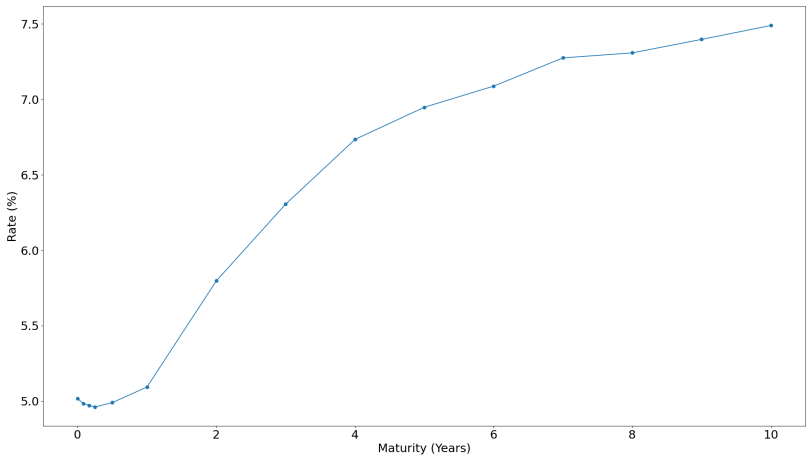

Figure A.1: Reference Data provided by John.C.Hull in [7] based on Deutschmark zero-coupon yield curve on 08/07/1994 [11].

B Reference Data: Philipp Schönbucher, A Tree Implementation of a Credit Spread Model for Credit Derivatives

Table B.1: Data provided for the pricing of Digital Default Swaps using the 3d-trinomial tree [1].

	Calibration Parameters	
	Short Rate (r)	**Default Intensity (λ)**
a	0.1	0.1
σ	0.01	0.01
ρ	0	
q	0	
Steps	21	
Δt	0.2831	

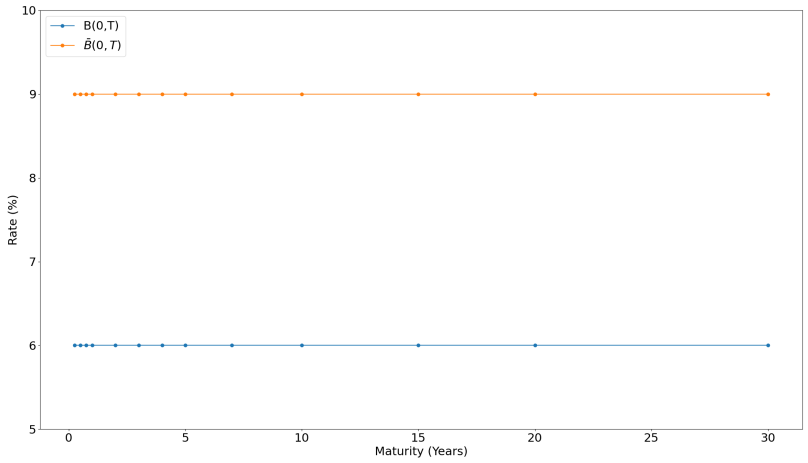

Figure B.1: Risk-free and intensity curves based on data provided by Schönbucher [1].

C Reference Data: John C.Hull & Alan White, Interest Trees: Extensions & Applications

Table C.1: Zero Rates and contract information used for calibrating the generalised short-rate tree in Section 7.3.2 and Section 7.3.3 [11].

Zero Rates	
Maturity (Months)	**Rate (%)**
1	-0.315
3	-0.353
6	-0.399
9	-0.42
12	-0.441
15	-0.456
18	-0.471
24	-0.477
36	-0.459
48	-0.401
60	-0.319
72	-0.209
84	-0.088
96	0.037
108	0.155
120	0.264
132	0.362
144	0.446
180	0.652
240	0.829
300	0.894
360	0.911

Contract Information	
a	0.25
s	0.02
σ	0.3
c	0.03
Steps	4
Δt	0.25

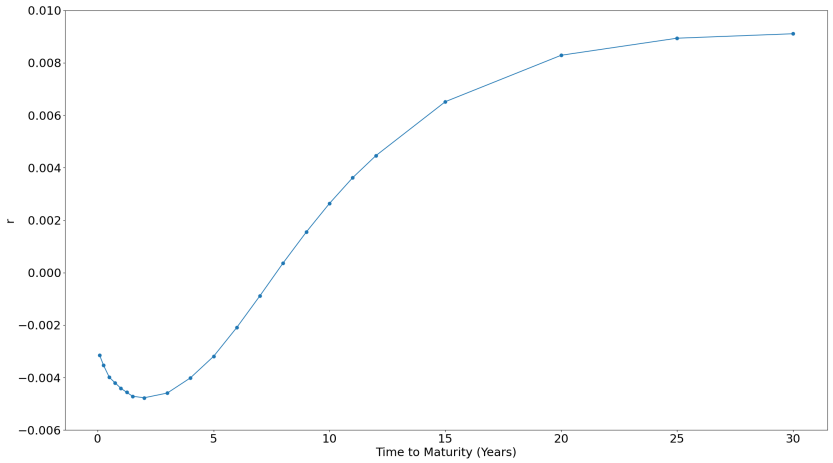

Figure C.1: Term Structure provided for creating short-rate trees in Section 7.3.2 and Section 7.3.3 [10].

D State Variable which follow a Brownian Motion with drift

Based on Lemma 7.1 in Schönbucher [9], a given distribution $x(t)$, which follows the following process:

$$dx(t) = [\kappa(t) - \alpha(t)x(t)]dt + \sigma(t)dW(t), \tag{D.1}$$

can be expressed as:

$$x(T) = x(t)e^{\int_t^T \alpha(s)ds} + \int_t^T e^{-\int_s^T \alpha(u)du}\kappa(s)ds + \int_t^T e^{-\int_s^T \alpha(u)du}\sigma(s)dW(s). \tag{D.2}$$

This is equivalent to stating that $x(T)|x(t)$, $t > T$ is a normally distributed random variable whereby:

$$\begin{aligned} \mathbb{E}\left(x(T)|x(t)\right) &= x(t)e^{\int_t^T \alpha(s)ds} + \int_t^T e^{-\int_s^T \alpha(u)du}\kappa(s)ds, \\ \mathbb{V}\left(x(T)|x(t)\right) &= \int_t^T e^{-2\int_t^T \alpha(u)du}\sigma^2(s)ds. \end{aligned} \tag{D.3}$$

Additionally, if one considers $\alpha(t) = \alpha$, the price of a default free zero-coupon bond with maturity T can be described as:

$$\mathbb{E}\left[e^{-\int_t^T x(s)ds}|\mathcal{F}_t\right] = e^{A(t,T)-B(t,T,\alpha)x(t)}, \tag{D.4}$$

whereby:

$$\begin{aligned} B(t,T;\alpha) &= \frac{1}{\alpha}\left(1 - e^{-\alpha(T-t)}\right), \\ A(t,T;\alpha,\kappa,\sigma) &= \frac{1}{2}\int_t^T \sigma^2(s)B(t,s;\alpha)^2 ds - \int_t^T B(t,s;\alpha)\kappa(s)ds. \end{aligned} \tag{D.5}$$

In order to prove this claim, let:

$$y(t) = x(t)e^{\int_0^t \alpha(s)ds}, \tag{D.6}$$

and by applying Ito's lemma, we arrive at:

$$dy(t) = e^{\int_0^t \alpha(s)ds}\left[\kappa(t)dt + \sigma dW(t)\right]. \tag{D.7}$$

Finally, by integrating Eq D.7 from t to T yields $y(T)$, which can be substituted back into Eq D.6 and solved for $x(T)$ [9].

Master's Theses in Mathematical Sciences 2022:E19
ISSN 1404-6342

LUNFMS-3108-2022

Mathematical Statistics
Centre for Mathematical Sciences
Lund University
Box 118, SE-221 00 Lund, Sweden

http://www.maths.lu.se/